Direct, indirect and composite adaptive control of robot manipulators

Vijverstra, F.J.

Award date:
1992

Direct, Indirect and Composite Adaptive Control of Robot Manipulators

F.J. Vijverstra

WFW report 92.076

Professor: Dr. Ir. J.J. Kok
Coach: Ir. I.M.M. Lammerts

July 1992

Eindhoven University of Technology
Department of Mechanical Engineering
Division of Mechanical Engineering Fundamentals

Contents

Summary III

Notation IV

1 Introduction 1

2 Theoretical properties of the controllers 3
- 2.1 The direct adaptive controller 3
- 2.2 Prediction model 5
- 2.3 Estimation methods 6
  - 2.3.1 The gradient estimator 6
  - 2.3.2 The standard least-squares estimator 7
  - 2.3.3 The exponential forgetting least-squares estimator 8
  - 2.3.4 The bounded-gain-forgetting estimator 8
- 2.4 The indirect adaptive controller 9
- 2.5 The composite adaptive controller 10
- 2.6 A comparison between the controllers 10

3 Simulations with the TR-robot 12
- 3.1 The TR-robot 12
- 3.2 The desired trajectories 13
- 3.3 Control parameters 15
- 3.4 Results of simulations with the TR-robot 16
  - 3.4.1 Equivalent models 16
  - 3.4.2 Unmodelled dynamics 18
  - 3.4.3 Time-varying parameters 19
- 3.5 Conclusions 20

4 Simulations with the XY-table 21
- 4.1 The XY-table 21
- 4.2 Control parameters and desired trajectory 23
- 4.3 Results of the simulations with the XY-table 24
  - 4.3.1 Results of situation 1 24
  - 4.3.2 Results of situation 2 26
- 4.4 Conclusions 28

5 Implementation on the XY-table 29
- 5.1 The XY-table 29
- 5.2 The observer 30
- 5.3 Results of the experiments with the XY-table 31
  - 5.3.1 Experiments with the rigid XY-table 31
  - 5.3.2 Experiments with the flexible XY-table 35
- 5.4 Conclusions 36

6 Conclusions and recommendations 37

References 39

Appendices

A The tracking convergence of the controllers A.1
A.1 The direct adaptive controller A.1
A.2 The indirect adaptive controller A.2
A.3 The composite adaptive controller with BGF estimator A.5
B Controller design for the TR-robot B.1
C Results of simulations with the TR-robot C.1
C.1 Data C.1
C.2 Results with equivalent models C.2
C.3 Results with unmodelled dynamics C.11
C.4 Results with time-varying parameters C.19
D Controller design for the XY-table D.1
E Results of simulations with the XY-table E.1
E.1 Data E.1
E.2 Results of situation 1 E.2
E.3 Results of situation 2 E.3
F The observer F.1
G The control parameters K_D and Λ G.1
H Results of the experiments H.1
H.1 Results of the rigid XY-table H.1
H.2 Results of the flexible XY-table H.7
H.3 Results of a non-adaptive controller H.8

Summary

In this report a comparison is made between three different adaptive controllers, namely the direct, indirect and composite adaptive controller. These controllers are based on the computed-torque control method, which takes full consideration of the non-linear, time-varying and coupled nature of robot dynamics. With an adaptation mechanism the unknown parameters of the robot and its load can be estimated. In the presence of unknown parameters the adaptive controller will achieve much better tracking of the desired trajectory than a non-adaptive controller. All three adaptive controllers, which will be investigated in this report, have a different adaptation mechanism for the unknown parameters.

The investigation of the controllers consists of four parts:

- Theory
- Simulations with a TR-robot
- Simulations with the XY-table
- Experiments with the XY-table

The simulations with the TR-robot are not only executed with equivalent models (model of the simulated proces and model of the controller are the same), but also with a simulation model with robot dynamics being unmodelled in the control model. Then, the controllers are investigated by simulating a control of a XY-table. In these simulations there are no unmodelled dynamics present. Finally, experiments with the experimental XY-table are done. In this practical situation there are always unmodelled dynamics present.

The main conclusion of this report is that the indirect and composite adaptive controller have better tracking performance than the direct adaptive controller. This is caused by better parameter estimation of the indirect and composite controller. The tracking performance of the indirect and composite controller does not differ much. Furthermore can be concluded that the indirect and composite adaptive controller are more robust against unmodelled dynamics than the direct controller.

Notation

A,a	:scalar
A	:matrix (capital *italic* characters)
A_{ij}	:term on row i, column j
a	:column (small *italic* characters)
a^T, A^T	:transposition of column or matrix
A^{-1}	:inverse of matrix
â, $\hat{a}$	:estimate of scalar or column
a_d, a_d	:desired scalar or column
$\tilde{a}$	:a-a_d (tracking error)
$\tilde{a}$	:$\hat{a}$-a (estimation error)
$\dot{a}$	:first order derivative
$\ddot{a}$	:second order derivative
I	:unity matrix

Chapter 1. Introduction

Advanced manipulator applications often require effective controller design in order to achieve accurate tracking of fast desired motions. If the parameters of a manipulator and its load are known a priori, the well-known **computed-torque control** (CTC) method can be used for this purpose. The CTC method takes full consideration of the non-linear, time-varying and coupled nature of robot dynamics and can theoretically guarantee exact tracking and stable robot performance.

However, for a manipulator handling various loads, the inertial parameters of the load change from time to time without being accurately known by the controller, and the performance of the computed-torque controller degrades substantially or may even become unstable. This parameter sensitivity is particularly severe for direct-drive robots and/or fast manipulator motions. Therefore, there has been active research in adaptive CTC control.

The difference between the adaptive and the non-adaptive CTC controllers is that the adaptive controllers have an adaptation mechanism for the unknown parameters. The adaptive CTC controllers can mainly be classified into three categories according to their adaptation mechanisms: direct, indirect and composite adaptive controllers.

- The **direct** adaptive controllers use tracking errors of the joint motion to drive the parameter adaptation. In this class of adaptive controllers, the predominant concern of the adaptation laws is to reduce the tracking errors. These controllers are also called tracking-error-based (TEB) adaptive controllers.

- The **indirect** adaptive controllers, on the other hand, use prediction errors in the filtered joint torques to generate parameter estimates to be used in the control law. For these adaptive controllers, the predominant concern is to extract information about the true parameters from the prediction errors, with no direct concern to adapt the parameters so that the tracking error converge to zero. These controllers are called prediction-error-based adaptive controllers.

- The **composite** adaptive controllers use both tracking errors in the joint motion and the prediction errors in the predicted filtered torque to drive the parameter adaptation. They are based on the observation that the parameter uncertainty is reflected in both the tracking error and the prediction error and, therefore, it is desirable to extract the parameter information from both sources.

In this report, a comparison will be made between the three different adaptive controllers, mentioned above.

In chapter 2, the theoretical properties of the controllers are explained and discussed.

In chapter 3, simulations with the TR-robot are presented. After given the mathematical model of the robot, the simulations are executed for three kinds of situations: either with equivalent models, or with unmodelled dynamics, or with time-varying parameters.

In chapter 4, simulations with the XY-table are presented. After given a description of the XY-table and the equations of motion, the simulations are only executed for the situation with equivalent models.

In chapter 5, the three adaptive controllers are applied to the experimental XY-table. To reduce errors, an observer is designed to estimate the position and speed one sample ahead with only the measurements of the positions.

In chapter 6, the main conclusions are summarized and recommendations are given for further research.

Chapter 2. Theoretical properties of the controllers

In this chapter, the principles of the direct, indirect and composite adaptive controllers will be discussed. First, the rigid-body model of the manipulator will be given. With this model the direct adaptive controller can be described. Then, a prediction model for the joint torque and some estimation methods will be given. The prediction model and one of the estimation methods will be used in the indirect and composite adaptation law.

2.1 The direct adaptive controller

In the absence of friction or other disturbances the dynamics of a rigid manipulator can be written as

$$H(q)\ddot{q} + C(q,\dot{q})\dot{q} + G(q) = \tau \tag{2.1}$$

with

q	the nx1 vector of joint displacements
τ	the nx1 vector of applied joint torques
$H(q)$	the nxn symmetric positive definite manipulator inertia matrix
$C(q,\dot{q})\dot{q}$	the nx1 vector of centripetal and Coriolis torques
$G(q)$	the nx1 vector of gravitational torques

The above robot dynamics are linear in terms of a suitable selected set of robot and load parameters. This property is called the linear parametrization property. The robot dynamics model of (2.1) can now be simply written as

$$\tau = Y_1(q,\dot{q},\ddot{q})\,a \tag{2.2}$$

with

Y_1	nxm non-linear matrix function
a	mx1 vector of equivalent robot and load parameters

The adaptive robot controller design problem is as follows: given the desired trajectories $q_d(t)$, $\dot{q}_d(t)$, $\ddot{q}_d(t)$, measurements (or reconstruction) of the joint positions q and velocities $\dot{q}$, derive a control law for the actuator torque τ, and an adaptation law for the unknown parameters, such that the manipulator joint positions $q(t)$ closely track the desired positions $q_d(t)$ and also that the joint velocities $\dot{q}(t)$ closely track the desired velocities $\dot{q}_d(t)$.

In Slotine and Li [1] the following direct adaptive controller was developed: Let $\hat{H}$, $\hat{C}$ and $\hat{G}$ be obtained by substituting the estimated parameters $\hat{a}$(t) into $H(q)$, $C(q,\dot{q})$ and $G(q)$. Then the control and adaptation law can be written as:

$$\tau = \hat{H}(q)\ddot{q}_r + \hat{C}(q,\dot{q})\dot{q}_r + \hat{G}(q) - K_D s \tag{2.3}$$

$$\dot{\hat{a}}(t) = -\Gamma Y^T(q,\dot{q},\dot{q}_r,\ddot{q}_r)s \tag{2.4}$$

where K_D and Γ are constant positive definite matrices, and

$$\dot{q}_r = \dot{q}_d - \Lambda\tilde{q} \tag{2.5}$$

$$s = \dot{q} - \dot{q}_r = \dot{\tilde{q}} + \Lambda\tilde{q} \tag{2.6}$$

with $\tilde{q}=q(t)-q_d(t)$ denoting the error in tracking the desired joint position $q_d(t)$ and Λ a constant p.d. matrix. The matrix Y of (2.4) is defined by the following linearity relation associated with the dynamics model (2.1):

$$\tilde{H}(q)\ddot{q}_r + \tilde{C}(q,\dot{q})\dot{q}_r + \tilde{G}(q) = Y(q,\dot{q},\dot{q}_r,\ddot{q}_r)\tilde{a} \tag{2.7}$$

where $\tilde{a}=\hat{a}-a$, $\tilde{H}=\hat{H}-H$, $\tilde{C}=\hat{C}-C$ and $\tilde{G}=\hat{G}-G$. As $\ddot{q}_r=\ddot{q}_d-\Lambda\dot{\tilde{q}}$, the matrix $Y(q,\dot{q},\dot{q}_r,\ddot{q}_r)$ can be computed from measurements of only q and $\dot{q}$.

Equation (2.3) can also be written as

$$\tau = Y(q,\dot{q},\dot{q}_r,\ddot{q}_r)\hat{a} - K_D s \tag{2.8}$$

This equation represents a feedforward + PD controller, with the feedforward action adaptively cancelling the robot dynamic forces, and the PD action ($K_D s$) regulating the tracking error to zero.

In appendix A the complete proof of the global asymptotic tracking convergence is given. It is important to know that tracking convergence of direct adaptive controllers does not require a persistent excitation condition. By persistent excitation (p.e.) of a matrix M is meant that there exist positive constants α_1, α_2 and δ, such that

$$\forall t \geq 0 \quad \alpha_1 I \leq \int_t^{t+\delta} M^T(r)M(r)dr \leq \alpha_2 I \tag{2.9}$$

Condition (2.9) means that, although the matrix M^TM is singular for all r, the integral of M^TM is uniformly positive definite over any interval of some length δ. In other words, condition (2.9) means that M must vary sufficiently over the interval δ so that the entire space is spanned. This persistent excitation condition is very important in the theoretical analyses of indirect and composite adaptive controllers and will be much used in the rest of this chapter.

However, exponential convergence of the tracking errors cannot be shown, even under a persistent excitation condition. Exponential convergence of an adaptive controller is an attractive property, since it favors robustness, as pointed out by Anderson and Johnson [2].

The issue of parameter error convergence is studied in Slotine and Li [1]. The condition for the estimated parameters to converge to the true parameters is found to be the persistent excitation of Y_d, where $Y_d = Y(q_d,\dot{q}_d,\dot{q}_d,\ddot{q}_d)$.

2.2 Prediction model

The robot model (2.2) is the only model that has information about the true parameters and therefore this model will be used for estimating the parameters. As (2.2) involves the joint acceleration $\ddot{q}$, which generally cannot be measured, it is desirable to eliminate $\ddot{q}$ from (2.2). This is done by filtering both sides of the equation through an exponentially stable and strictly proper filter. Let $w(t)$ be the impulse response of a stable, proper filter. Then, convolving both sides of (2.1) by w yields

$$\int_0^t w(t-r)\tau(r)dr = \int_0^t w(t-r)[H\ddot{q} + C\dot{q} + G]dr \tag{2.10}$$

Using partial integration, the first term on the right-hand side of (2.10) can be written as

$$\int_0^t w(t-r)[H\ddot{q}]dr = w(t-r)H\dot{q}\Big|_0^t - \int_0^t \frac{d}{dr}[wH]\dot{q}dr \tag{2.11}$$

Define $y(t) = \int_0^t w(t-r)\tau(r)\,dr$ as the filtered torque, then with (2.11) equation (2.2) can be can be written as

$$y(t) = W(q,\dot{q})a \tag{2.12}$$

where W is the filtered version of Y_1. Thus, the matrix W can be computed from measurements of q and $\dot{q}$ only.

From (2.12) a prediction of the filtered output torque $y(t)$ and a prediction error can be generated based on the estimated parameters $\hat{a}$

$$\hat{y}(t) = W(q,\dot{q})\hat{a}(t) \tag{2.13}$$

$$e = \hat{y} - y = W\tilde{a} \tag{2.14}$$

where $\tilde{a}=\hat{a}-a$ is the parameter estimation error. The estimation methods in the following paragraph extract parameter information from the prediction error.

2.3 Estimation methods

All the estimators which will be considered have a common form of parameter update, namely

$$\dot{\hat{a}} = -PW^T e \tag{2.15}$$

where $P(t)$ is a constant or time-varying, positive definite gain matrix. The difference between the estimation methods lies in the fact that the gain matrix P is generated in different forms and from different perspectives.

2.3.1 The gradient estimator

In the gradient estimator, the gain matrix is simply held constant

$$P(t) = P_0 \tag{2.16}$$

Advantages:

1 If W is persistently exciting, there is exponential convergence of the estimated parameters.

2 The estimator can track time-varying parameters and it works quite well in the presence of disturbances.

Disadvantages:

1 Persistent excitation is essential for the robustness of the estimator. If W is not p.e., the parameters will not converge even in the absence of uncertainties.

2 Convergence of the parameters is usually slow. This is a disadvantage, since faster parameter convergence will lead to better tracking performance of the controller.

3 If P is chosen too large, the convergence will become oscillatory and the parameter error will become large.

2.3.2 The standard least-squares estimator

The gain update equation in SLS estimation is

$$\dot{P} = -PW^TWP \tag{2.17}$$

Advantages:

1 The estimated parameters are guaranteed to be bounded. If W is such that it satisfies the "infinite integral" condition

$$\lambda_{min}\{\int_0^t W^TW\mathrm{d}r\} \to \infty \quad \text{as} \quad t \to \infty \tag{2.18}$$

then the estimated parameters will asymptotically converge to the true parameters. By (2.18) is meant that the smallest eigenvalue λ_{min} of the integral approaches infinity, if t goes to infinity.

2 The SLS method has good robustness with respect to noise and disturbances.

3 If P is chosen large, the estimated parameters are much smoother than those from the gradient method.

Disadvantages:

1 The SLS method has poor ability in tracking time-varying parameters. This is

caused by the fact that $P(t)$ converges to zero when W is p.e. (see Slotine and Li [1]). Because $P(t)$ converges to zero, the parameter update is shut off after some time, and the changing parameters cannot be estimated any more.

2 The exponential convergence of the estimated parameters can NOT be shown, even under p.e. condition of W.

2.3.3 The exponential forgetting least-squares estimator

Exponential forgetting of data is a solution to the problem of the inability of tracking time-varying parameters. Exponential forgetting implies that past data must be discounted when being used for the estimation of the current parameters. The gain update equation is:

$$\dot{P} = \lambda(t)P - PW^TWP \tag{2.19}$$

Advantages:

1 The EFLS estimator always improves parameter convergence over the SLS method.

2 The EFLS estimator can track time-varying parameters.

3 The estimated parameters are guaranteed to be bounded. If W satisfies the infinite integral condition, the estimated parameters are asymptotically convergent. If W is p.e., the estimated parameters are exponential convergent.

Disadvantage:

1 A constant positive λ leads to exploding gain matrix P in the absence of p.e. (see Slotine and Li [1]). Unboundedness of the gain matrix is undesirable, since it implies that the disturbance and noise in the prediction error may lead to violent oscillations of the estimated parameters.

2.3.4 The bounded-gain-forgetting estimator

To keep the benefits of data forgetting (parameter tracking ability) while avoiding the possibility of gain unboundedness, it is desirable to tune the forgetting factor variation so that data forgetting is activated when W is p.e. and suspended when W is not. Since the magnitude of the gain matrix P is an indicator of the excitation level of W, it is reasonable to correlate the forgetting factor variation with $\|P(t)\|$. A specific technique is to choose:

$$\dot{P} = \lambda(t)P - PW^TWP \tag{2.20}$$

$$\lambda(t) = \lambda_0(1 - \frac{\|P\|}{k_0}) \tag{2.21}$$

where k_0 and λ_0 are two positive constants specifying the upper bound of the gain matrix norm and the maximum forgetting rate, respectively. This implies forgetting at a maximum factor λ_0 if the norm of P is zero (which indicates infinitely strong p.e.) and stops forgetting if the norm reaches the specified upper bound (indicating weak excitation).

Advantages:

1 The estimated parameters are always bounded and the gain matrix P is always uniformly upper bounded, i.e., $P(t) \leq k_0 I$

2 If W is p.e., the estimated parameters converge exponentially with a rate dependent on the p.e. strength and the gain matrix is uniformly bounded from both below and above by positive definite matrices, i.e., $k_2 I \leq P(t) \leq k_1 I$.

3 The advantage of the BGF method over the gradient method is that the estimated parameters are smooth. This implies that much larger gain bound can be used. As a result, faster parameter convergence can be achieved.

Disadvantage:

1 If W is not p.e., the boundedness of parameter errors in the presence of parameter variation and disturbances cannot be guaranteed.

2.4 The indirect adaptive controller

The indirect controller has the same control law as in the direct controller:

$$\tau = Y(q,\dot{q},\dot{q}_r,\ddot{q}_r)\hat{a} - K_D s \tag{2.22}$$

In an indirect controller, the parameter update of the last paragraph is used as adaptation law:

$$\dot{\hat{a}} = -PW^T e \tag{2.23}$$

where P can be chosen according to one of the estimation methods mentioned above. In the following chapters of this report a BGF estimator will be used, since this estimator has the best properties.

2.5 The composite adaptive controller

The control law is the same as in the direct and indirect adaptive controller:

$$\tau = Y(q,\dot{q},\dot{q}_r,\ddot{q}_r)\hat{a} - K_D s \tag{2.24}$$

The new adaptation law extracts information from both the tracking error s and the prediction error e. This composite adaptation law has the following form:

$$\dot{\hat{a}}(t) = -P(t)[Y^T s + W^T R(t) e] \tag{2.25}$$

where $R(t)$ is a uniformly p.d. weighting matrix indicating how much attention should be payed to the parameter information in the prediction error. The adaptation gain $P(t)$ is a uniformly p.d. gain matrix determined by the estimation methods described above.

For the composite adaptive controller, the gain update techniques of the various parameter estimators can be used. The gradient estimator is computationally simple, but leads to relatively slow convergence. The SLS estimator is good for constant parameters, but it is unsuitable for time-varying parameters. The BGF estimator, on the other hand, has desirable convergence and robustness properties. Under p.e. of W_d, the parameter estimation errors are exponentially convergent if the unknown parameters are constant and no disturbance is present. And they are uniformly bounded if the unknown parameters vary with bounded derivative and if disturbances are bounded. So in the following chapters of this report we will use the BGF estimator in the adaptation law of the composite controller.

2.6 A comparison between the controllers

In appendix A, the stability proofs of the three different controllers are given, based on two different methods. The proof of the global tracking convergence of the direct and composite adaptive controller is based on a Lyapunov analysis. The convergence proof of the indirect adaptive controller is based on the square-integrable property of the prediction error e. A disadvantage of this proof is the necessity to explicitly guarantee that the estimated inertia matrix $\hat{H}$ remains positive definite in the course of adaptation. This is avoided by both the direct and the composite adaptive controller.

The controllers have the following theoretical differences, which are shown in appendix A: as mentioned before, the direct adaptive controller does not require a persistent excitation condition of the desired trajectories to proof the global asymptotic tracking convergence. However, desirable exponential convergence of the tracking errors cannot be shown, even not under a persistent excitation condition.

The indirect and composite adaptive controller with BGF estimators have globally convergent tracking errors $\tilde{q}$ and $\dot{\tilde{q}}$ and a globally convergent prediction error e if the desired trajectories are bounded. Furthermore, if W_d is persistent exciting, the parameter errors, the tracking errors and prediction errors are globally exponentially convergent. As said before, exponential convergence favors robustness and leads to better tracking performance.

To compare the composite adaptation law with the direct adaptation law, choose $P(t)=\Gamma=\gamma I$ and $R(t)=I$. With $e=W\tilde{a}$ the composite adaptation law is

$$\dot{\tilde{a}} - \gamma W^T W\tilde{a} = -\gamma Y^T s \tag{2.26}$$

The adaptation law in the direct adaptive controller is

$$\dot{\tilde{a}} = -\gamma Y^T s \tag{2.27}$$

We see that (2.27) represents an integrator while (2.26) can be considered as a time-varying low-pass filter. The gradient nature of (2.27) accounts for the violent oscillations of the estimated parameters if a large adaptation gain is used. From (2.26) we see that the parameter errors are now a filtered version of the gradient direction. Thus, the parameter search in the composite adaptation goes along a filtered direction. This indicates that parameter and tracking error convergence in composite adaptive control has less oscillations than in TEB adaptive control. The adaptation gain in composite adaptive control can now be increased much higher than in TEB adaptation, yielding faster parameter convergence and better tracking accuracy.

Chapter 3. Simulations with the TR-robot

To investigate the three different adaptive controllers, simulations will be executed on a TR-robot. First a model of the TR-robot will be derived. Then the desired trajectories will be given, followed by the results of the simulations which are executed for various situations.

3.1 The TR-robot

The TR-robot has two degrees of freedom, namely a translation x(t) (prismatic joint) and a rotation φ(t) (revolute joint). In figure 3.1 a model of the TR-robot is given.

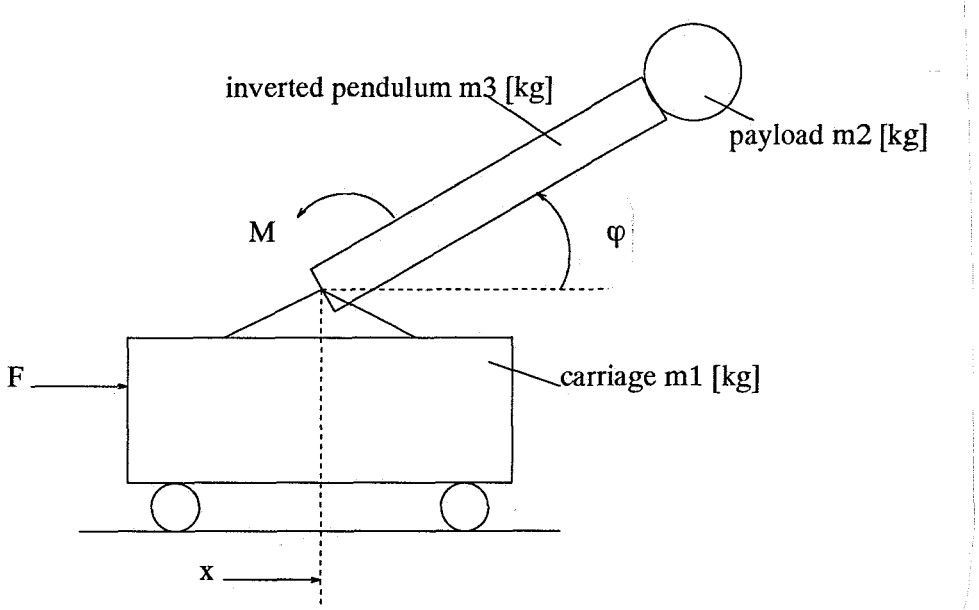

Figure 3.1: The TR-robot

The TR-robot consists of a carriage and an inverted pendulum. The carriage with mass m_1 can be translated by the force F(t). The pendulum with mass m_3 has a concentrated payload m_2 at the end and can be rotated by the torque M(t). If there is no friction and the TR-robot moves in a vertical plane without gravity, the dynamics of the TR-robot can be written in the form $H(q)\ddot{q}+C(q,\dot{q})\dot{q}+G(q)=\tau$:

$$\begin{bmatrix} m_1+m_2+m_3 & -(m_2+\frac{m_3}{2})l\sin(\varphi) \\ -(m_2+\frac{m_3}{2})l\sin(\varphi) & (m_2+\frac{m_3}{3})l^2 \end{bmatrix} \begin{bmatrix} \ddot{x} \\ \ddot{\varphi} \end{bmatrix} + \begin{bmatrix} 0 & -(m_2+\frac{m_3}{2})l\cos(\varphi)\dot{\varphi} \\ 0 & 0 \end{bmatrix} \begin{bmatrix} \dot{x} \\ \dot{\varphi} \end{bmatrix} = \begin{bmatrix} F \\ M \end{bmatrix} \tag{3.1}$$

Using the linear parametrization property, we can write the robot dynamics in the form $\tau = Y_1(q,\dot{q},\ddot{q})a$:

$$\begin{bmatrix} \ddot{x} & -l\sin(\varphi)\ddot{\varphi} - l\cos(\varphi)\dot{\varphi}^2 & 0 \\ 0 & -l\sin(\varphi)\ddot{x} & l^2\ddot{\varphi} \end{bmatrix} \begin{bmatrix} a_1 \\ a_2 \\ a_3 \end{bmatrix} = \begin{bmatrix} F \\ M \end{bmatrix} \tag{3.2}$$

with:

$a_1 = m_1 + m_2 + m_3$
$a_2 = m_2 + m_3/2$
$a_3 = m_2 + m_3/3$

3.2 The desired trajectories

The desired trajectory of the payload, $q_d=[x_d\ \varphi_d]^T$, is shown in figure 3.2. The payload at the end of the inverted pendulum has to rotate in a circle, from which the centre is fixed at a vertical distance l/2 to the ground. The circle has a radius r and the rotation velocity of the payload is ω.

To make a circle, the x and the φ have to be solved from the following equations, which are derived from figure 3.2:

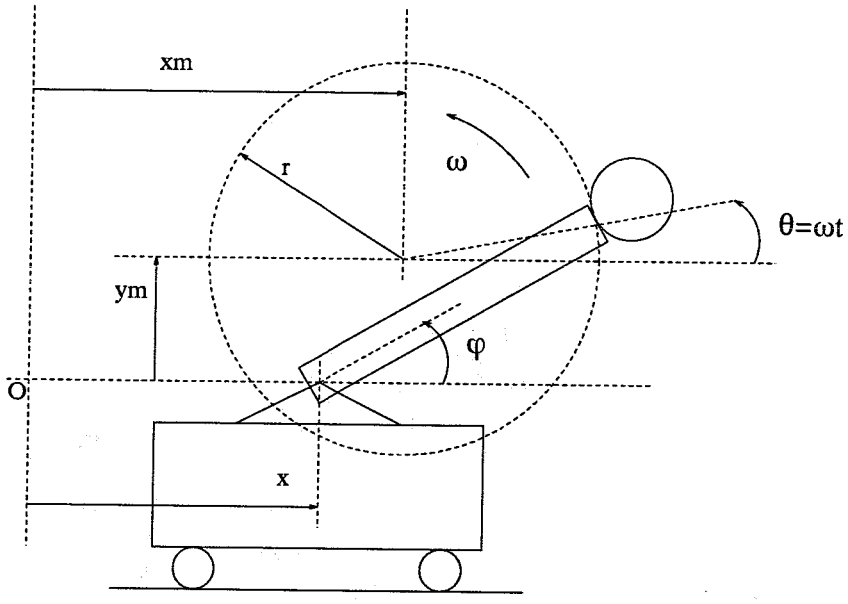

Figure 3.2: The desired trajectory

$$x + l\cos(\varphi) = x_M + r\cos(\omega t) \tag{3.3}$$

$$l\sin(\varphi) = y_M + r\sin(\omega t) \tag{3.4}$$

The solution is:

$$x_d = x_M + r\cos(\omega t) - l\cos(\varphi_d) \tag{3.5}$$

$$\varphi_d = \arcsin\left(\frac{y_M + r\sin(\omega t)}{l}\right) \tag{3.6}$$

The controllers also need the first and second derivative of x_d and φ_d:

$$\dot{x}_d = -\frac{1}{\cos(\varphi_d)} r\omega \sin(\omega t - \varphi_d) \tag{3.7}$$

$$\dot{\varphi}_d = \frac{1}{l\sin(\varphi_d)}(\dot{x}_d + r\omega\sin(\omega t)) \tag{3.8}$$

$$\ddot{x}_d = \frac{1}{\cos(\varphi_d)}(l\dot{\varphi}_d^2 - r\omega^2\cos(\omega t - \varphi_d)) \tag{3.9}$$

$$\ddot{\varphi}_d = \frac{1}{l\sin(\varphi_d)}(\ddot{x}_d + r\omega^2\cos(\omega t) - l\cos(\varphi_d)\dot{\varphi}_d^2) \tag{3.10}$$

3.3 Control parameters

In this paragraph, the different control parameters will be discussed. In the case of the direct adaptive controller the matrices Γ, K_D and Λ have to be chosen. The choice of the gain matrix Γ has a fundamental influence on the convergence of the parameters. Generally speaking, an increasing gain matrix leads to faster parameter convergence. But beyond some point, further increasing of the gain matrix leads to oscillatory and slower convergence.

The tracking performance of the adaptive controller depends much on the choice of the gain matrices K_D and Λ. Increasing the gain matrix K_D leads to a better tracking accuracy (a smaller error s). But if K_D is chosen too large, the controller has no robustness to noise, unmodelled dynamics and disturbances. The matrix Λ has influence on the desired speed of the position convergence.

In the case of the composite adaptive controller, the matrices K_D and Λ have the same influence on the tracking performance as in the direct adaptive controller. Instead of the matrix Γ in the direct adaptive controller, now the gains λ_0 and k_0 have to be chosen. The choice of λ_0 means a tradeoff between the speed of parameter tracking and the oscillation of the estimated parameters. Namely, a larger value of λ_0 means faster parameter convergence, but also more oscillations in the estimated parameters. The gain bound k_0 has the same tradeoff.

In the indirect adaptive controller the same gain matrices and constants have to be chosen as in the composite adaptive controller.

A disadvantage of the composite and the indirect adaptive controller is that we cannot increase λ_0 very much. If we take λ_0 too large, the computer goes out of memory or gives a singularity at the beginning of the simulation. But we need a large λ_0, because otherwise the parameter convergence is too slow. A solution to this problem is to take the following composite adaptation law:

$$\dot{\hat{a}} = -k_1 P(t)(Y^T s + W^T e) \tag{3.11}$$

In case of the indirect adaptation we get the following law:

$$\dot{\hat{a}} = -k_1 P(t) W^T e \tag{3.12}$$

3.4 Results of simulations with the TR-robot

In this paragraph, the three different controllers will be compared with each other. In appendix B, the designs of the three controllers are given. In this appendix is also the matrix $W(q,\dot{q})$ calculated. First, the situation will be investigated with equivalent models, i.e., the model of the controller is of the same order as the model of the proces. Then, the simulations are executed with unmodelled dynamics, i.e., there are dynamics present in the proces, but these dynamics are not accounted for in the controller. At last the results are given when we are dealing with time-varying parameters.

3.4.1 Equivalent models

The manipulator link parameters, the manipulator initial state variables, the initial mass parameters and the desired trajectories are given in appendix C. Now, only the control parameters have to be chosen. A suitable choice of the control parameters is found by trial and error. We want to tune the control parameters as large as possible, but not too large since we want to avoid large oscillations.

A suitable choice of the control parameters of the direct adaptive controller is:

$$\Gamma = \begin{bmatrix} 1000 & 0 & 0 \\ 0 & 1000 & 0 \\ 0 & 0 & 1000 \end{bmatrix}, \quad K_D = \begin{bmatrix} 100 & 0 \\ 0 & 100 \end{bmatrix}, \quad \Lambda = \begin{bmatrix} 10 & 0 \\ 0 & 10 \end{bmatrix}$$

A suitable choice of the composite adaptive controller with BGF estimator is:

$$K_D = \begin{bmatrix} 100 & 0 \\ 0 & 100 \end{bmatrix}, \quad \Lambda = \begin{bmatrix} 10 & 0 \\ 0 & 10 \end{bmatrix}, \quad \lambda_0 = 100, \quad k_0 = 1$$

$$\lambda_f = 10, \quad R(t) = I, \quad k_1 = 100, \quad P(t=0) = I$$

A suitable choice of the parameter set of the indirect adaptive controller with BGF estimator is the same as for the composite adaptive controller, except that $R(t)$ is not used.

In the figures 3.3 and 3.4 the estimated parameter a_1 and the position tracking error of x of all three controllers with the above choice of the control parameters are shown.

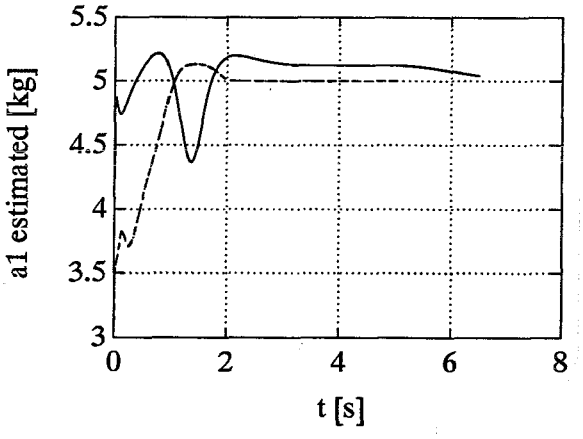

Figure 3.3: estimated parameter a_1
—— :direct, ----:indirect, -·-·:composite

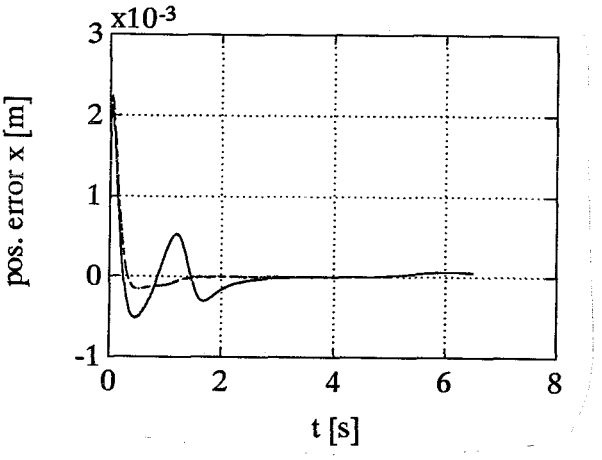

Figure 3.4: Pos. tr. error x
—— :direct, ----:indirect, -·-·:composite

From figure 3.3 we see that in the composite and indirect adaptive controller the estimated parameter a_1 converges within 2 seconds to the true value of 5 [kg]. In the direct adaptive controller the estimated parameter a_1 does not exactly converge to the true value. The other two estimated parameters a_2 and a_3 have the same tendencies as the estimated parameter a_1 and are given in appendix C.

From figure 3.4 we see that in case of the composite and indirect controller the position tracking error of the translation x converges within 1.5 second to zero. In the direct controller this position tracking error does not exactly converge to zero even in 6 seconds. Furthermore, the position tracking error of the translation x in the direct controller is more oscillatory than in the composite and indirect controller. The same remarks as above can be made about the position tracking error of the rotation φ, which is given in appendix C. So, the conclusion can be made that, compared with the direct method, the position tracking errors of the composite and indirect method are less oscillatory and have faster convergence.

Now the three different controllers will be discussed separately. First the direct adaptive controller will be investigated. In appendix C the simulations are shown for three different values of Γ, namely $\Gamma=100I$, $1000I$ and $3000I$. The matrices K_D and Λ remain the same as above. We see that for $\Gamma=100I$ the parameter and tracking convergence are slow, but also that they are smooth. For $\Gamma=1000I$ the parameter and tracking convergence are better, but the errors are more oscillatory. For $\Gamma=3000I$ the parameter convergence and the tracking errors are very oscillatory.

In appendix C simulations are also done for the composite and indirect controller. These simulations are done with different values of k_1, namely k_1=10, 30 and 100. Now we see that the parameter and tracking errors do not become oscillatory (remain smooth) with increasing gain k_1. So, the conclusion can be made that the adaptation gain in the composite and indirect controller can be increased much higher than in the direct controller, without causing oscillations.

3.4.2 Unmodelled dynamics

To compare the robustness of the different controllers simulations are done with unmodelled dynamics. Unmodelled dynamics are introduced by an extra damping -bφ̇ in the revolute joint. This damping is not accounted for in the controller. For b is the value 100 chosen.

The most suitable choice of the control parameters of the direct adaptive controller is not the same anymore as in the case with equivalent models. The matrices K_D and Λ are the same, but Γ is now $100I$.

The control parameters of the composite and indirect adaptive controller are the same as in the case with equivalent models, except for k_1 which is now 30. In the figures 3.5, 3.6 and 3.7 the estimated parameter a_1 and the position tracking errors with these control parameters are shown.

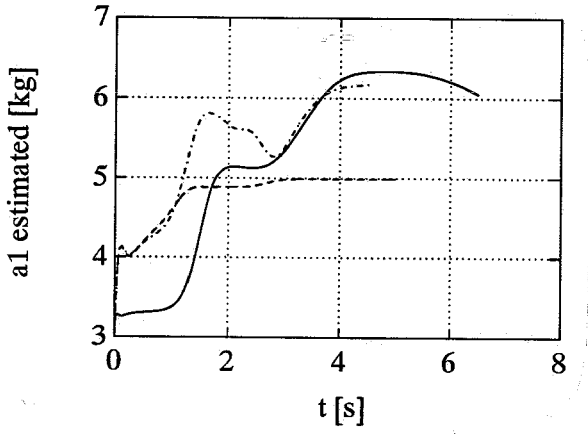

Figure 3.5: estimated parameter a_1
—— :direct, ----:indirect, -·-·:composite

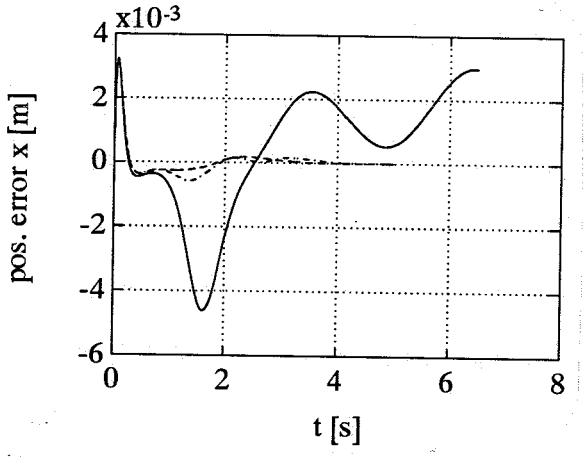

Figure 3.6: Pos. tr. error x
—— :direct, ----:indirect, -·-·:composite

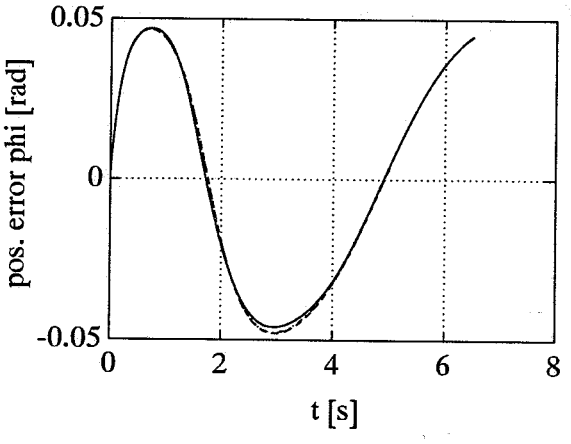

Figure 3.7: Pos. tr. error phi
—— :direct, ----:indirect, -·-·:composite

From figure 3.5 we see that in the indirect adaptive controller the estimated parameter a_1 converges within 3 seconds to the true value of 5 [kg] even in the presence of unmodelled dynamics. The estimated parameter a_1 in the composite controller is worse than in the indirect controller, but is still better than in the direct controller. The other two estimated parameters a_2 and a_3 have the same phenomena as the estimated parameter a_1 and are given in appendix C.

From figure 3.6 we see that in the direct controller the position tracking error of the translation x does not converge to zero, but increases instead. In the composite and indirect controller this error does converge to zero and is much smoother. Also the velocity tracking error of the translation x is smaller and smoother in case of the composite and indirect controller. This velocity tracking error is given in appendix C. So, we can say that in the situation with unmodelled dynamics the composite and indirect controller have better performance than the direct controller. However, looking at figure 3.7 we see that the position tracking error of the rotation φ does not converge to zero in all three controllers, but increases instead. The conclusion is now that all three controllers are not robust to unmodelled dynamics.

Now the three different controllers will be discussed separately. First the direct adaptive controller will be discussed. In appendix C the simulations are shown for two values of Γ, namely $\Gamma=100I$ and $1000I$. Matrices K_D and Λ remain the same. In the case of $\Gamma=1000I$ the estimated parameters are much oscillatory. Also the tracking errors are larger and more oscillatory than in the case of $\Gamma=100I$. So, increasing the adaptation gain in the direct controller too much leads to oscillatory and larger tracking errors.

The simulations of the composite and indirect adaptive controller are done with two different values of k_1, namely $k_1=10$ and 30. We see that even with increasing k_1 the tracking errors remain small and smooth. The conclusion is that the composite and indirect adaptive controller are more robust than the direct controller, since variations in the control parameters of the composite and indirect method have little influence on the responses, while in the direct method variations quickly causes oscillations in the responses. Furthermore, the adaptation gain in the composite and indirect method can increased much higher than in the direct controller.

3.4.3 Time-varying parameters

Suppose that the load of the TR-robot is time-varying with $m_2(t)=2+\sin(0.5*t)$. The simulations are done without unmodelled dynamics.

The most suitable choice of the control parameters is for each controller the same as in the simulations with equivalent models. In figures 3.8 the estimated parameter a_1 for all three controllers is shown:

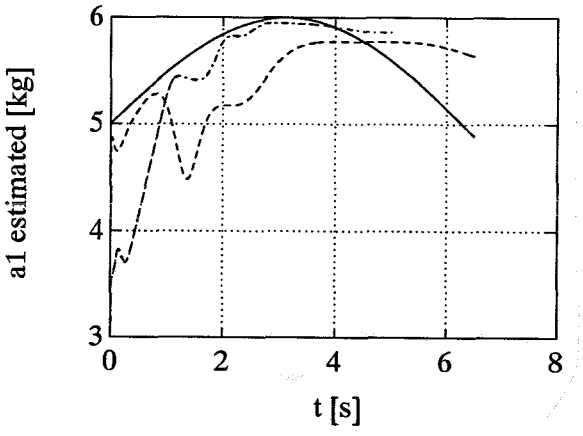

Figure 3.8: estimated parameter a_1
—— :real, ----:dir., -·-·:ind. and comp.

We see that in case of the direct adaptive controller the estimated parameter a_1 cannot track the time-varying real parameters. In case of the composite and indirect adaptive controller the estimated parameter a_1 tracks the time-varying parameter reasonably well. This counts also for the other two estimated parameters a_2 and a_3, which are given in appendix C. The tracking errors of all three controllers are in the time-varying case the same as in the case of equivalent models.

3.5 Conclusions

The main conclusion of this chapter is that the indirect and composite adaptive controller have better tracking performance than the direct adaptive controller, since the tracking errors in the indirect and composite controller are less oscillatory and have faster convergence. Furthermore, the indirect and composite controller are more robust against unmodelled dynamics than the direct controller and the adaptation gains in the composite and indirect controller can increased much higher than in the direct controller, without causing oscillations.

Chapter 4. Simulations with the XY-table

In paragraph 4.1 a description of the XY-table and the equations of motion will be given. The control parameters are determined with a method according to L.J.W. van Gerwen [3]. After given the desired trajectories, the results of the simulations will be shown.

4.1 The XY-table

In figure 4.1 a schematic representation of the XY-table is given. A model of the XY-table is shown in figure 4.2. Notice the difference between the definition of the positive y-direction in these figures.

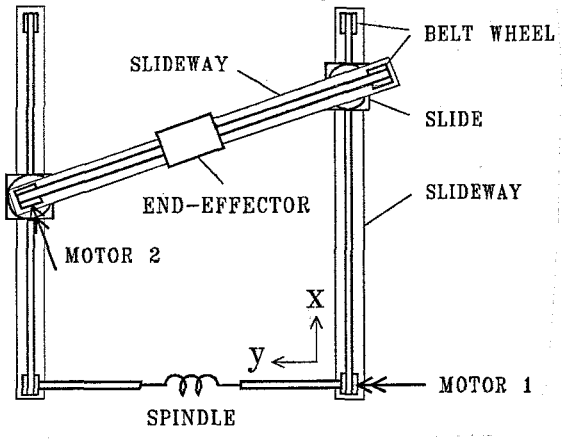

Figure 4.1: The XY-table

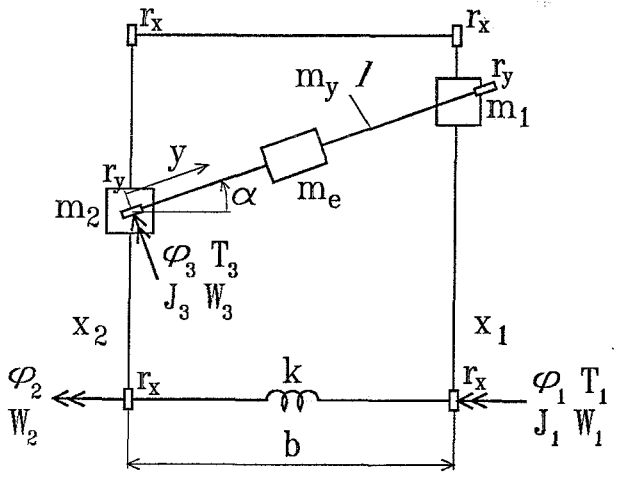

Figure 4.2: Diagram of the XY-table

φ_1	angular displacement of belt wheel 1
φ_2	angular displacement of belt wheel 2
φ_3	angular displacement of belt wheel 3
x_1	position of x-slide 1 on slideway 1
x_2	position of x-slide 2 on slideway 2
y	position of end-effector on y-slideway
b	distance between slideway 1 and 2
l	length of y-slideway
r_x	radius of belt wheels 1 and 2
r_y	radius of belt wheel 3
m_1	mass of x-slide 1
m_2	mass of x-slide 2
m_e	mass of end-effector
m_y	mass of y-slideway including y-motor
J_1	moment of inertia associated with φ_1
J_2	moment of inertia associated with φ_2 (assumed to be zero)

J_3	moment of inertia associated with φ_3
W_1	friction torque associated with φ_1
W_2	friction torque associated with φ_2
W_3	friction torque associated with φ_3
T_1	motor torque on belt wheel 1
T_3	motor torque on belt wheel 3
k	torsion spring constant

$x_1=\varphi_1 r_x$
$x_2=\varphi_2 r_x$
$y=\varphi_3 r_y$
$\alpha=\arctan((x_1-x_2)/b)$

The end-effector is a slide with mass m_e, which can move in the xy-plane by means of three slides, namely two slides in x-direction and one slide in y-direction. The belt wheels of the slideways in x-direction are connected with a torsion spring with stiffness k. However, this spring can be replaced by a rigid bar. If the torsion spring is connected between the belt wheels, there are three degrees of freedom, namely the rotations φ_1, φ_2 and φ_3. If the rigid bar is connected, there are two degrees of freedom, since the rotations φ_1 and φ_2 are equal. In this chapter the simulations are only executed with the rigid bar. So, in the simulations there are no unmodelled dynamics present. In the following chapter the XY-table with torsion spring will be used. The belt wheels of slideway 1 and 3 are driven by servomotors with couples T_1 and T_3. Coulomb friction is modelled for movements along the three slideways. This friction is represented by the torques W_1, W_2 and W_3. The two degrees of freedom model of the XY-table is used to simulate the real system and is also used in the controllers. The equations of motion of this model are derived by L.J.W. van Gerwen [3] and are given below:

$$\begin{bmatrix} J_1+(m_1+m_2+m_e+m_y)r_x^2 & 0 \\ 0 & J_3+m_e r_y^2 \end{bmatrix}\begin{bmatrix} \ddot{\varphi}_1 \\ \ddot{\varphi}_3 \end{bmatrix} + \begin{bmatrix} (W_1+W_2)\,\mathrm{sign}(\dot{\varphi}_1) \\ W_3\,\mathrm{sign}(\dot{\varphi}_3) \end{bmatrix} = \begin{bmatrix} T_1 \\ T_3 \end{bmatrix} \qquad (4.1)$$

Using the linear parametrization property:

$$\begin{bmatrix} \ddot{\varphi}_1 & 0 & \mathrm{sign}(\dot{\varphi}_1) & 0 \\ 0 & \ddot{\varphi}_3 & 0 & \mathrm{sign}(\dot{\varphi}_3) \end{bmatrix}\begin{bmatrix} a_1 \\ a_2 \\ a_3 \\ a_4 \end{bmatrix} = \begin{bmatrix} T_1 \\ T_3 \end{bmatrix} \qquad (4.2)$$

with: $a_1=J_1+(m_1+m_2+m_e+m_y)r_x^2$
$a_2=J_3+m_e r_y^2$
$a_3=W_1+W_2$
$a_4=W_3$

4.2 Control parameters and desired trajectory

The three adaptive controllers make use of a PD feedback $-K_D s$ (see equation (2.8)). This term can also be written as: $-K_D(\dot{\tilde{q}}+\Lambda\tilde{q}) = -K_D\dot{\tilde{q}}-K_D\Lambda\tilde{q} = -K_D\dot{\tilde{q}}-K_P\tilde{q}$. The gain matrices K_D and K_P can be written as a function of the eigenfrequencies and damping factors. To determine these matrices, the two degrees of freedom model of (4.2) without friction is used:

$$\ddot{\varphi}_1 a_1 = T_1 \tag{4.3}$$

$$\ddot{\varphi}_3 a_2 = T_3 \tag{4.4}$$

The PD-feedback of the motor rotations are:

$$T_1 = -K_{D1}(\dot{\varphi}_1-\dot{\varphi}_{1d})-K_{P1}(\varphi_1-\varphi_{1d}) \tag{4.5}$$

$$T_3 = -K_{D3}(\dot{\varphi}_3-\dot{\varphi}_{3d})-K_{P3}(\varphi_3-\varphi_{3d}) \tag{4.6}$$

Substitution of (4.5) in (4.3) and (4.6) in (4.4) leads to the following equations

$$\ddot{\varphi}_1+\frac{K_{D1}}{a_1}\dot{\varphi}_1+\frac{K_{P1}}{a_1}\varphi_1 = \frac{K_{D1}}{a_1}\dot{\varphi}_{1d}+\frac{K_{P1}}{a_1}\varphi_{1d} \tag{4.7}$$

$$\ddot{\varphi}_3+\frac{K_{D3}}{a_2}\dot{\varphi}_3+\frac{K_{P3}}{a_2}\varphi_3 = \frac{K_{D3}}{a_2}\dot{\varphi}_{3d}+\frac{K_{P3}}{a_2}\varphi_{3d} \tag{4.8}$$

This can be written as:

$$\ddot{\varphi}+2\beta\omega_0\dot{\varphi}+\omega_0^2\varphi = 2\beta\omega_0\dot{\varphi}_d+\omega_0^2\varphi_d \tag{4.9}$$

This results in:

$$K_P = \begin{bmatrix}\omega_0^2 a_1 & 0\\ 0 & \omega_0^2 a_2\end{bmatrix}, \qquad K_D = \begin{bmatrix}2\beta\omega_0 a_1 & 0\\ 0 & 2\beta\omega_0 a_2\end{bmatrix}$$

In the simulations the choice of the gain matrices is now replaced by a choice of the eigenfrequency ω_0 and the dampingfactor β.

The desired trajectory, that is used in the simulations, is chosen to be circle:

$$x_d = 0.5 - 0.25\cos(2\pi t) \qquad [m] \tag{4.10}$$

$$y_d = 0.5 + 0.25\sin(2\pi t) \qquad [m] \tag{4.11}$$

4.3 Results of the simulations with the XY-table

The simulations are executed for two different situations. The difference between these two situations are the values of the control parameters. In appendix D the controller designs are given. The data, which are used in the simulations, are given in appendix E.

4.3.1 Results of situation 1

The eigenfrequency and the damping are chosen as follows:

$$\omega_0=10 \text{ [rad/s]} \quad \text{and} \quad \beta=1 \text{ [-]}$$

For these values, the control parameters are:

$$K_D = \begin{bmatrix} 20*3.7*10^{-3} & 0 \\ 0 & 20*3.88*10^{-4} \end{bmatrix}, \qquad \Lambda = \begin{bmatrix} 5 & 0 \\ 0 & 5 \end{bmatrix}$$

In the direct adaptive controller now only the matrix Γ has to be chosen. We want to choose the matrix Γ as large as possible, since a large Γ means a fast convergence of the tracking errors. But a too large Γ means many oscillations in the parameter estimates and the tracking errors. If Γ is chosen too small, the convergence of the parameter estimates and the tracking errors is very slow. A suitable choice of Γ is difficult to find, because a small change in Γ causes a large change in the convergence rate of the tracking errors. A suitable choice of Γ is found by trial and error:

$$\Gamma = \begin{bmatrix} 7.5*10^{-7} & 0 & 0 & 0 \\ 0 & 7.5*10^{-8} & 0 & 0 \\ 0 & 0 & 1*10^{-1} & 0 \\ 0 & 0 & 0 & 5*10^{-2} \end{bmatrix}$$

For the indirect adaptive controller the same matrices K_D and Λ are chosen as in the direct controller. The other control parameters are found by trial and error:

$$\lambda_0 = 0.01, \quad \lambda_f = 10, \quad k_0 = 1, \quad k_1 = 1, \quad R(t) = I$$

$$P(t=0) = \begin{bmatrix} 2.5*10^{-4} & 0 & 0 & 0 \\ 0 & 7.5*10^{-5} & 0 & 0 \\ 0 & 0 & 6 & 0 \\ 0 & 0 & 0 & 22 \end{bmatrix}$$

For the composite adaptive controller the same control parameters are used as in the indirect controller, except for $P(t=0)$. A suitable choice of $P(t=0)$ is in the composite controller:

$$P(t=0) = \begin{bmatrix} 2.5*10^{-6} & 0 & 0 & 0 \\ 0 & 2.5*10^{-6} & 0 & 0 \\ 0 & 0 & 0.5 & 0 \\ 0 & 0 & 0 & 0.1 \end{bmatrix}$$

The matrix $P(t=0)$ in the indirect and composite controller has the same great influence on the convergence of the tracking errors as the matrix Γ in the direct controller. So a suitable choice of $P(t=0)$ is also difficult to find.

In the figures 4.3 and 4.4 the estimated parameters a_1 and a_2 of all three controllers are shown for the control parameters mentioned above. The estimated parameter a_1 is a moment of inertia in x-direction and a_2 a moment of inertia in y-direction. In the figures 4.5 and 4.6 the position tracking errors are given.

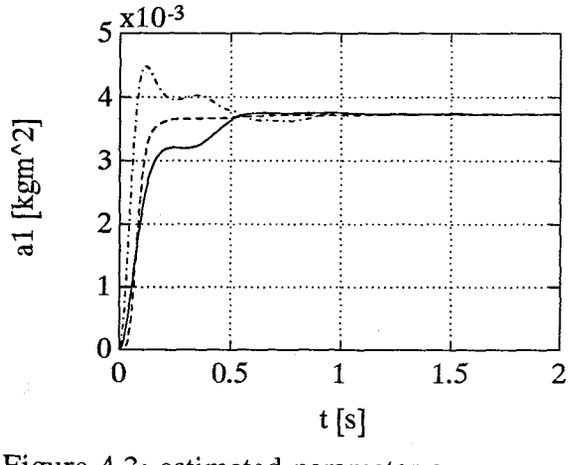

Figure 4.3: estimated parameter a_1
—— :direct, ----:indirect, -·-·:composite

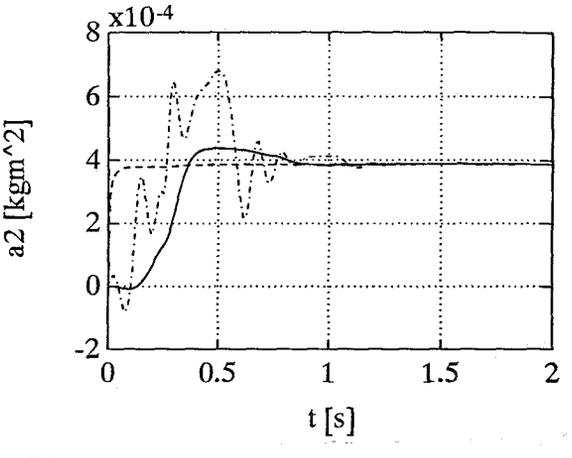

Figure 4.4: estimated parameter a_2
—— :direct, ----:indirect, -·-·:composite

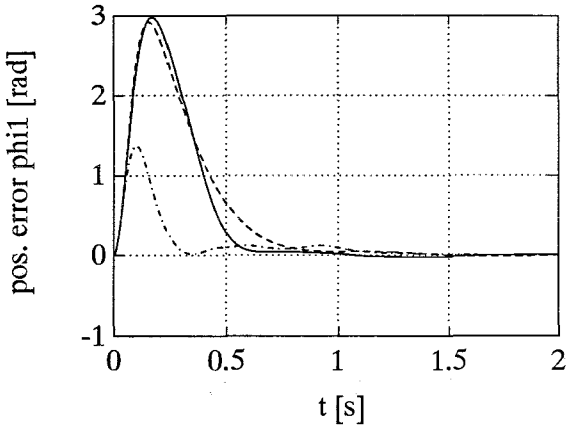

Figure 4.5: Pos. tr. error x-direction
—— :direct, ----:indirect, -·-·:composite

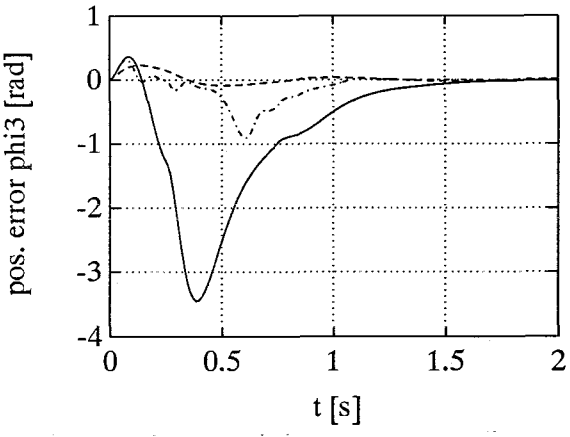

Figure 4.6: Pos. tr. error y-direction
—— :direct, ----:indirect, -·-·:composite

Looking at the figures 4.5 and 4.6 the conclusion can be made that the composite adaptive controller has the smallest position tracking error in x-direction. However, in y-direction the indirect adaptive controller has the smallest position tracking error. Furthermore, the position tracking error of the composite controller has in y-direction a more oscillatory behaviour than in x-direction. The direct adaptive controller has the largest tracking errors. The velocity tracking errors, which are given in appendix E, have the same phenomena.

From the figures 4.3 and 4.4 we can say that the parameter estimates in the indirect controller have the best performance. These conclusions can also be made for the estimated parameters a_3 and a_4, which are given in appendix E. The estimated parameters of the indirect controller are in the y-direction (a_2 and a_4) smoother than in the composite controller and this is the reason why the tracking errors in y-direction are also smoother than in the composite controller.

The performance of the composite controller is better in x-direction. However, the indirect controller has better performance in y-direction. This difference is caused by the choice of the control parameters λ_0 and k_0 and $P(t=0)$. With another choice of the control parameters the indirect controller can have a better performance in x-direction or the composite controller a better performance in y-direction.

4.3.2 Results of situation 2

The oscillatory behaviour of the composite adaptive controller in the y-direction can be remedied by another choice of the eigenfrequency ω_0 and the dampingfactor β:

$$\omega_0=50 \text{ [rad/s]} \quad \text{and} \quad \beta=5 \text{ [-]}$$

This results in:

$$K_D = \begin{bmatrix} 500*3.7*10^{-3} & 0 \\ 0 & 500*3.88*10^{-4} \end{bmatrix}, \qquad \Lambda = \begin{bmatrix} 5 & 0 \\ 0 & 5 \end{bmatrix}$$

In this case the PD-action $-K_D s$ has more influence in the control law than the feedforward action, so the estimated parameters have less influence in the controller. A suitable choice of the control parameters, that belongs to these values of K_D and Λ, is for the direct adaptive controller:

$$\Gamma = \begin{bmatrix} 2.5*10^{-5} & 0 & 0 & 0 \\ 0 & 2.5*10^{-6} & 0 & 0 \\ 0 & 0 & 5 & 0 \\ 0 & 0 & 0 & 2.5 \end{bmatrix}$$

A suitable choice of the control parameters for the indirect adaptive controller is the same as the control parameters of the indirect controller in paragraph 4.3.1. For the composite adaptive controller a suitable choice of $P(t=0)$ is:

$$P(t=0) = \begin{bmatrix} 5*10^{-5} & 0 & 0 & 0 \\ 0 & 5*10^{-5} & 0 & 0 \\ 0 & 0 & 5 & 0 \\ 0 & 0 & 0 & 5 \end{bmatrix}$$

The other control parameters are the same as in paragraph 4.3.1. The results of the simulations with these control parameters are shown in figure 4.7 to 4.8. The estimated parameter a_2 and the position tracking error in y-direction are given resp. in figure 4.7 and 4.8. The other estimated parameters and tracking errors are given in appendix E.

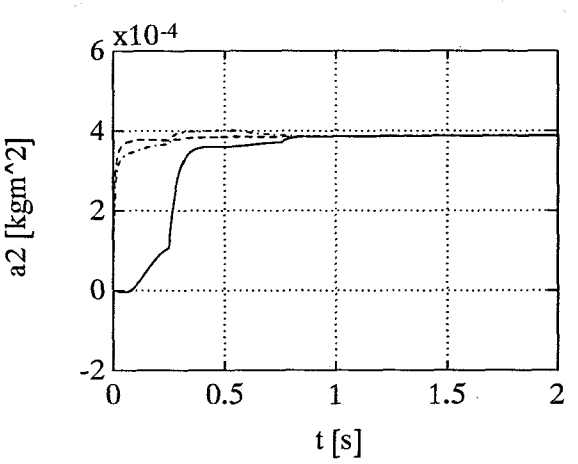

Figure 4.7: estimated parameter a_2
—— :direct, ----:indirect, -·-·:composite

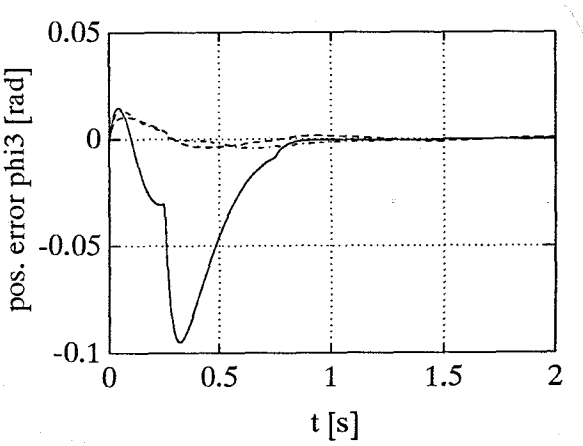

Figure 4.8: Pos. tr. error y-direction
—— :direct, ----:indirect, -·-·:composite

From these figures we see that now the position tracking error in y-direction of the composite adaptive controller is smooth. The velocity tracking error in y-direction and the parameter estimates in y-direction of the composite controller are now also smooth.

4.4 Conclusions

The performance of the controllers is strongly dependent on the choice of the control parameters. A small change in the control parameters causes a large change in the behaviour of the tracking errors. This counts for all controllers. So, the controllers are difficult to compare, but with a good choice of the control parameters the indirect and the composite controller have better performance than the direct controller.

Chapter 5. Implementation on the XY-table

In this chapter the application of the controllers to the experimental XY-table will be discussed. First, a description of the model is given. To compensate time delays and discretization effects an observer is designed. The results of some experiments with both the rigid and flexible system are given.

5.1 The XY-table

The XY-table has already been discussed in paragraph 4.1. The model of the XY-table, that is used to design the controllers, is almost the same as the model in chapter 4. Only, the torques and rotations are replaced by forces and translations. This leads to the following two degrees of freedom model of the XY-table, that is used in the controllers:

$$\begin{bmatrix} \ddot{x} & 0 & \text{sign}(\dot{x}) & 0 \\ 0 & \ddot{y} & 0 & \text{sign}(\dot{y}) \end{bmatrix} \begin{bmatrix} a_1 \\ a_2 \\ a_3 \\ a_4 \end{bmatrix} = \begin{bmatrix} F_1 \\ F_3 \end{bmatrix} \tag{5.1}$$

with parameter values:

a_1=40 [kg]
a_2=4 [kg]
a_3=50 [N]
a_4=15 [N]

These parameter values will not correspond to the exact parameter values, but better information was not available. The forces F_1 and F_3 in (5.1) are acting on the end-effector. The inputs to the servomotors, which have to be calculated by the controller, can be found as follows:

$$\begin{aligned} F_1 &= k_1.u_1 \\ F_3 &= k_2.u_2 \end{aligned} \tag{5.2}$$

where u_1 and u_2 are the commands to the x-axis and y-axis servomotors and k_1 and k_2 are the constant conversion factors, with k_1=0.12 and k_2=0.02. With these conversion factors the model of the XY-table becomes:

$$\begin{bmatrix} \ddot{x} & 0 & \text{sign}(\dot{x}) & 0 \\ 0 & \ddot{y} & 0 & \text{sign}(\dot{y}) \end{bmatrix} \begin{bmatrix} a_1/k_1 \\ a_2/k_2 \\ a_3/k_1 \\ a_4/k_2 \end{bmatrix} = \begin{bmatrix} u_1 \\ u_2 \end{bmatrix} \tag{5.3}$$

In the practical situation, the simple model of the XY-table is not exactly the same as the real system. First there is the possibility to use the flexible bar, but also other unmodelled dynamics are present, such as:

- Harmonic friction terms in x- and y-direction, caused by some bad bearings.
- Backlash in one of the bearings in x-direction. When the motor shaft starts moving in another direction, only one of the two x-slides moves.
- Extra flexibility caused by little springs used in the transmission between motor and slide.
- When the belts touch the sides of the belt wheels, the friction changes. This happens in x- and y-direction.
- Motors and amplifiers have their own dynamics, which are not modelled. They have been modelled as constant gains.
- The sampling frequency influences the error made by the observer.

As mentioned in L.J.W. van Gerwen [3], the gain matrices of the controllers cannot be chosen too large, due to these unmodelled dynamics. This will be discussed in appendix G.

5.2 The observer

The three adaptive controllers use in their control laws the rotations and the angular speeds of the servomotors. The servomotor rotations can be measured with incremental encoders. However, the angular speeds cannot directly be measured. An observer is used to determine the angular speeds. The observer determines the speed not only with the measured rotations but also with the knowledge of the dynamics. It estimates the position and speed one sample ahead using the measurements, the last estimated position and speed, the last inputs and the knowledge of the dynamics. The computer calculates the input with the estimated position and speed. The calculated input is applied at the point of time, at which position and speed have been estimated. The design of the observer is based on a continious Kalman observer and is shown in appendix F. In a Kalman observer

the covariance Q of the process noise and the covariance R of the measurement noise are needed to calculate the optimum gain matrix of the Kalman filter. Since the covariance Q of the process noise is not known, the optimum gain matrix is determined by placing the filterpoles at a desired position in the s-plane (see appendix F).

5.3 Results of the experiments with the XY-table

In chapter 3 and 4 a BGF estimator is used in the indirect and composite adaptive controller. In this chapter the BGF estimator is replaced by an exponential forgetting least squares estimator (EFLS estimator). This is done because in the BGF estimator $\lambda(t)$ is updated according to equation (2.21). In this equation the norm of P has to be calculated. For this calculation the eigenvalues of P are needed, but the programming language C^{++}, that is used for on-line control, cannot calculate eigenvalues. So, in the experiments we use the EFLS estimator, since this estimator has a constant λ. The EFLS estimator has the same theoretical convergence properties as the BGF estimator. The only difference is that in the EFLS estimator the gain matrix P can become large in the absence of p.e.

Another difference in this chapter is the determination of the prediction error e (equation (2.14)). Because in the simulations the "real" parameters a were known, the prediction error e could be determined with:

$$e = W(\hat{a} - a) \tag{5.4}$$

However in the experiments the real parameters are not known. Now, the prediction error e has to be determined with:

$$e = W\hat{a} - y \tag{5.5}$$

Note that y can be computed by filtering the measured torque τ through a first-order filter. In our case the measured torque τ consists of the measured currents to the x-axis and y-axis servomotors.

The desired trajectory is chosen to be a circle with a radius of R=0.25 [m]. Now only the angular speed ω has to be chosen. The experiments are executed for ω is 0.5π [rad/s]. The sample time t_s is chosen to be 0.005 [s] in all the experiments.

5.3.1 Experiments with the rigid XY-table

In appendix G the values of K_D and Λ are determined. In this appendix is found that the following values of K_D and Λ give the best results:

$$K_D = \begin{bmatrix} 6000 & 0 \\ 0 & 3600 \end{bmatrix}, \qquad \Lambda = \begin{bmatrix} 18 & 0 \\ 0 & 18 \end{bmatrix}$$

These values are used in the experiments for all three controllers.

For the direct adaptive controller now only the matrix Γ has to be chosen. This matrix is found by trial and error:

$$\Gamma = \begin{bmatrix} 10 & 0 & 0 & 0 \\ 0 & 100 & 0 & 0 \\ 0 & 0 & 25 & 0 \\ 0 & 0 & 0 & 750 \end{bmatrix}$$

For the indirect adaptive controller the following control parameters are chosen:

$$\lambda_f = 10, \qquad P(t=0) = I, \qquad \lambda = \begin{bmatrix} 0.5 & 0 & 0 & 0 \\ 0 & 0.5 & 0 & 0 \\ 0 & 0 & 1 & 0 \\ 0 & 0 & 0 & 5 \end{bmatrix}$$

The control parameters of the composite adaptive controller are the same as for the indirect controller. In the composite controller now only the matrix R has to be chosen. For R is the unity matrix chosen.

The experiments are executed for two different situations. In these situations the initial parameter estimates are different.

situation 1: $\hat{a}(t_0) = [40/0.12 \quad 4/0.02 \quad 50/0.12 \quad 15/0.02]^T$

situation 2: $\hat{a}(t_0) = \frac{1}{2}[40/0.12 \quad 4/0.02 \quad 50/0.12 \quad 15/0.02]^T$

In the figures 5.1, 5.2 and 5.3 the estimated parameter a_4 and the position tracking errors of situation 1 are shown. The other estimated parameters and the velocity tracking errors are given in appendix H.

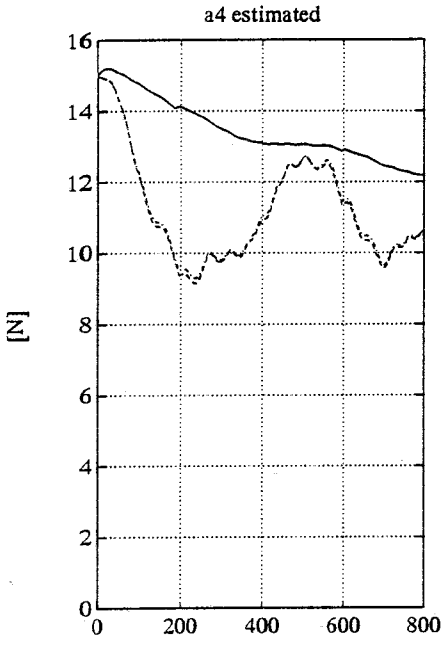

Figure 5.1: estimated a_4

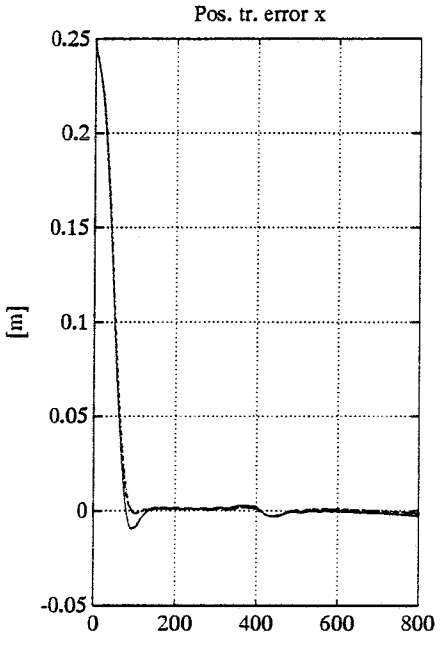

Figure 5.2: Pos. error x
—— :direct, ----:indirect, -·-·:composite

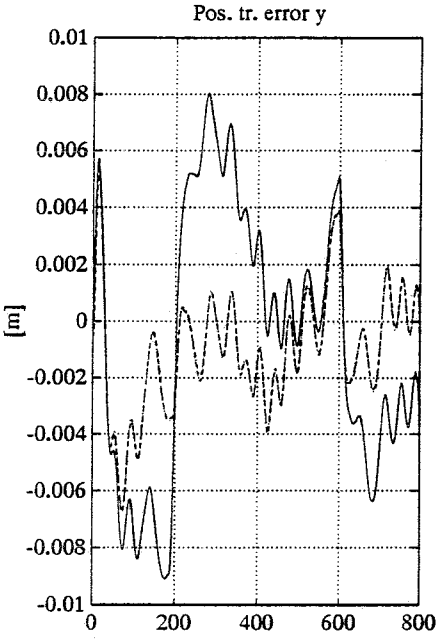

Figure 5.3: Pos. error y

From the figures of the parameter estimates can be concluded that the parameter estimates of the indirect controller are similar to the estimates of the composite controller. These estimates of the indirect and composite controller correspond better to the real system parameters than the estimates of the direct controller. For example, in the friction estimate in y-direction ($\hat{a}_4$) we see the harmonic term, which is mentioned in paragraph 5.1 as unmodelled dynamics. Furthermore, we see another (smaller) harmonic friction term with higher frequency on this larger harmonic term. This smaller harmonic term is caused by the fact that the shaft of the bearing is bent. Each revolution of the bearing shaft corresponds to one vibration.

From figure 5.2 and 5.3 we see that the position tracking errors of the direct controller are larger than the position tracking errors of the indirect and composite controller. We see that the tracking errors do not converge to zero. These remaining tracking errors are caused by unmodelled dynamics and measurement noise. Furthermore, in the direct controller the overshoot of the position tracking error in x-direction has a maximum of 1 cm. In the indirect and composite controller this overshoot is much smaller. The velocity tracking error in x-direction of the direct controller has also a larger overshoot.

The larger tracking errors of the direct controller are probably caused by the worse parameter estimates, since the parameter adaptation is the only difference with the indirect and composite controller. The control matrices K_D and Λ are in all three controllers the same.

In the figures 5.4, 5.5 and 5.6 the results of situation 2 are given. The estimated parameter a_4 is given in figure 5.4 and the position tracking errors are given in figure 5.5 and 5.6.

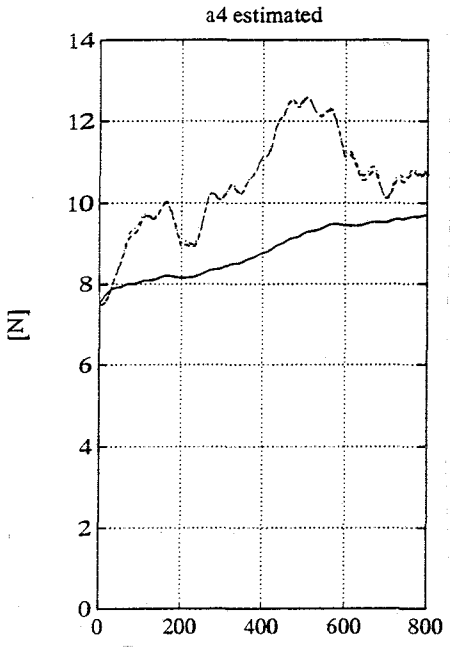

Figure 5.4: estimated a_4

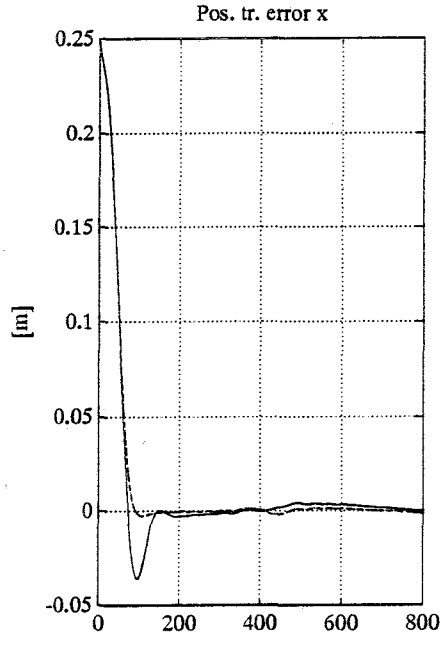

Figure 5.6: Pos. error x
—— :direct, ----:indirect, -·-·:composite

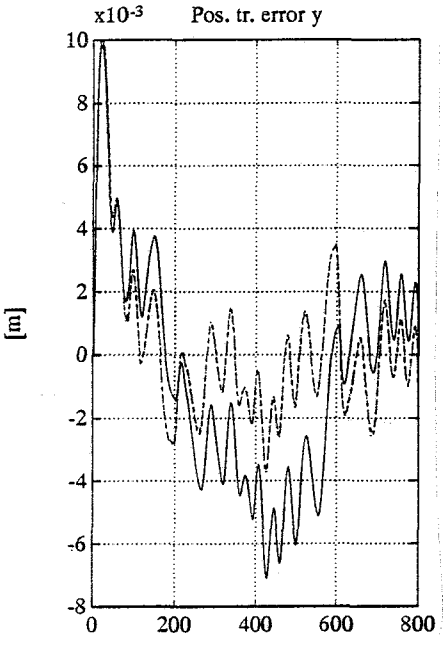

Figure 5.7: Pos. error y

In these experiments the initial parameter estimates are 50% of the initial estimates of situation 1. We see that the estimated parameter a_4 is almost similar with the estimated parameter a_4 of situation 1. Also the other estimated parameters are similar with situation 1 (see appendix H).

Furthermore, we see that again the position tracking errors of the direct controller are larger than those of the indirect and composite controller. The overshoot of the position tracking error in x-direction in the direct controller has become larger than in situation 1. In situation 1 this overshoot of the position tracking error x was 1 cm and has become 4 cm in situation 2. Also the overshoot of the velocity tracking error in x-direction has become significantly larger. The overshoot in the indirect and composite controller in situation 2 remains the same as in situation 1. So we can conclude that the indirect and composite controller are more robust than the direct controller if the initial parameter estimates have larger wrong values. This behaviour is also explained by the fact that the parameter estimates of the direct controller are worse than in situation 1.

In this paragraph we have only shown the parameter estimates and the tracking errors. In appendix H the desired and real trajectory and also the calculated and real inputs to the x-axis and y-axis servomotors are given for situation 1. Furthermore, in appendix H results are given of experiments, which are executed for $\omega=\pi$ [rad/s], instead of $\omega=0.5\pi$ [rad/s].

In appendix H, also a comparison is made between a non-adaptive CTC controller and the adaptive controllers. The main conclusion of this comparison is that, if the parameters are known a priori, the non-adaptive controller shows good results. If the parameters are unknown and we choose the unknown parameters reasonably well, the results of the non-adaptive controller are as good as the results of the direct adaptive controller. If we choose the parameters in the non-adaptive controller completely wrong (i.e. not corresponding with the real system parameters), the results of the non-adaptive controller are not good and can become unstable.

5.3.2 Experiments with the flexible XY-table

These experiments are executed with the same control parameters as in the case with the rigid XY-table. The results of the experiments with the flexible XY-table for situation 1 are shown in figure 5.7 and 5.8. In these figures, the estimated parameter a_4 and the position tracking error in x-direction are shown. The other estimated parameters and other tracking errors are given in appendix H.

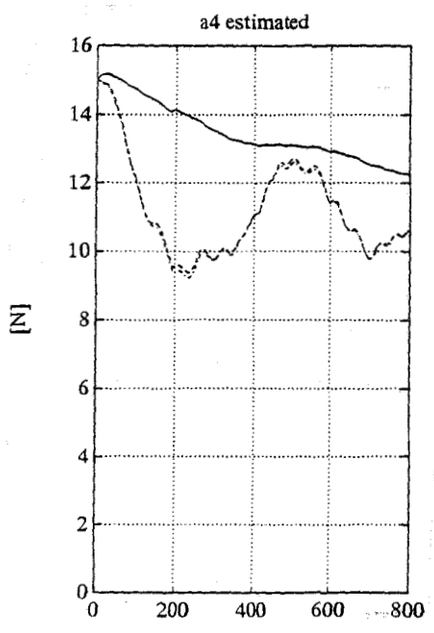

Figure 5.7: estimated a_4

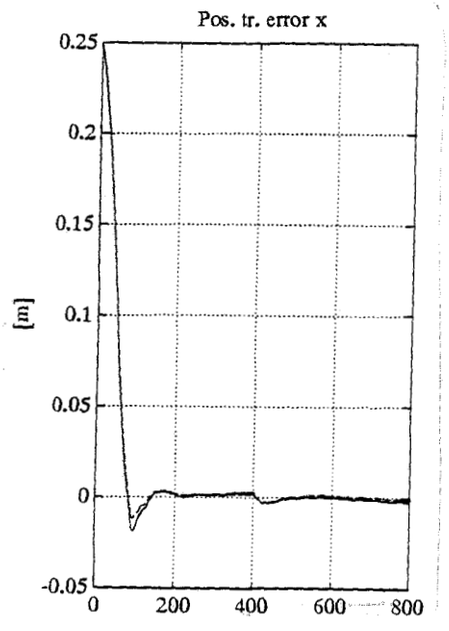

Figure 5.8: Pos. error x

—— :direct, ----:indirect, -·-·:composite

Looking at figure 5.7 we see that the estimated parameter a_4 is the same as for the rigid XY-table. The other estimated parameters are also the same as for the rigid XY-table. From figure 5.8 we see that for situation 1 the position tracking error in x-direction for the

flexible XY-table are larger than for the rigid XY-table. The tracking errors in y-direction for the flexible XY-table (see appendix H) are the same as for the rigid XY-table. Futhermore, we see that the behaviour of the tracking errors in x-direction has become more oscillatory. This oscillatory behaviour can be explained by the presence of the torsion spring between the belt wheels in x-direction.

The only disadvantage of the flexible system is the oscillatory behaviour of the tracking errors in x-direction. The minimum and maximum values of the tracking errors of the flexible and rigid XY-table do not differ much from each other. This can be explained by the fact that we have a desired trajectory φ_{1d} and φ_{3d} for the servomotors and that we measure the servomotor-positions φ_1 and φ_3. The difference between the desired and the measured position of the servomotors is the tracking error.

In case of the rigid XY-table the position of the end-effector is directly fixed by the servomotor-positions φ_1 and φ_3. So, the tracking errors of the servomotors are also the tracking errors of the end-effector in the rigid XY-table. However, in the case of the flexible XY-table the position of the end-effector is fixed by φ_1, φ_2 and φ_3. Due to the difference in φ_1 and φ_2 the y-slideway does not make an angle of 90° with the x-slideway as it does in the rigid XY-table. The fact that the y-slideway does not make an angle of 90° with the x-slideway is not accounted for in the desired trajectory φ_{1d} and φ_{3d} of the servomotors. So, the tracking errors of the end-effector are larger than the tracking errors of the servomotors.

Because we look at the tracking errors of the servomotors, there is no much difference between the tracking errors of the flexible and the rigid XY-table. If we should look at the tracking errors of the end-effector, the flexible XY-table would have larger tracking errors than the rigid XY-table. The purpose of manipulator control is to achieve accurate tracking for the end-effector. As explained above this is more difficult to achieve for the flexible XY-table.

5.4 Conclusions

The tracking accuracy of the indirect and composite controller is better than in case of the direct controller. This difference is probably caused by the different parameter estimates of the direct controller. The used adaptation laws are the only difference, since the control matrices K_D and Λ are the same in all three controllers.

Furthermore, the indirect and composite controller are more robust to less good initial parameter estimates than the direct controller. The conclusions made above are valid for both the rigid and flexible XY-table.

The parameter estimates do not converge to constant values, but there still remain some fluctuations. These fluctuations and the remaining tracking errors after parameter convergence are caused by the unmodelled dynamics and measurement noise. If a better model of the XY-table is used in the controllers, a better tracking accuracy will be achieved. Especially, the harmonic friction term due to bad bearings has a large influence on the tracking errors. A better tracking accuracy would be achieved by expanding the model, used for the controller designs, with the harmonic friction term.

Chapter 6. Conclusions and recommendations

- Theoretically it can be proven that the indirect and composite adaptive controller have faster parameter convergence and better tracking accuracy than the direct adaptive controller. These theoretical properties can be verified by simulations. Simulations have indeed shown that the tracking errors of the indirect and composite controller are less oscillatory and have faster convergence. Experiments with the XY-table show the same results.

- Simulations have shown that the indirect and composite controller are more robust against unmodelled dynamics than the direct controller. Furthermore, the adaptation gain in the indirect and composite controller can be increased much higher than in the direct controller and this in turn leads to better tracking accuracy. From the experiments can be concluded that the indirect and composite controller are more robust to less good initial parameter estimates than the direct controller.

- In the simulations the parameter estimates of the indirect and composite controller converge to the true values. In the situation with equivalent models the convergence of the parameter estimates in the direct controller is much slower than in the indirect and composite controller, but they converge to the true values. In the presence of unmodelled dynamics the parameter estimates of the direct controller do not converge at all to the true values.

- In the experiments there are always unmodelled dynamics present. The experiments show that the parameter estimates of the direct controller do not correspond to the real system parameters. The parameter estimates of the indirect and composite controller correspond much better to the real system parameters. The worse parameter estimation of the direct controller is probably the reason why the tracking errors of the direct controller are larger, since the parameter adaptation is the only difference between the controllers.

- In the situation with unmodelled dynamics the indirect and composite controller have better performance than the direct controller. However, in the simulations with the TR-robot the position tracking error of the rotation φ does not converge to zero, but increases instead. This counts for all three controllers. So, the conclusion can be made that all three controllers are not robust to unmodelled dynamics.

- The BGF estimator in the indirect and composite controller can reasonably track time-varying parameters. The direct adaptive controller cannot track time-varying parameters. In the experiments the EFLS estimator is used. This EFLS estimator can also track time-varying parameters.

- In the experiments with the XY-table the unmodelled dynamics and the measurement noise are the reason of the remaining tracking errors and the remaining fluctuations of the parameter estimates after convergence. Besides the torsion spring other unmodelled dynamics are present like flexible springs between belts

and belt wheels, backlash in one of the bearings, harmonic friction due to bad bearings, dynamics of motors and amplifier and contact between the belts and the sides of the belt wheels. Especially the harmonic friction has a large influence on the remaining tracking errors. It would be interesting to expand the model, used for the controllers, with this harmonic friction term.

- The optical measurement system, which measures the end-effector position, could not be used during this study. Therefore only the measurements of the motor positions were used. When the end-effector position measurements are available, it would be possible to compare the controllers again.

- For the indirect and composite controller simulations with the TR-robot give more promising results than simulations with the XY-table. The TR-robot is in contrast with the XY-table a system, which has centripetal- and Coriolis forces. In such a system the full capacities of the controllers can be compared. For example, experiments should be done with a TR-robot.

References

1. Slotine, J.J.E. and W. Li. Composite adaptive control of robot manipulators. Automatica, Vol. 25, No. 4, pp. 509-519, 1989.

2. Anderson, B.D.O. and C.R. Johnson. Exponential convergence of adaptive identification and control algorithms. Automatica, Vol. 18, No. 1, pp. 1-13, 1982.

3. Gerwen, L.J.W. van. An adaptive robot controller: Design, simulation and implementation. Report WFW 90.036, Department of Mechanical Engineering, Eindhoven University of technology, 1990.

4. Kok, J.J.. Werktuigkundig regelen 2. Lecture notes 4594, Dep. of Mechanical Engineering, Eindhoven University of Technology, 1985.

5. Hsu, P., S. Sastry, M. Bodson and B. Paden. Adaptive identification and control for manipulators without using joint accelerations. IEEE Int. Conf. on Robotics and Automation, Raleigh, North Carolina, 1987.

6. Li, W. and J.J.E. Slotine. Parameter estimation strategies for robot applications. A.S.M.E. Winter Annual Meeting, Boston, Massachusetts, 1987.

7. Li, W. and J.J.E. Slotine. Indirect adaptive robot control. IEEE Int. Conf. on Decision and Control, Austin, Texas, 1988.

8. Slotine, J.J.E. and W. Li. Adaptive robot control: a new perspective. IEEE Int. Conf. on Decision and Control, Los Angeles, California, 1987.

9. Craig, J.J.. Adaptive control of mechanical manipulators. Amsterdam: Addison-Wesley, 1988.

10. Goodwin, G.C. and K.S. Sin. Adaptive Filtering, Prediction and Control. Englewood Cliffs: Prentice Hall, 1984.

11. Narendra, K.S. and A.M. Annaswamy. Stable adaptive systems. Englewood Cliffs: Prentice Hall, 1989.

12. Sastry, S. and M. Bodson. Adaptive control: Stability, convergence and robustness. Englewood Cliffs: Prentice Hall, 1989.

13. Slotine, J.J.E. and W. Li. Applied nonlinear control. Englewood Cliffs: Prentice Hall, 1991.

Direct, Indirect and Composite Adaptive Control of Robot Manipulators

Appendices

F.J. Vijverstra
WFW report 92.076

Professor: Dr. Ir. J.J. Kok
Coach: Ir. I.M.M. Lammerts

July 1992

Eindhoven University of Technology
Department of Mechanical Engineering
Division of Mechanical Engineering Fundamentals

Appendix A: The tracking convergence of the controllers

In this appendix the proofs of the tracking convergence of the different controllers will be given.

A.1 The direct adaptive controller

Consider the Lyapunov function candidate

$$V(t) = \frac{1}{2}[s^T H s + \tilde{a}^T \Gamma^{-1} \tilde{a}] \tag{A.1}$$

Differentiating this function gives

$$\dot{V}(t) = s^T H \dot{s} + \frac{1}{2} s^T \dot{H} s + \dot{\tilde{a}}^T \Gamma^{-1} \tilde{a} \tag{A.2}$$

$$\dot{V}(t) = s^T (H\ddot{q} - H\ddot{q}_r) + \frac{1}{2} s^T \dot{H} s + \dot{\tilde{a}}^T \Gamma^{-1} \tilde{a} \tag{A.3}$$

$$\dot{V}(t) = s^T (\tau - C\dot{q} - G - H\ddot{q}_r) + \frac{1}{2} s^T \dot{H} s + \dot{\tilde{a}}^T \Gamma^{-1} \tilde{a} \tag{A.4}$$

$$\dot{V}(t) = s^T (\tau - C(s+\dot{q}_r) - G - H\ddot{q}_r) + \frac{1}{2} s^T \dot{H} s + \dot{\tilde{a}}^T \Gamma^{-1} \tilde{a} \tag{A.5}$$

Using the fact that $\dot{H}$-$2C$ is skew-symmetric, leads to

$$\dot{V}(t) = s^T (\tau - H\ddot{q}_r - C\dot{q}_r - G) + \dot{\tilde{a}}^T \Gamma^{-1} \tilde{a} \tag{A.6}$$

$$\dot{V}(t) = s^T (\tau - Ya) + \dot{\tilde{a}}^T \Gamma^{-1} \tilde{a} \tag{A.7}$$

The control law is chosen to be:

$$\tau = Y\hat{a} - K_D s \tag{A.8}$$

This gives:

$$\dot{V}(t) = s^T(Y\tilde{a}-K_D s) + \dot{\hat{a}}^T\Gamma^{-1}\tilde{a} \tag{A.9}$$

Updating the parameter estimates $\hat{a}$ according to

$$\dot{\hat{a}} = -\Gamma Y^T s \tag{A.10}$$

then yields

$$\dot{V}(t) = -s^T K_D s \leq 0 \tag{A.11}$$

Since $V \geq 0$ and $\dot{V} \leq 0$, we can say that V remains bounded. Given (A.1), this implies that both s and $\tilde{a}$ are bounded. This in turn implies that q, $\dot{q}$ and $\hat{a}$ are all bounded. The closed-loop dynamics are:

$$H\dot{s} + (C+K_D)s = Y\tilde{a} \tag{A.12}$$

This shows that $\dot{s}$ is also bounded (if H^{-1} exists and is bounded). Since s and $\dot{s}$ are bounded this means that $\ddot{V}=-2s^T K_D\dot{s}$ is bounded.

$$\ddot{V} \text{ bounded} \Rightarrow \dot{V} \rightarrow 0$$

Given (A.11) we see that $s \rightarrow 0$ as $t \rightarrow \infty$:

$$\ddot{V} \text{ bounded} \Rightarrow \dot{V} \rightarrow 0 \Rightarrow s \rightarrow 0$$

Given the definition of s, we have proven that $\tilde{q}$ and $\dot{\tilde{q}}$ tend to zero as t tends to infinity.

A.2 The indirect adaptive controller

Li and Slotine [7] state that the tracking convergence of the indirect controller which I used cannot be proven. They say that only their indirect controller has a complete proof of the global tracking convergence. But in the following I will give a complete proof of the global tracking convergence of my indirect controller. Let us consider:

$$\tau = \hat{H}\ddot{q}_r + \hat{C}\dot{q}_r + \hat{G} - K_D s \tag{A.13}$$

$$\tau = \hat{H}(\ddot{q}_d-\lambda\dot{\tilde{q}}) + \hat{C}(\dot{q}-s) + \hat{G} - K_D s \tag{A.14}$$

$$\tau = \hat{H}(\ddot{q}-\ddot{\tilde{q}}-\lambda\dot{\tilde{q}}) + \hat{C}(\dot{q}-s) + \hat{G} - K_D s \tag{A.15}$$

This substituting in (2.1):

$$\hat{H}(\ddot{q}-\ddot{\tilde{q}}-\lambda\dot{\tilde{q}}) + \hat{C}(\dot{q}-s) + \hat{G} - K_D s = H\ddot{q} + C\dot{q} + G \tag{A.16}$$

Rearranging terms gives:

$$\hat{H}(\ddot{\tilde{q}}+\lambda\dot{\tilde{q}}) + \hat{C}s + K_D s = \tilde{H}\ddot{q} + \tilde{C}\dot{q} + \tilde{G} = Y\tilde{a} \tag{A.17}$$

$$\hat{H}\dot{s} + (\hat{C}+K_D)s = Y\tilde{a} \tag{A.18}$$

Take

$$\hat{C}+K_D = \lambda\hat{H} \tag{A.19}$$

Then

$$\hat{H}\dot{s} + \lambda\hat{H}s = Y\tilde{a} \tag{A.20}$$

With p the Laplace operator:

$$\hat{H}\,(p+\lambda)s = Y\tilde{a} \tag{A.21}$$

Using a first-order filter for generating the matrix W gives:

$$\hat{H}\,\frac{\lambda_f(p+\lambda)}{p+\lambda_f}s = W\tilde{a} = e \tag{A.22}$$

$$\hat{H}s = \frac{p+\lambda_f}{p+\lambda}e/\lambda_f \tag{A.23}$$

$$\hat{H}s = \left(\frac{(p+\lambda)e-(\lambda-\lambda_f)e}{p+\lambda}\right)/\lambda_f \tag{A.24}$$

So

$$s = \hat{H}^{-1}(e-v)/\lambda_f \tag{A.25}$$

with

$$v = \frac{(\lambda-\lambda_f)}{p+\lambda}e \tag{A.26}$$

To proof the convergence, we first state a lemma

Lemma 1: Consider the filter relation $y=L(p)u$, with y being the output, u the input and $L(p)$ an exponentially stable and strictly proper transfer function. 1: If $u \in L^2$, then $y \in L^2$, $y \in L_\infty$ and $y(t) \to 0$ as $t \to \infty$. 2: If u is exponentially convergent to zero, so is y.

The performances of the estimators are different from each other, but they have a common theoretical property. This property is that the prediction-error e is square-integrable, which mathematically means that $e \in L^2$. Using the first part of lemma 1, we see that $v(t) \in L^2$ and v converges (see formula (A.26)). If we multiply a square-integrable function by an upper bounded function, the result of this multiplication retains the square-integrable property. Since e and v are both square-integrable, we can say from

$$\dot{\tilde{q}} + \Lambda\tilde{q} = \hat{H}^{-1}(e-v)/\lambda_f \tag{A.27}$$

that $\tilde{q}$ must be square-integrable and asymptotically convergent to zero. Since $\dot{\tilde{q}}$ is square-integrable from (A.27) and $\ddot{q}$ is bounded if q_d, $\dot{q}_d$ and $\ddot{q}_d$ are bounded (see Hsu, Bodson, Sastry and Paden), we can conclude that $\dot{\tilde{q}}$ is also convergent to zero. In summary,

Theorem 1: The indirect adaptive controller guarantees the convergence of the prediction error e, position tracking error $\tilde{q}$ and velocity tracking error $\dot{\tilde{q}}$ if the desired trajectories q_d, $\dot{q}_d$ and $\ddot{q}_d$ are bounded.

Now we say something about the exponential convergence of the tracking errors and the estimated parameters:

Theorem 2: If $Y(q_d,\dot{q}_d,\ddot{q}_d)$ is p.e. and uniformly continuous, or $W(q_d,\dot{q}_d)$ is p.e., the tracking errors, parameter errors and prediction errors in the indirect adaptive controller based on the BGF estimator will exponentially converge to zero.

This can be proven with two lemmas:

Lemma 2: If $W(q_d,\dot{q}_d)$ is p.e., and $q \to q_d$, $\dot{q} \to \dot{q}_d$ as $t \to \infty$, then $W(q,\dot{q})$ is also p.e.

Lemma 3: If the input matrix of an exponentially stable and strictly proper filter is p.e. and u.c., then the output matrix is also p.e. and u.c.

Proof: From lemmas 2 and 3, the p.e. and u.c. of Y_d guarantees the p.e. of $W(q,\dot{q})$, which implies the exponential convergence of the estimated parameters as said in chapter 2. The exponential convergence of the parameter error implies the exponential convergence of the prediction error e. This in turn leads to the exponential convergence of s, $\tilde{q}$ and $\dot{\tilde{q}}$ from (A.27) and lemma 1.

A.3 The composite adaptive controller with BGF estimator

Consider the Lyapunov function candidate

$$V(t) = \frac{1}{2}[s^T H s + \tilde{a}^T P^{-1} \tilde{a}] \tag{A.28}$$

Differentiating this function

$$\dot{V}(t) = s^T H \dot{s} + \frac{1}{2} s^T \dot{H} s + \frac{1}{2} \tilde{a}^T \dot{P}^{-1} \tilde{a} + \dot{\tilde{a}}^T P^{-1} \tilde{a} \tag{A.29}$$

With

$$\dot{\hat{a}} = -P[Y^T s + W^T e] \tag{A.30}$$

this leads to

$$\dot{V}(t) = s^T H \dot{s} + \frac{1}{2} s^T \dot{H} s + \frac{1}{2} \tilde{a}^T \dot{P}^{-1} \tilde{a} - s^T Y \tilde{a} - e^T W \tilde{a} \tag{A.31}$$

$$\dot{V}(t) = -s^T K_D s + \frac{1}{2} \tilde{a}^T \dot{P}^{-1} \tilde{a} - e^T W \tilde{a} \tag{A.32}$$

For the BGF estimator we get

$$\dot{P}^{-1} = -\lambda(t) P^{-1} + W^T W \tag{A.33}$$

This yields

$$\dot{V}(t) = -s^T K_D s - \frac{1}{2} \lambda(t) \tilde{a}^T P^{-1} \tilde{a} + \frac{1}{2} \tilde{a}^T W^T W \tilde{a} - e^T W \tilde{a} \tag{A.34}$$

$$\dot{V}(t) = -s^T K_D s - \frac{1}{2}\lambda(t)\tilde{a}^T P^{-1}\tilde{a} - \frac{1}{2}\tilde{a}^T W^T W\tilde{a} \leq 0 \tag{A.35}$$

$$\dot{V}(t) = -s^T K_D s - \frac{1}{2}\lambda(t)\tilde{a}^T P^{-1}\tilde{a} - \frac{1}{2}e^T e \leq 0 \tag{A.36}$$

The convergence of s and e can be shown in the same way as in the direct adaptive controller. Note also that $\lambda(t)\tilde{a}^T P^{-1}\tilde{a}$ converges to zero. Now we will proof the exponential convergence of s and $\tilde{a}$:

The BGF estimator has the following properties

$$P(t) \leq k_0 I \tag{A.37}$$

and if W_d, and thus W, is p.e. then

$$\lambda(t) \geq \lambda_1 > 0 \tag{A.38}$$

With (A.37) and (A.38)

$$\lambda(t)\tilde{a}^T P^{-1}\tilde{a} \geq \lambda_1 \tilde{a}^T\tilde{a}/k_0 \tag{A.39}$$

Therefore the convergence of $\lambda(t)\tilde{a}^T P^{-1}\tilde{a}$ to zero implies that of $\tilde{a}$. If we take $K_D=\lambda_1 H/2$ we get

$$\dot{V}(t) \leq -\frac{1}{2}\lambda_1 s^T H s - \frac{1}{2}\lambda_1\tilde{a}^T P^{-1}\tilde{a} - \frac{1}{2}e^T e \tag{A.40}$$

With (A.28) this leads to

$$\dot{V}(t) \leq -\lambda_1 V(t) - \frac{1}{2}e^T e \tag{A.41}$$

$$\dot{V}(t) + \lambda_1 V(t) \leq 0 \tag{A.42}$$

Therefore, $V(t) \leq V(0)e^{-\lambda_1 t}$. This implies the exponential convergence of s and $\tilde{a}$.

Appendix B: Controller design for the TR-robot

Control law

All three controllers: $\tau = Y(q,\dot{q},\dot{q}_r,\ddot{q}_r)\hat{a} - K_D s$

Adaptation law

Direct controller: $\dot{\hat{a}} = -\Gamma Y^T(q,\dot{q},\dot{q}_r,\ddot{q}_r)s$

Indirect controller: $\dot{\hat{a}} = -PW^T(q,\dot{q})e$

Composite controller: $\dot{\hat{a}} = -P[Y^T s + W^T R(t)e]$

BGF estimator:

$$\dot{P} = \lambda(t)P - PW^T WP$$
$$\lambda(t) = \lambda_0(1 - \frac{\|P\|}{k_0})$$

This yields for the TR-robot:

$$\tau = \begin{bmatrix} F \\ M \end{bmatrix}, \quad q = \begin{bmatrix} x \\ \varphi \end{bmatrix}, \quad a = \begin{bmatrix} m_1+m_2+m_3 \\ m_2+m_3/2 \\ m_2+m_3/3 \end{bmatrix}, \quad s = \begin{bmatrix} \dot{x}-\dot{x}_r \\ \dot{\varphi}-\dot{\varphi}_r \end{bmatrix}, \quad e = W(\hat{a}-a)$$

$$Y(q_r,\dot{q}_r,\dot{q}_r,\ddot{q}_r) = \begin{bmatrix} \ddot{x}_r & -l\sin(\varphi)\ddot{\varphi}_r - l\cos(\varphi)\dot{\varphi}\dot{\varphi}_r & 0 \\ 0 & -l\sin(\varphi)\ddot{x}_r & l^2\ddot{\varphi}_r \end{bmatrix} \tag{B.1}$$

with

$$\dot{x}_r = \dot{x}_d - \Lambda_{11}(x - x_d)$$

$$\dot{\varphi}_r = \dot{\varphi}_d - \Lambda_{22}(\varphi - \varphi_d)$$

$$\ddot{x}_r = \ddot{x}_d - \Lambda_{11}(\dot{x} - \dot{x}_d)$$

$$\ddot{\varphi}_r = \ddot{\varphi}_d - \Lambda_{22}(\dot{\varphi} - \dot{\varphi}_d)$$

The matrix $W(q,\dot{q})$ is generated by filtering the matrix $Y_1(q,\dot{q},\ddot{q})$ through a first-order filter:

$$W(q,\dot{q}) = \frac{\lambda_f}{p+\lambda_f}\begin{bmatrix} \ddot{x} & -l\sin(\varphi)\ddot{\varphi} - l\cos(\varphi)\dot{\varphi}^2 & 0 \\ 0 & -l\sin(\varphi)\ddot{x} & l^2\ddot{\varphi} \end{bmatrix} \tag{B.2}$$

Rearranging term by term:

W(1,1):

$$\ddot{x} = (p+\lambda_f)\dot{x} - \lambda_f\dot{x} \tag{B.3}$$

$$\frac{\lambda_f}{p+\lambda_f}\ddot{x} = \lambda_f\dot{x} - \lambda_f^2\frac{\dot{x}}{p+\lambda_f} \tag{B.4}$$

$$W(1,1) = \lambda_f\dot{x} - \lambda_f^2\dot{x}_f \tag{B.5}$$

with $\dot{x}_f = \dfrac{\dot{x}}{p+\lambda_f}$

W(1,2):

$$-l\sin(\varphi)\ddot{\varphi} = -(p+\lambda_f)l\sin(\varphi)\dot{\varphi} + \lambda_f l\sin(\varphi)\dot{\varphi} + l\cos(\varphi)\dot{\varphi}^2 \tag{B.6}$$

$$\frac{\lambda_f}{p+\lambda_f}(-l\sin(\varphi)\ddot{\varphi}) = -\lambda_f l\sin(\varphi)\dot{\varphi} + \lambda_f^2\frac{1}{p+\lambda_f}(l\sin(\varphi)\dot{\varphi}) + \frac{\lambda_f}{p+\lambda_f}(l\cos(\varphi)\dot{\varphi}^2) \tag{B.7}$$

$$W(1,2) = \frac{\lambda_f}{p+\lambda_f}(-l\sin(\varphi)\ddot{\varphi} - l\cos(\varphi)\dot{\varphi}^2) \tag{B.8}$$

Equation (B.7) and (B.8) give

$$W(1,2) = -\lambda_f l\sin(\varphi)\dot{\varphi} + \lambda_f^2 \frac{1}{p+\lambda_f}(l\sin(\varphi)\dot{\varphi}) \tag{B.9}$$

$$W(1,2) = -\lambda_f l\sin(\varphi)\dot{\varphi} + \lambda_f^2 h \tag{B.10}$$

with $h = \frac{1}{p+\lambda_f}(l\sin(\varphi)\dot{\varphi})$

W(2,2):

$$-l\sin(\varphi)\ddot{x} = -(p+\lambda_f)l\sin(\varphi)\dot{x} + \lambda_f l\sin(\varphi)\dot{x} + l\cos(\varphi)\dot{\varphi}\dot{x} \tag{B.11}$$

$$\frac{\lambda_f}{p+\lambda_f}(-l\sin(\varphi)\ddot{x}) = -\lambda_f l\sin(\varphi)\dot{x} + \frac{\lambda_f^2}{p+\lambda_f}(l\sin(\varphi)\dot{x}) + \frac{\lambda_f}{p+\lambda_f}(l\cos(\varphi)\dot{\varphi}\dot{x}) \tag{B.12}$$

$$W(2,2) = -\lambda_f l\sin(\varphi)\dot{x} + g \tag{B.13}$$

with $g = \frac{\lambda_f}{p+\lambda_f}(\lambda_f l\sin(\varphi)\dot{x} + l\cos(\varphi)\dot{\varphi}\dot{x})$

W(2,3):

$$l^2\ddot{\varphi} = (p+\lambda_f)l^2\dot{\varphi} - \lambda_f l^2\dot{\varphi} \tag{B.14}$$

$$\frac{\lambda_f}{p+\lambda_f} l^2\ddot{\varphi} = \lambda_f l^2\dot{\varphi} - \lambda_f^2 \frac{1}{p+\lambda_f}\dot{\varphi} \tag{B.15}$$

$$W(2,3) = \lambda_f l^2\dot{\varphi} - \lambda_f^2\dot{\varphi}_f \tag{B.16}$$

with $\dot{\varphi}_f = \frac{\dot{\varphi}}{p+\lambda_f}$

Result:

$$W(q,\dot{q}) = \begin{bmatrix} \lambda_f\dot{x}-\lambda_f^2\dot{x}_f & -\lambda_f l\sin(\varphi)\dot{\varphi}+\lambda_f^2 h & 0 \\ 0 & -\lambda_f l\sin(\varphi)\dot{x}+g & \lambda_f l^2\dot{\varphi}-\lambda_f^2\dot{\varphi}_f \end{bmatrix} \qquad \text{(B.17)}$$

Appendix C: Results of simulations with the TR-robot

C.1 Data

The simulations are executed with the following data:

Manipulator parameters:

m_1	the mass of the carriage	m_1=2 [kg]
m_2	the mass of the payload	m_2=2 [kg]
m_3	the mass of the inverted pendulum	m_3=1 [kg]
l	the length of the inverted pendulum	l=0.75 [m]

The payload is desired to rotate in a circle, which centre is situated at a vertical distance of 0.375 [m] to the ground.

r	the radius of this circle	r=0.3 [m]
ω	the rotation velocity of the payload	ω=1 [rad/s]
θ	the rotation angle of the payload with regard to the horizontal axis through the centre of the circle	$\theta(t_0)$=0 [rad]
x_m	the horizontal distance of the centre of the circle to the origin	x_m=0 [m]
y_m	the vertical distance of the centre of the circle to the origin	y_m=0.375 [m]

Manipulator state variables:

x	translation position of the carriage
φ	rotation angle of the inverted pendulum
$\dot{x}$	translation velocity of the carriage
$\dot{\varphi}$	rotation velocity of the inverted pendulum

The initial system state conditions:

	$x(t_0)$ [m]	$\varphi(t_0)$ [rad]	$\dot{x}(t_0)$ [m/s]	$\dot{\varphi}(t_0)$ [rad/s]
initial system state variables	r-l*0.5*$\sqrt{3}$	$\pi/6$	0	0
ideal initial state variables	r-l*0.5*$\sqrt{3}$	$\pi/6$	1.7321	4.6188

The system input signals:

F=u(1)	the actuator force acting upon the carriage	[N]
M=u(2)	the actuator torque acting upon the pendulum	[Nm]

The actuators were assumed to have no dynamics and no power limitations.

The initial mass parameters:

$a_1(t_0)=3$ [kg] $a_2(t_0)=2$ [kg] $a_3(t_0)=2$ [kg]

The real mass parameters are:

$a_1=5$ [kg] $a_2=2.5$ [kg] $a_3=2.33$ [kg]

C.2 Results with equivalent models

The direct adaptive controller:

The simulations are done for different values of control parameters:

1. $\Gamma=100I$, $K_D=100I$ and $\Lambda=10I$:

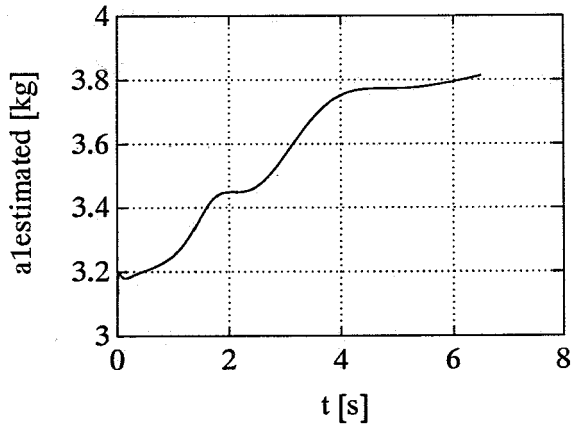

Figure C.1: a1 estimated

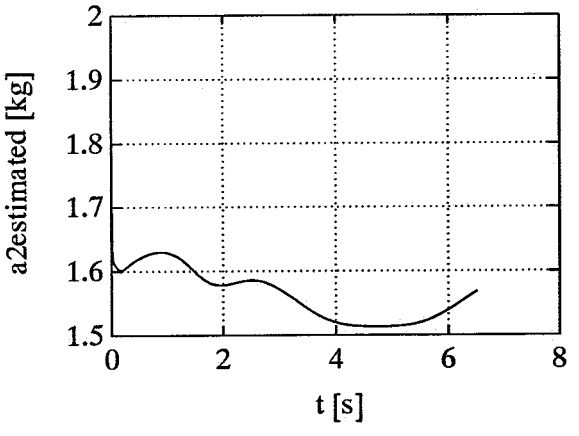

Figure C.2: a2 estimated

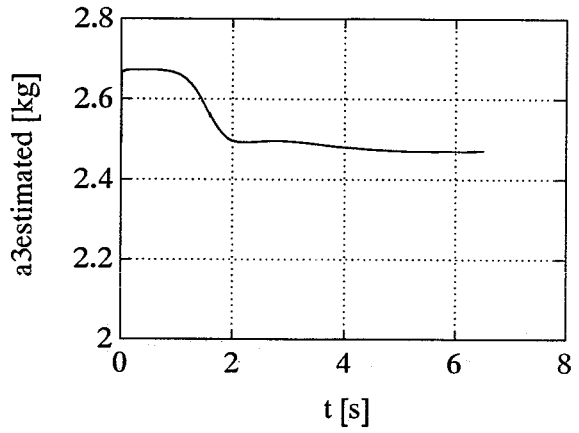

Figure C.3: a3 estimated

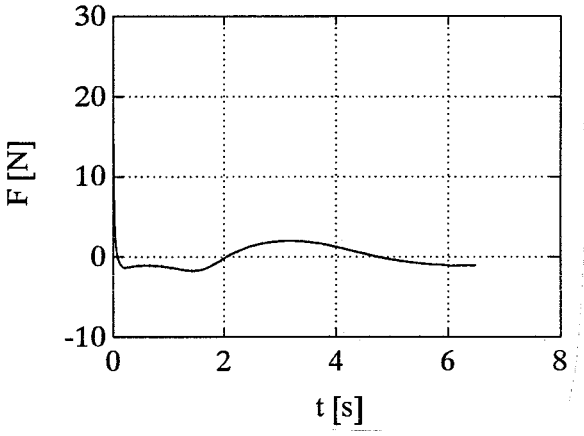

Figure C.4: Input force F

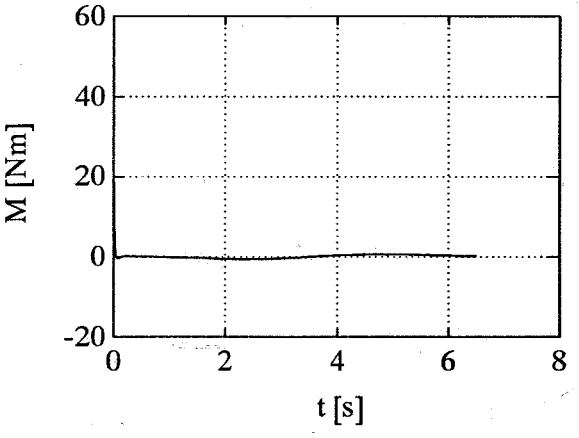

Figure C.5: Input torque M

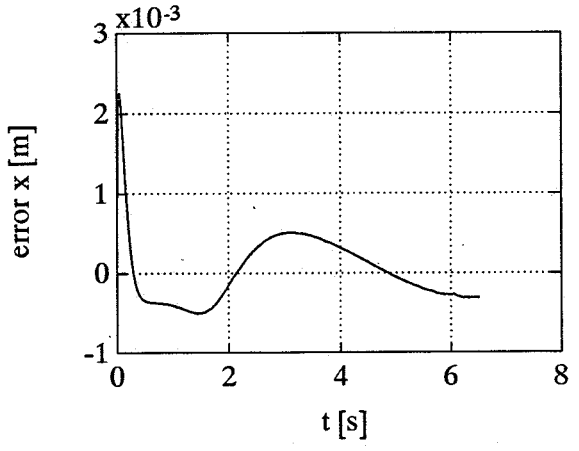

Figure C.6: Position error x

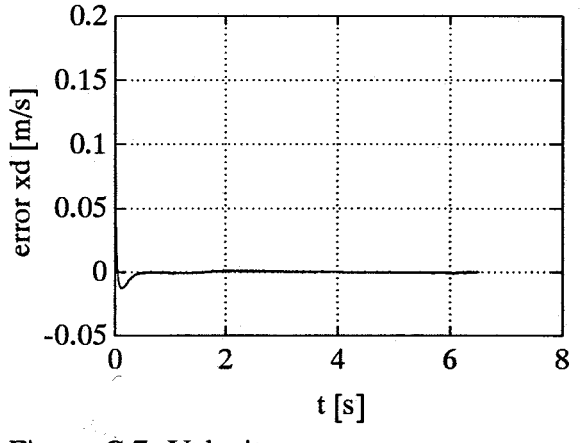

Figure C.7: Velocity error x

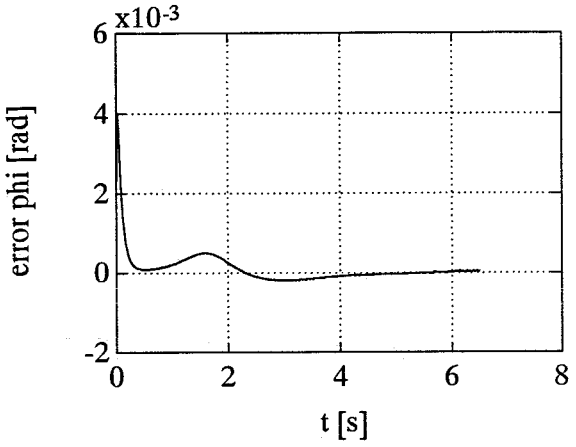

Figure C.8: Position error phi

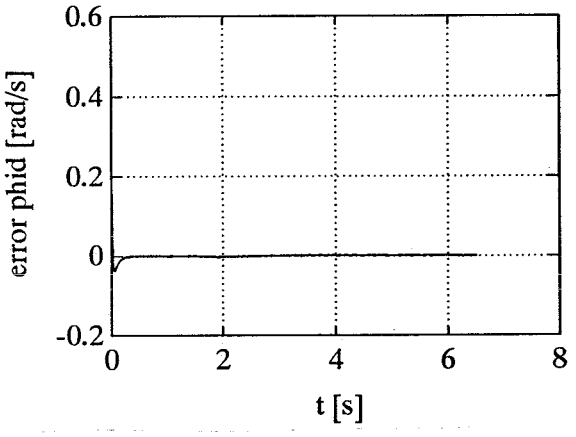

Figure C.9: Velocity error phi

2. Γ=1000*I*, K_D=100*I* and Λ=10*I*

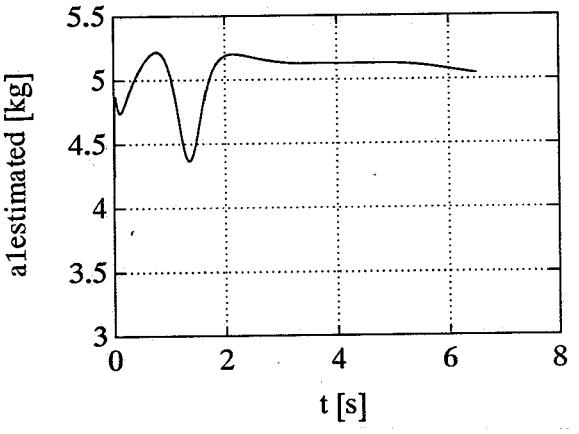

Figure C.10: a1 estimated

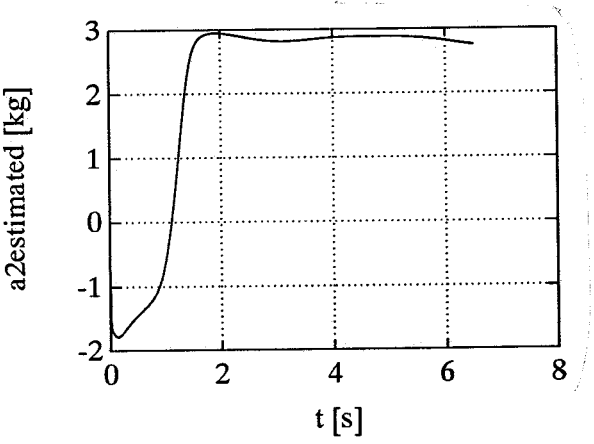

Figure C.11: a2 estimated

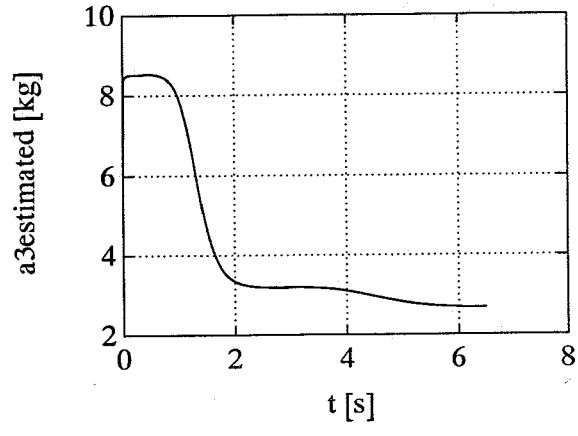

Figure C.12: a3 estimated

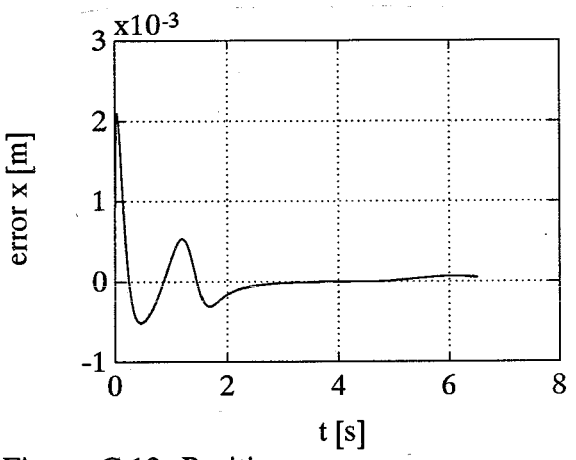

Figure C.13: Position error x

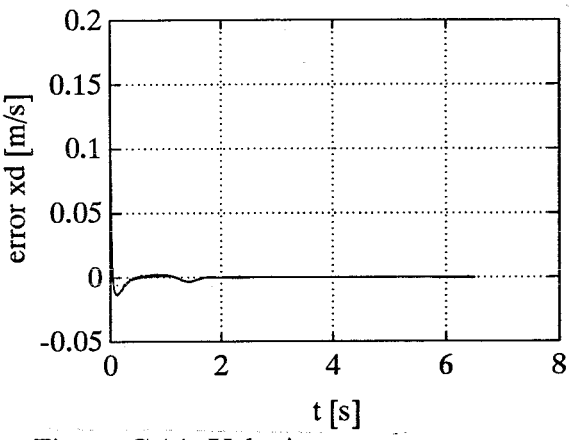

Figure C.14: Velocity error x

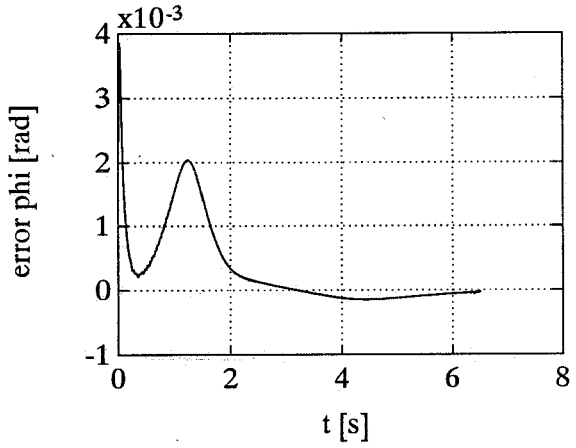

Figure C.15: Position error phi

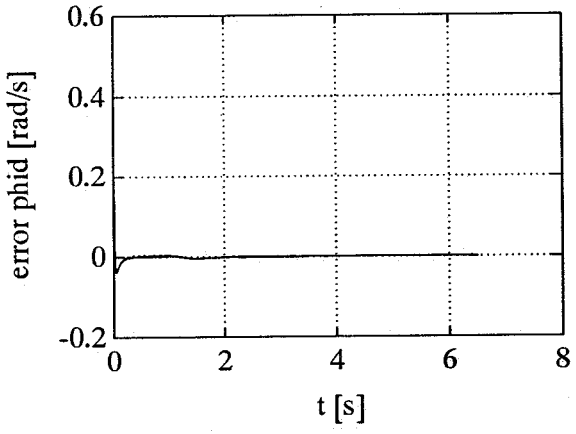

Figure C.16: Velocity error phi

3. Γ=3000I, K_D=100I and Λ=10I

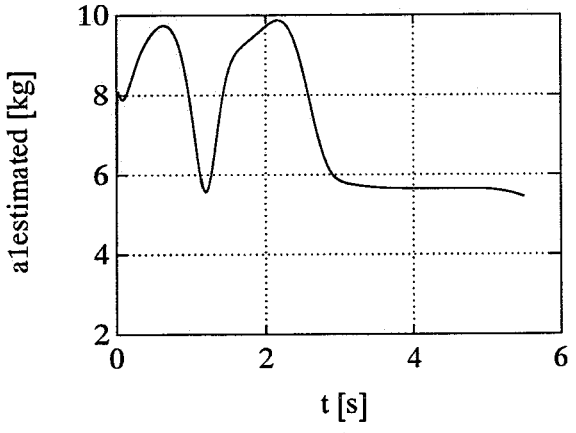

Figure C.17: a1 estimated

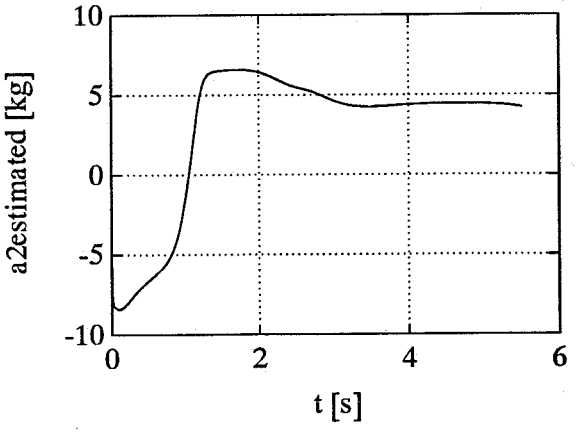

Figure C.18: a2 estimated

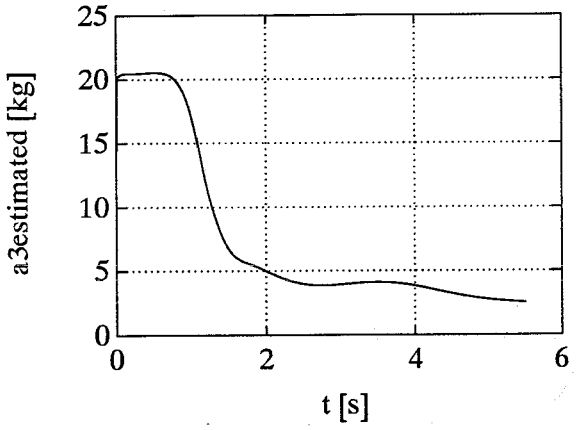

Figure C.19: a3 estimated

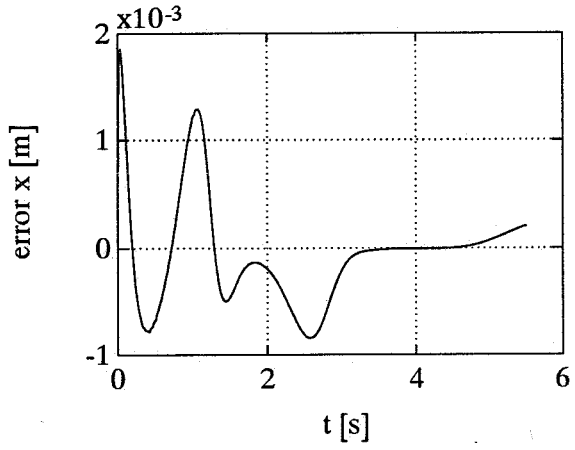

Figure C.20: Position error x

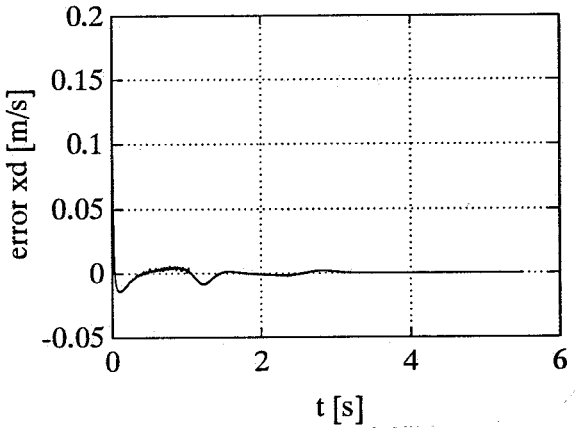

Figure C.21: Velocity error x

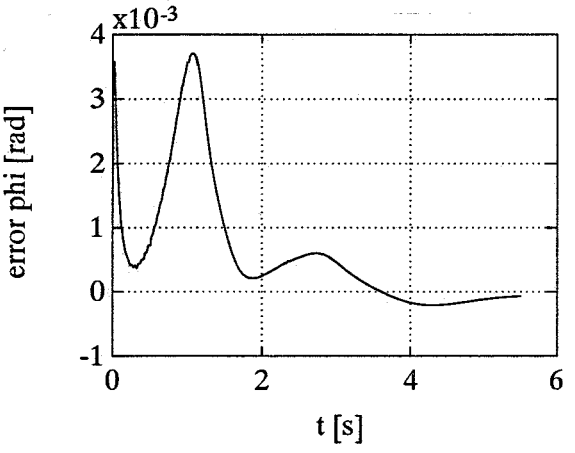

Figure C.22: Position error phi

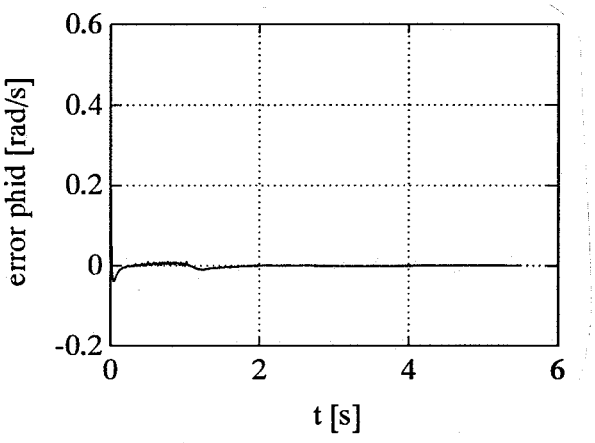

Figure C.23: Velocity error phi

The indirect and composite adaptive controller:

The results of the indirect and composite controller are the same.

1. K_D=100I, Λ=10I, λ_1=10, λ_0=100 k_0=1 and k_1=10

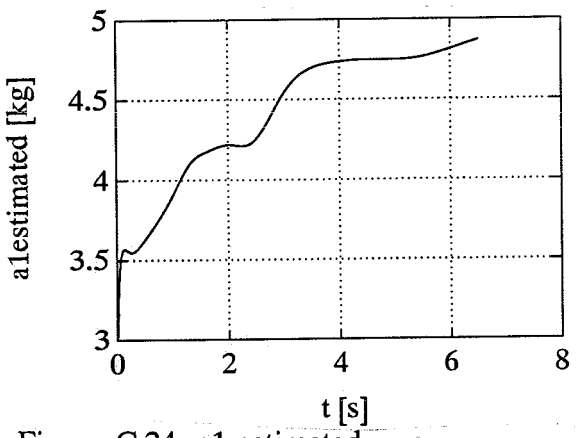

Figure C.24: a1 estimated

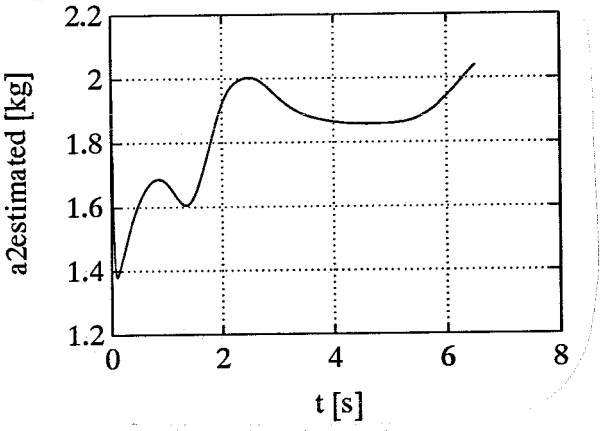

Figure C.25: a2 estimated

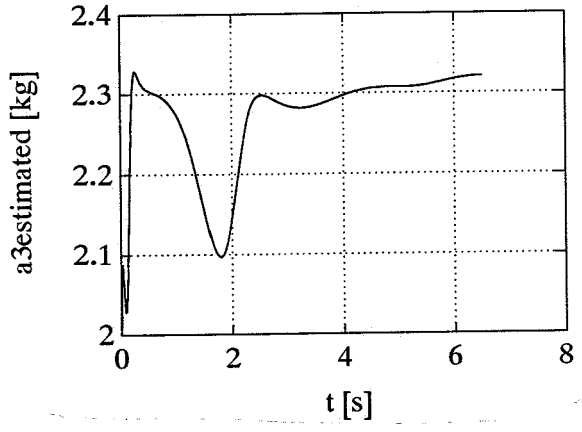

Figure C.26: a3 estimated

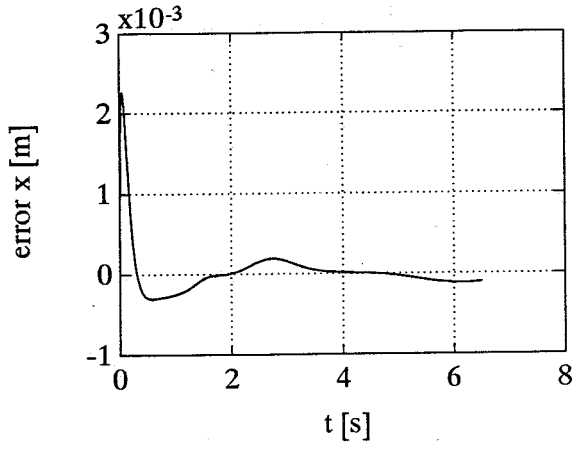

Figure C.27: Position error x

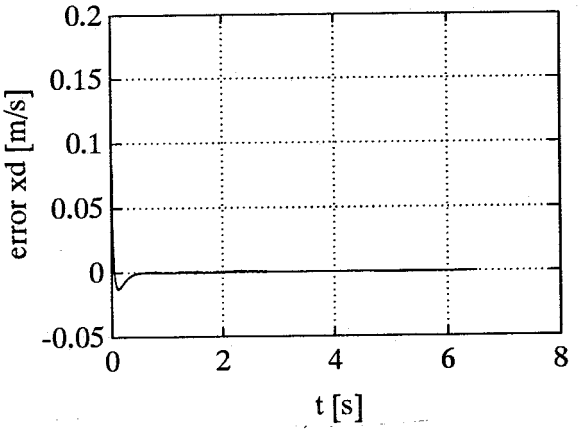

Figure C.28: Velocity error x

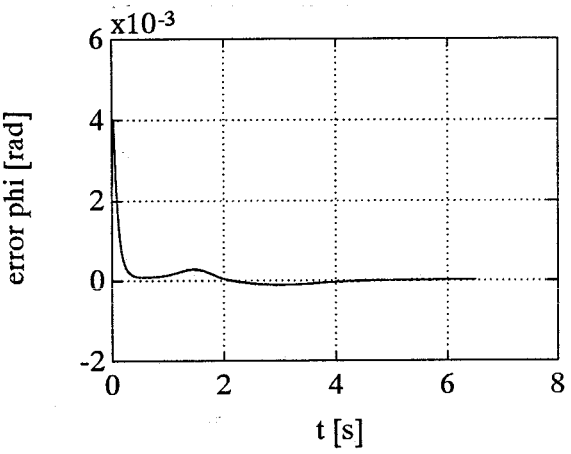

Figure C.29: Position error phi

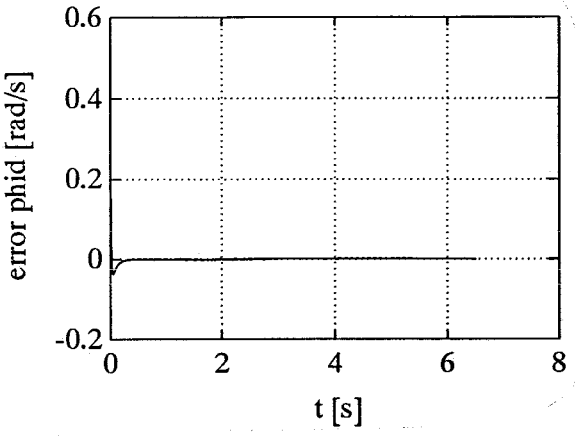

Figure C.30: Velocity error phi

2. K_D=100I, Λ=10I, λ_f=10, λ_0=100 k_0=1 and k_1=30

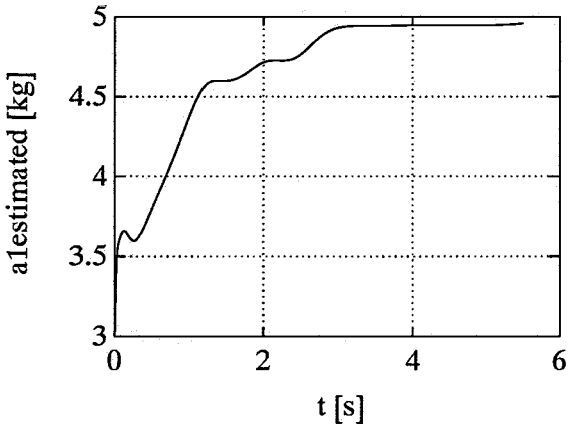

Figure C.31: a1 estimated

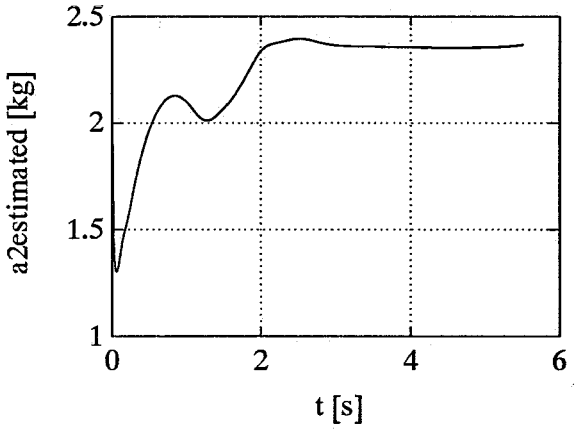

Figure C.32: a2 estimated

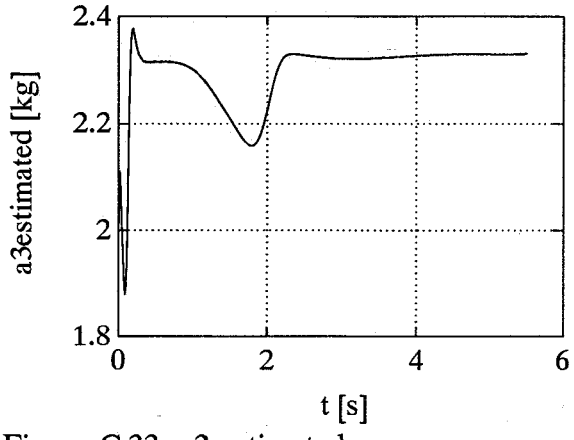

Figure C.33: a3 estimated

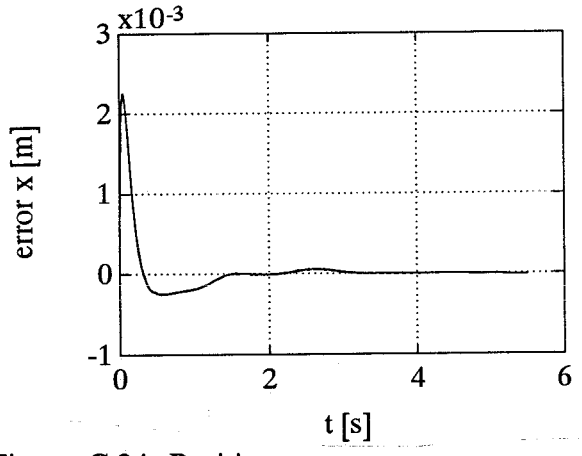

Figure C.34: Position error x

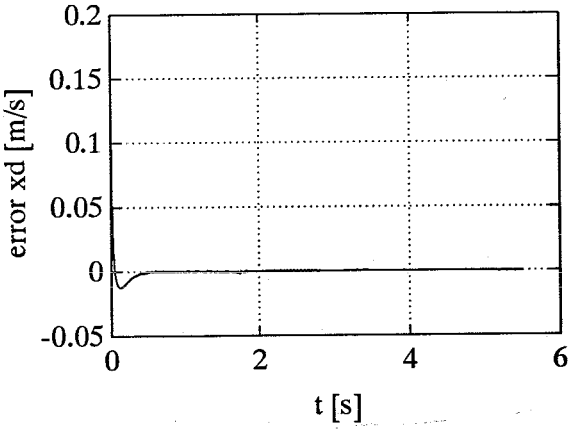

Figure C.35: Velocity error x

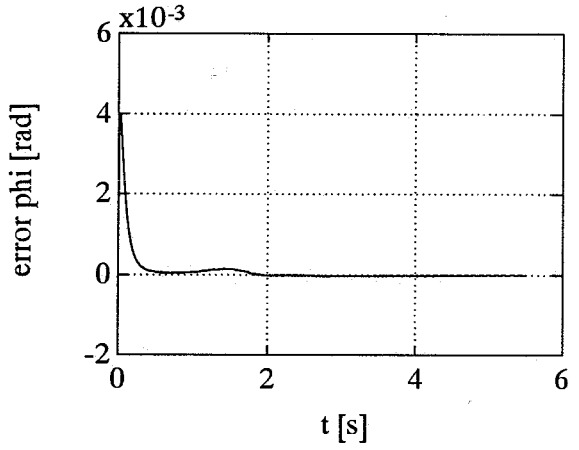

Figure C.36: Position error phi

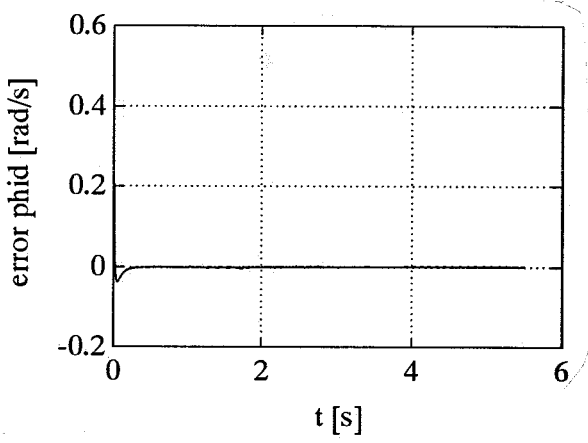

Figure C.37: Velocity error phi

3. K_D=100I, Λ=10I, λ_f=10, λ_0=100, k_0=1 and k_1=100

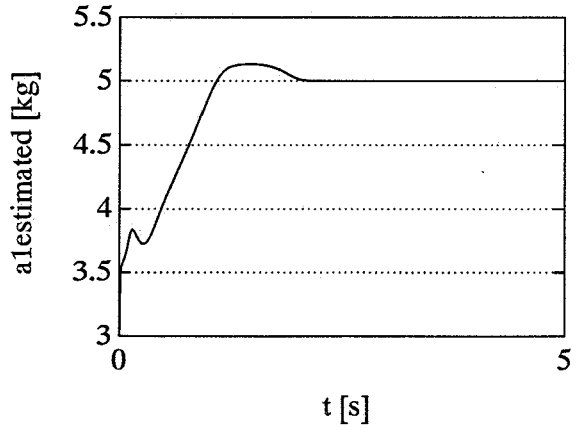

Figure C.38: a1 estimated

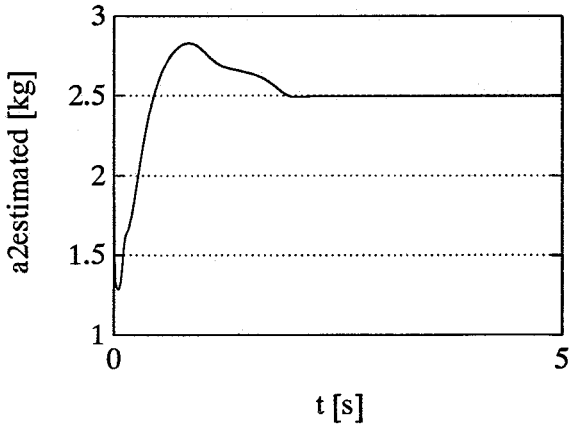

Figure C.39: a2 estimated

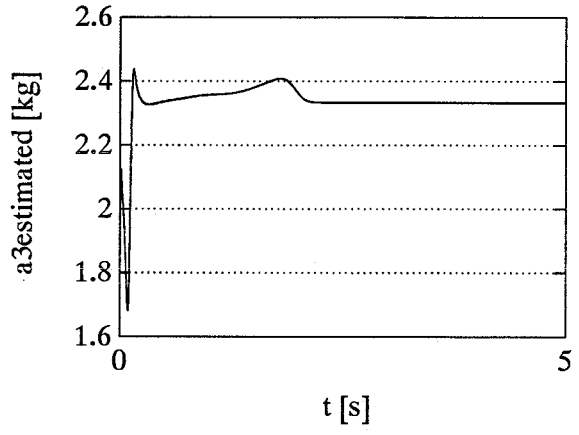

Figure C.40: a3 estimated

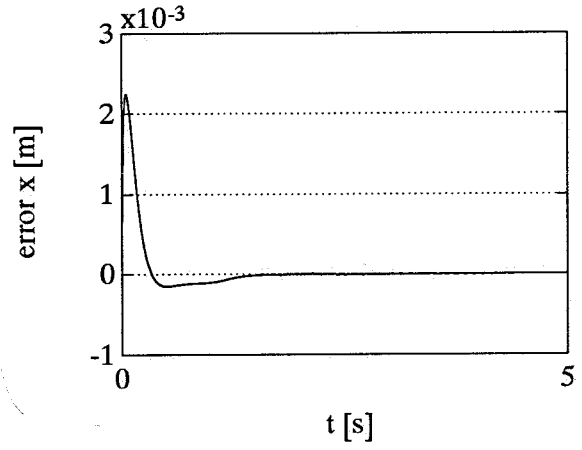

Figure C.41: Position error x

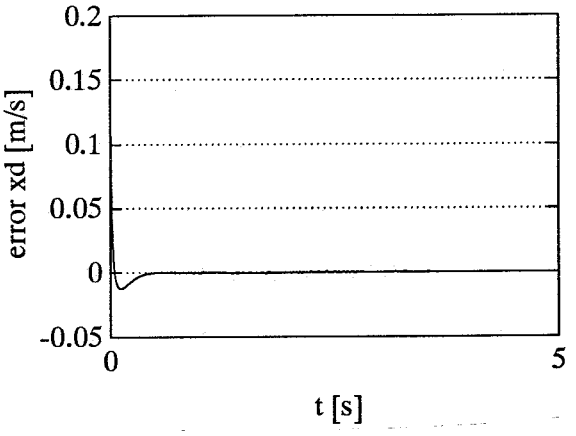

Figure C.42: Velocity error x

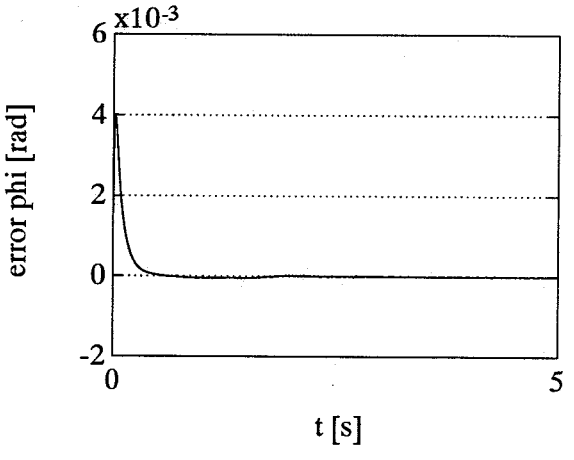

Figure C.43: Position error phi

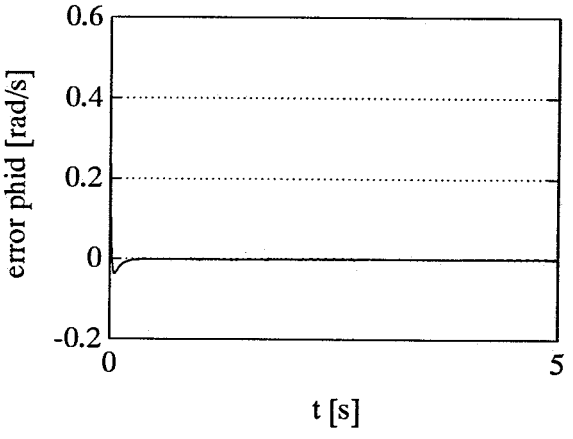

Figure C.44: Velocity error phi

C.3 Results with unmodelled dynamics

The direct adaptive controller:

1. Γ=100I, K_D=100I and Λ=10I

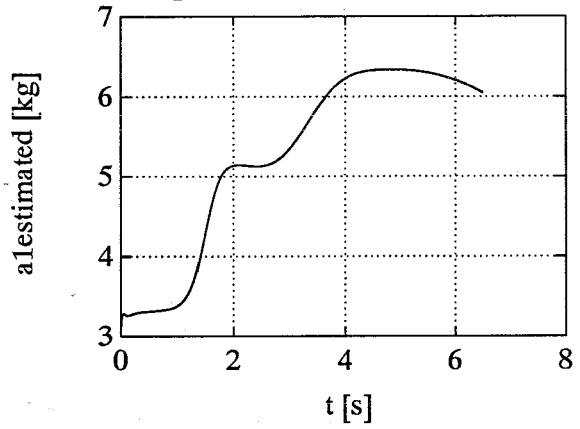

Figure C.45: a1 estimated

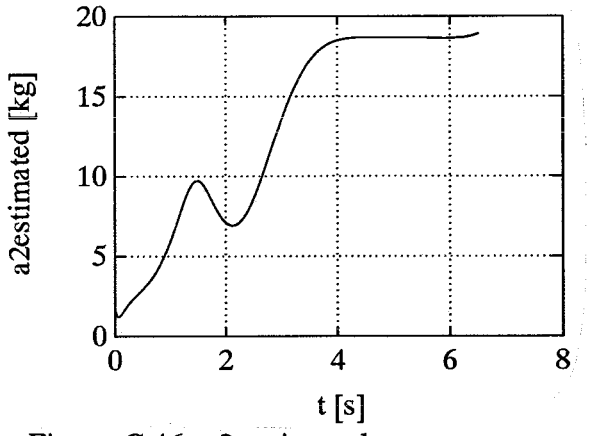

Figure C.46: a2 estimated

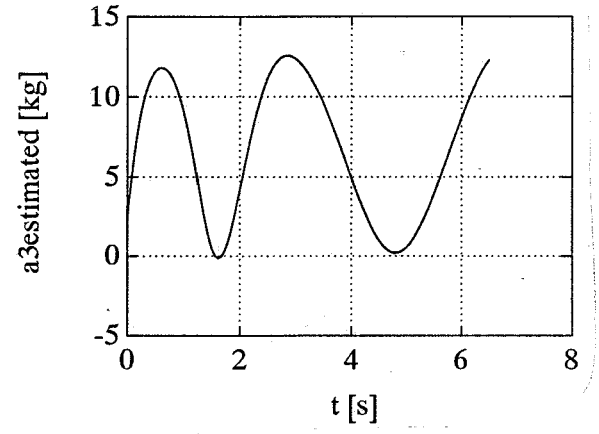

Figure C.47: a3 estimated

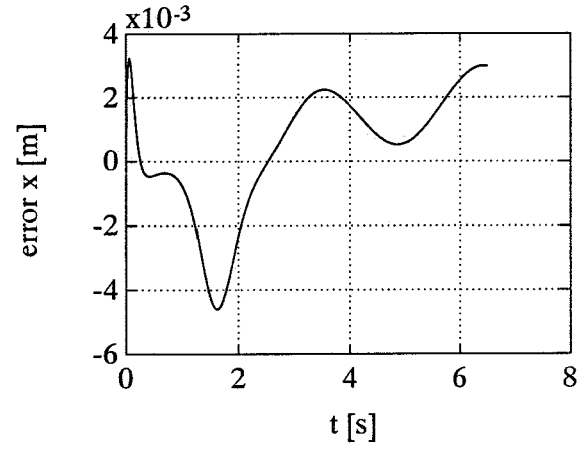

Figure C.48: Position tracking error x

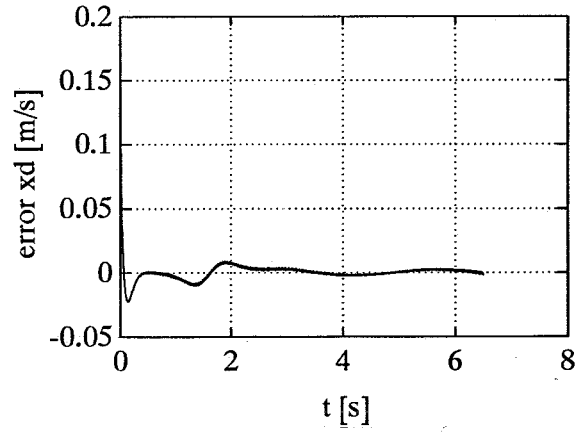

Figure C.49: Velocity tracking error x

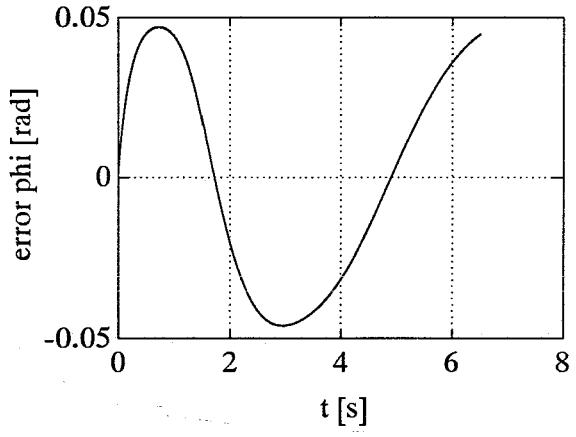

Figure C.50: Position tracking error phi

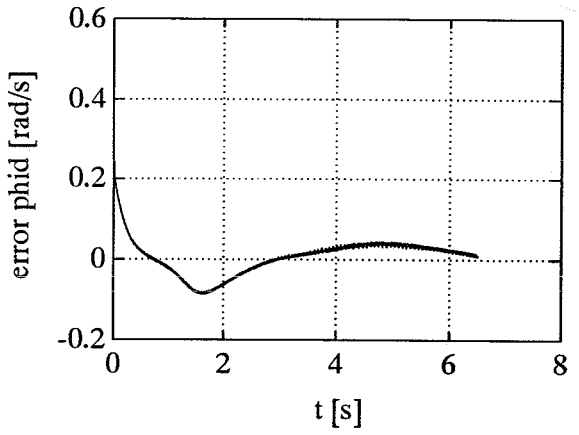

Figure C.51: Velocity tracking error phi

2. Γ=1000*I*, K_D=100*I* and Λ=10*I*

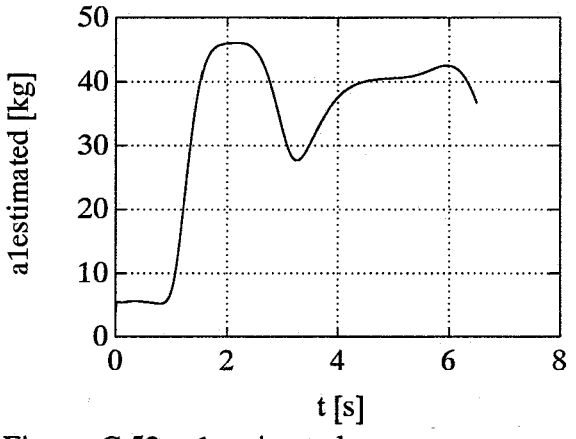

Figure C.52: a1 estimated

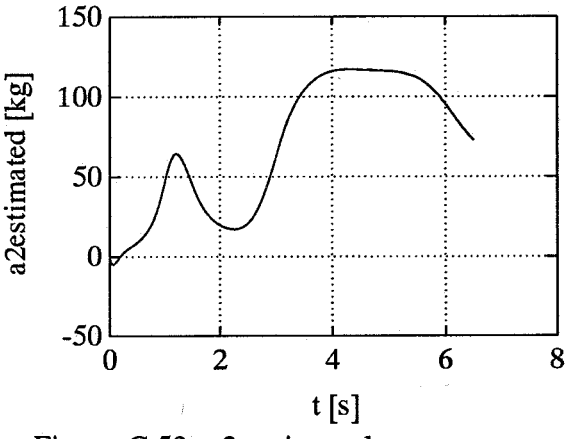

Figure C.53: a2 estimated

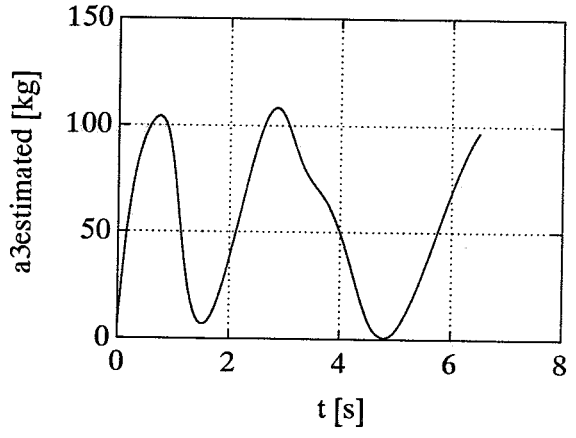

Figure C.54: a3 estimated

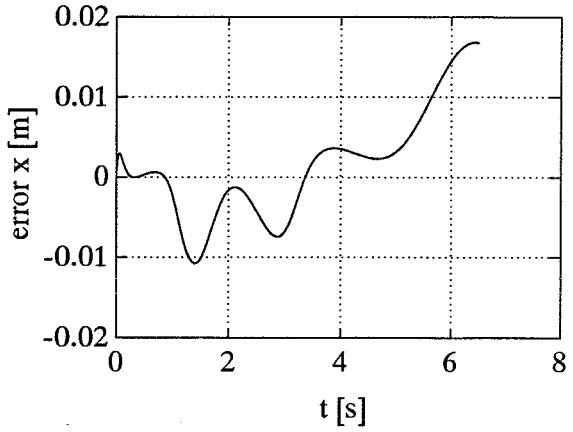

Figure C.55: Position tracking error x

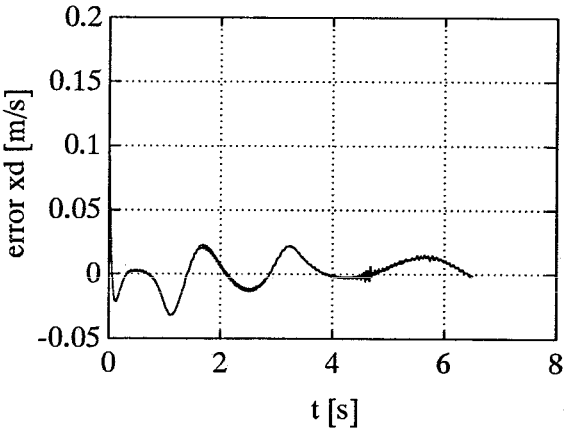

Figure C.56: Velocity tracking error x

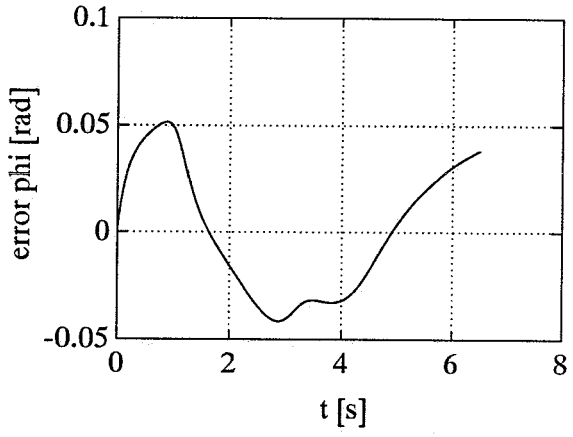

Figure C.57: Position tracking error phi

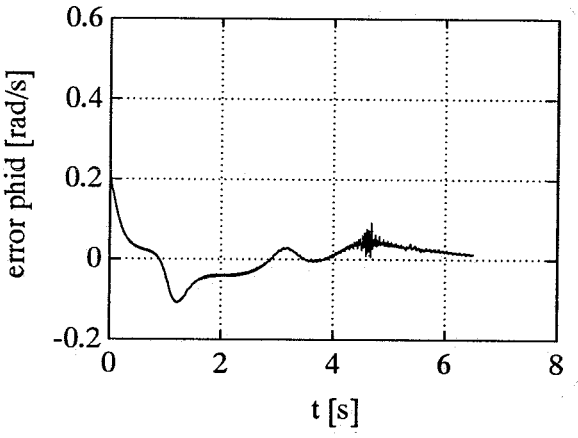

Figure C.58: Velocity tracking error phi

<u>The composite adaptive controller:</u>

1. K_D=100I, Λ=10I, λ_1=10, λ_0=100, k_0=1 and k_1=10

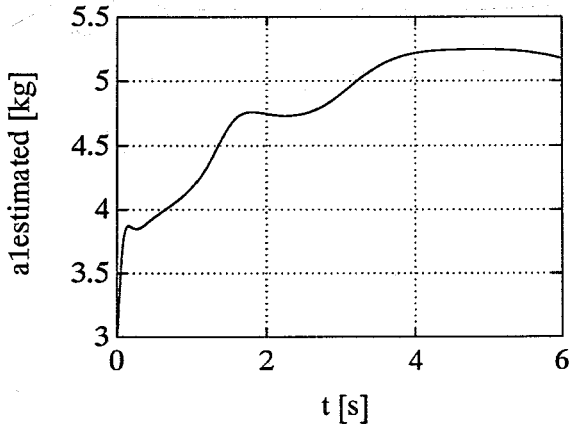

Figure C.59: a1 estimated

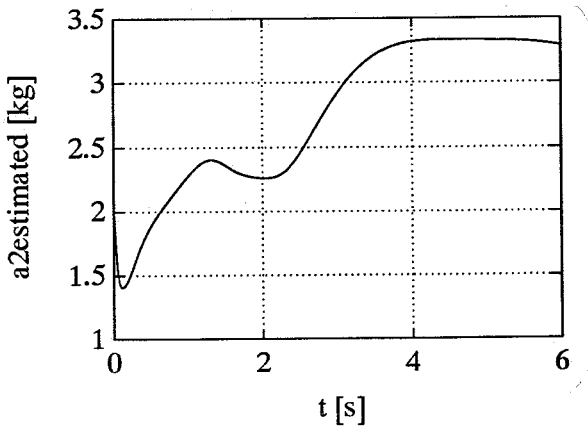

Figure C.60: a2 estimated

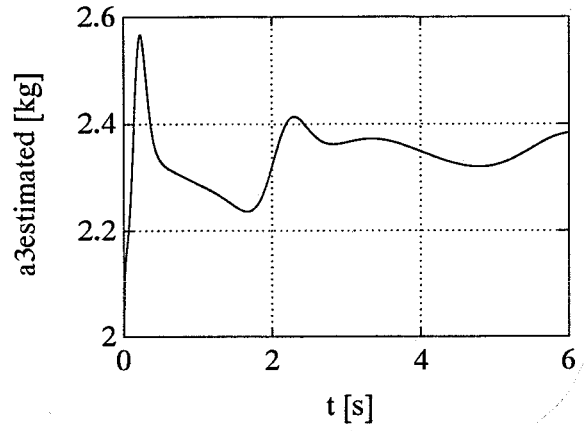

Figure C.61: a3 estimated

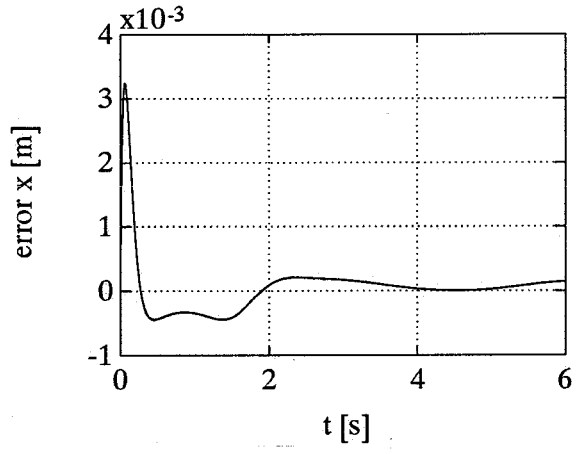

Figure C.62: Position tracking error x

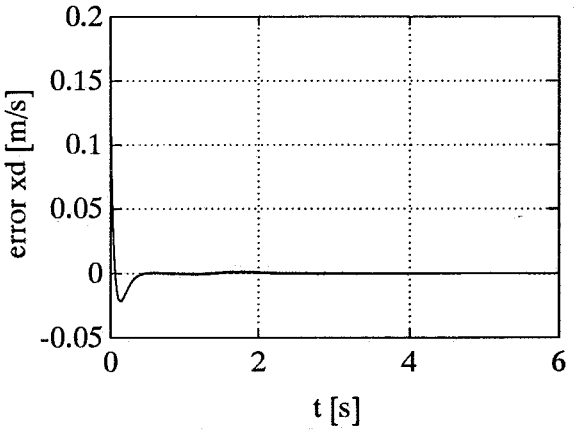

Figure C.63: Velocity tracking error x

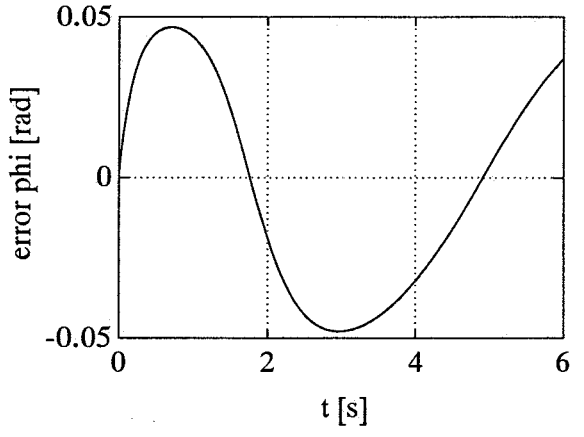

Figure C.64: Position tracking error phi

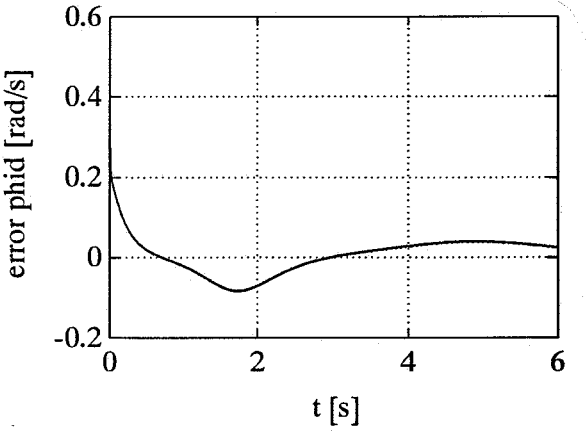

Figure C.65: Velocity tracking error phi

2. K_D=100I, Λ=10I, λ_f=10, λ_0=100, k_0=1 and k_1=30

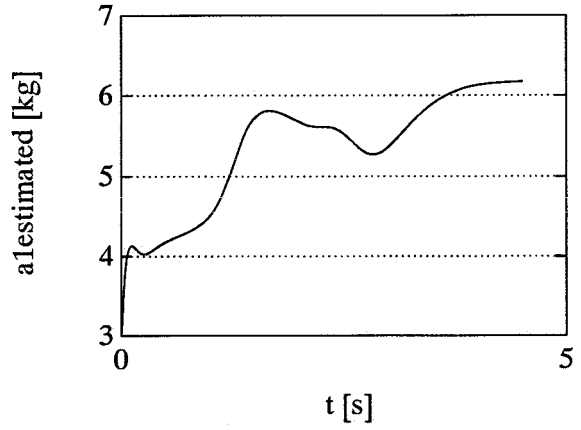

Figure C.66: a1 estimated

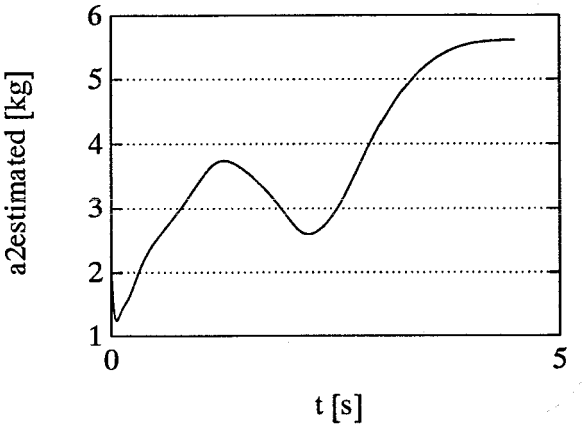

Figure C.67: a2 estimated

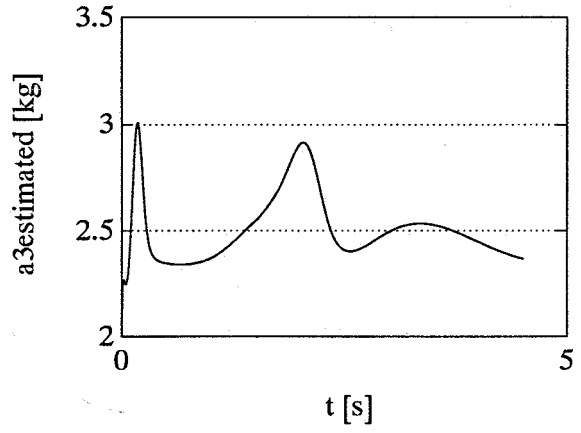

Figure C.68: a3 estimated

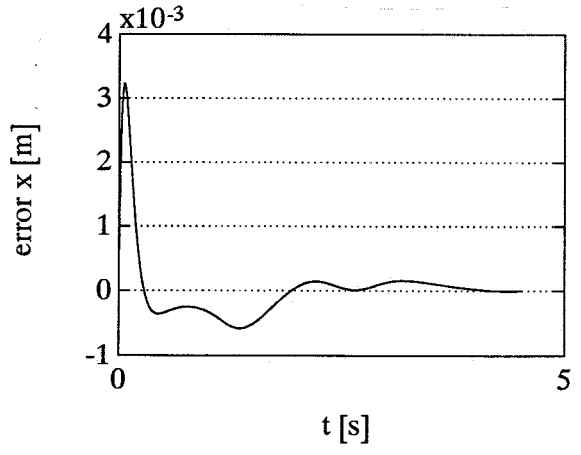

Figure C.69: Position tracking error x

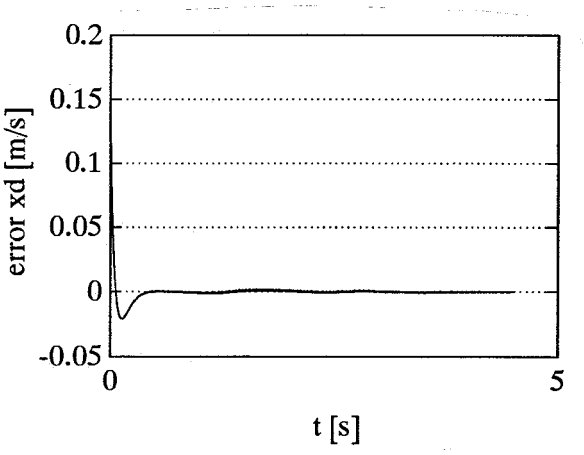

Figure C.70: Velocity tracking error x

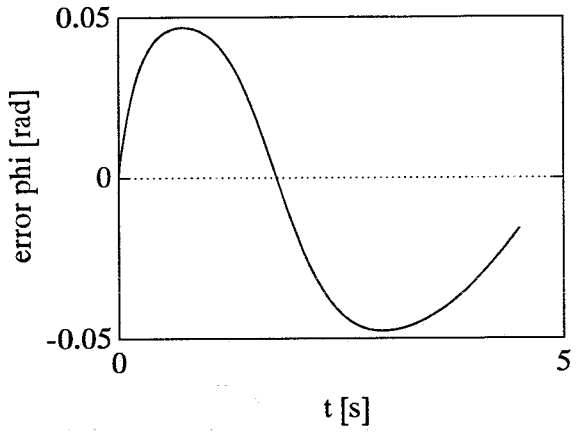

Figure C.71: Position tracking error phi

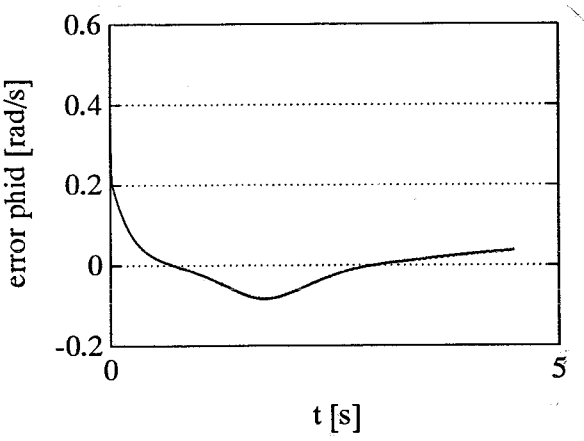

Figure C.72: Velocity tracking error phi

The indirect adaptive controller:

1. K_D=100I, Λ=10I, λ_f=10, λ_0=100, k_0=1 and k_1=10

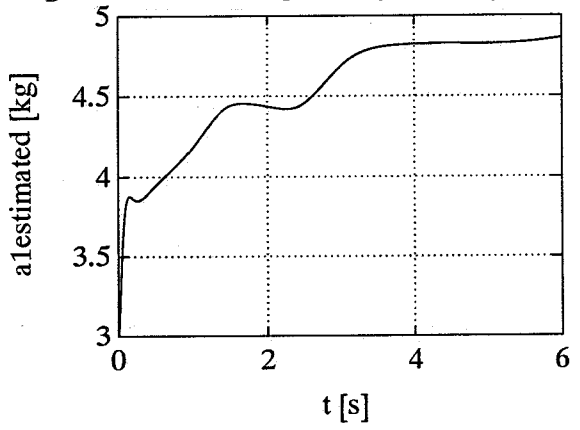

Figure C.73: a1 estimated

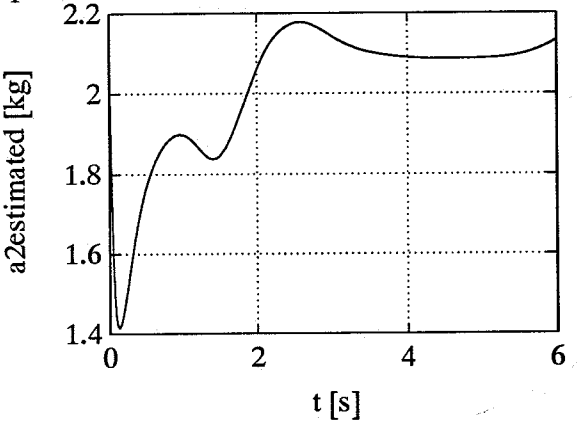

Figure C.74: a2 estimated

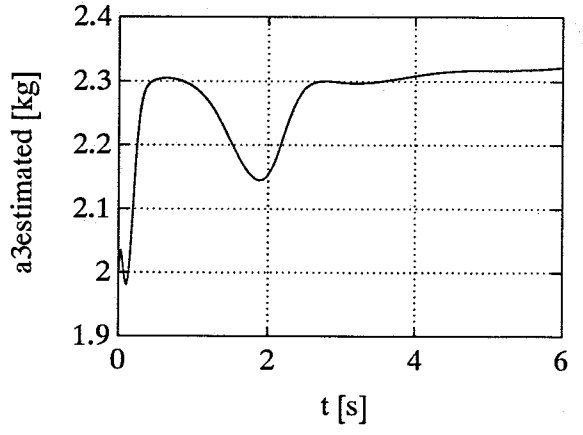

Figure C.75: a3 estimated

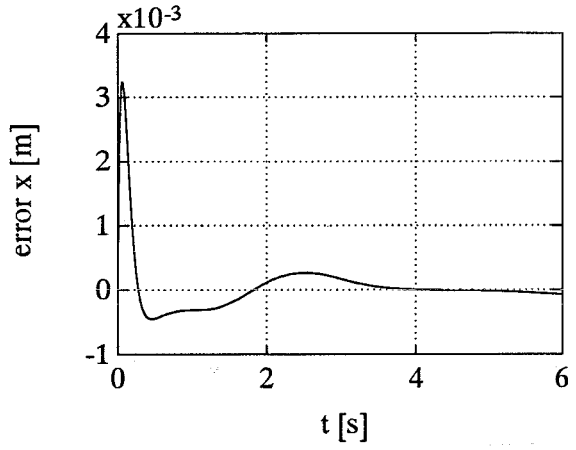

Figure C.76: Position tracking error x

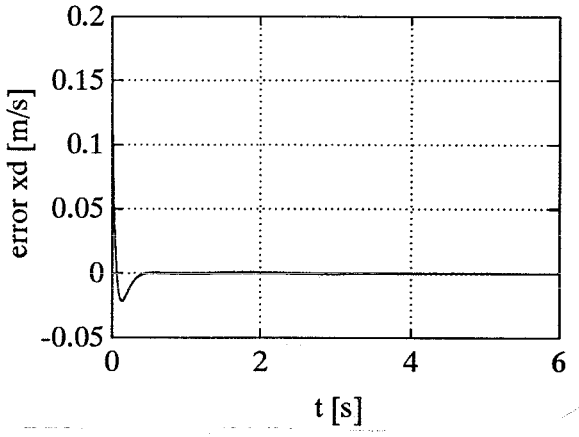

Figure C.77: Velocity tracking error x

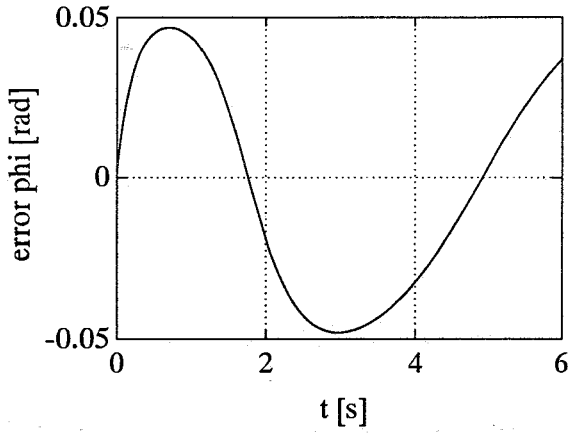

Figure C.78: Position tracking error phi

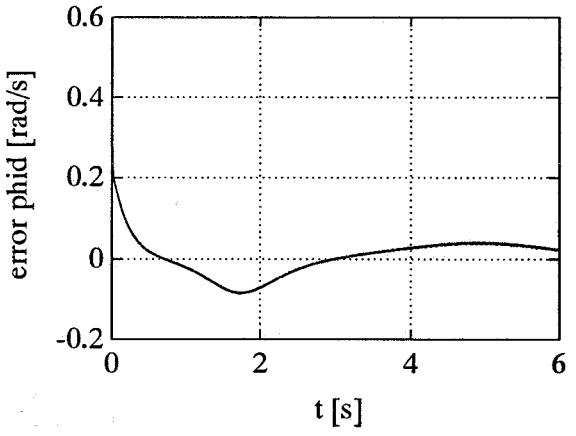

Figure C.79: Velocity tracking error phi

2. K_D=1000I, Λ=10I, λ_f=10, λ_0=100, k_0=1 and k_1=30

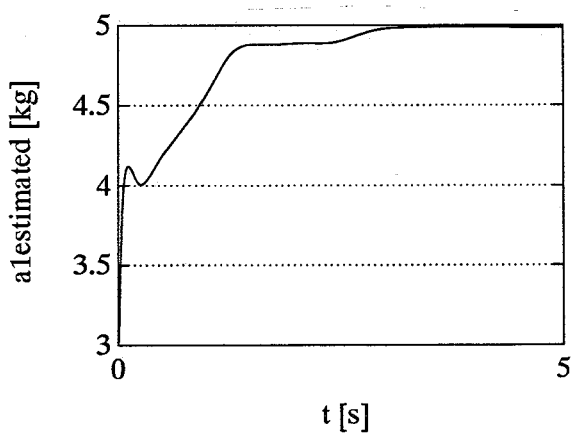

Figure C.80: a1 estimated

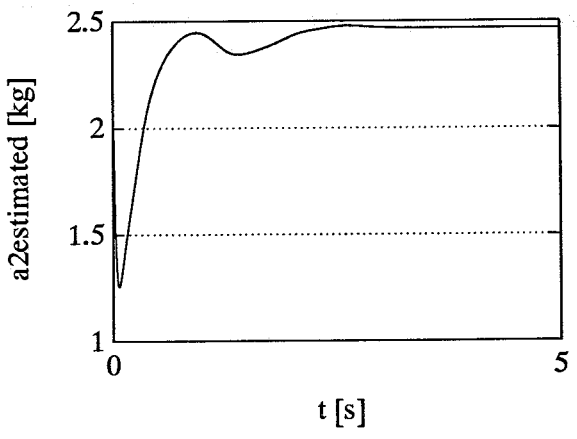

Figure C.81: a2 estimated

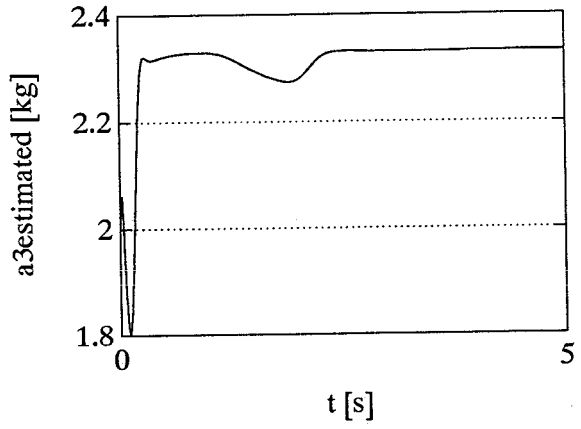

Figure C.82: a3 estimated

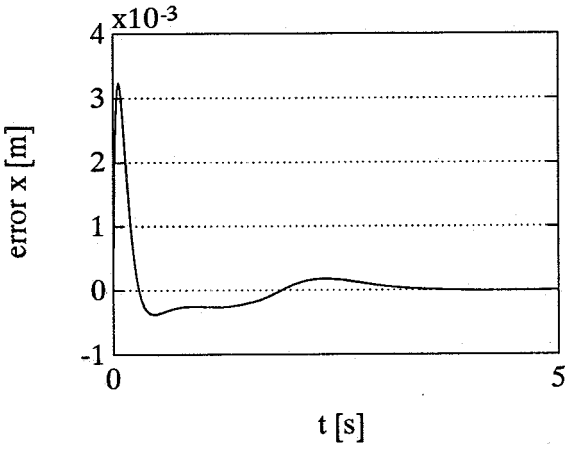

Figure C.83: Position tracking error x

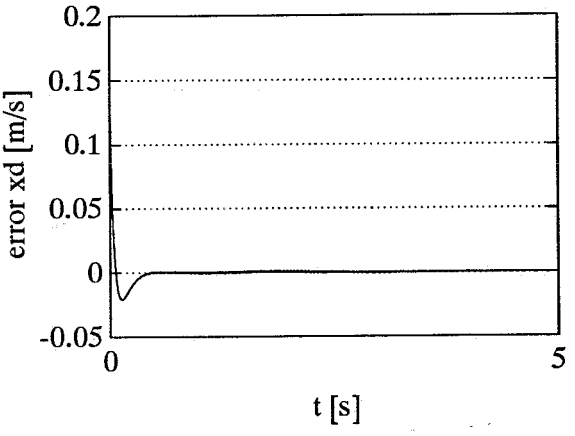

Figure C.84: Velocity tracking error x

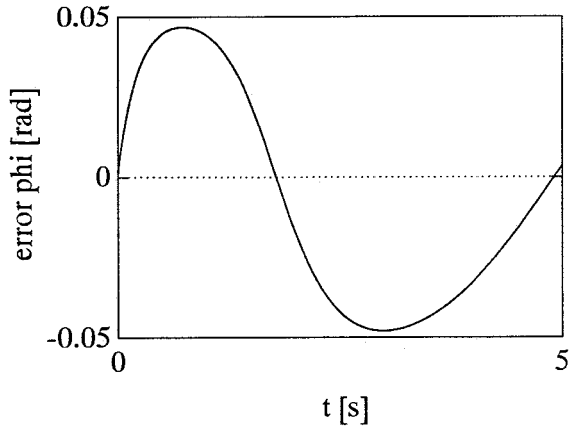

Figure C.85: Position tracking error phi

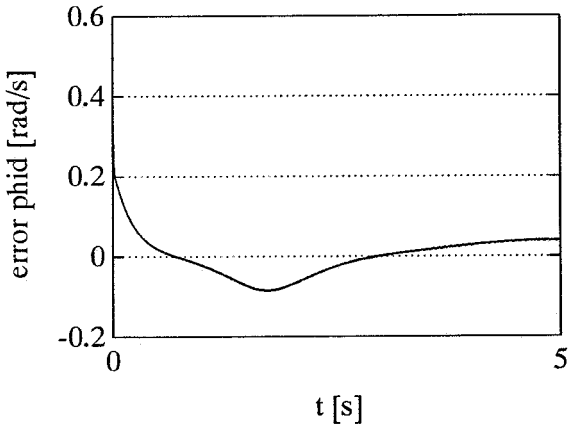

Figure C.86: Velocity tracking error phi

C.4 Results with time-varying parameters

The load of the TR-robot is time-varying with $m_2=2+\sin(0.5*t)$

The simulations are executed for the following control parameters:

direct controller: $\Gamma=1000I$, $K_D=100I$ and $\Lambda=10I$
indirect controller: $K_D=100I$, $\Lambda=10I$, $\lambda_f=10$, $\lambda_0=100$, $k_0=1$ and $k_1=100$, $P(t=0)=I$
composite controller: $K_D=100I$, $\Lambda=10I$, $\lambda_f=10$, $\lambda_0=100$, $k_0=1$ and $k_1=100$, $P(t=0)=I$, $R(t)=I$

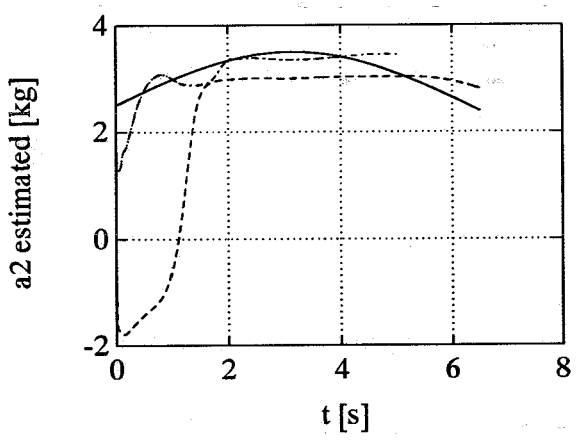

Figure C.87: estimated parameter a_2
—— :real, ----:dir., -·-·:ind. and comp.

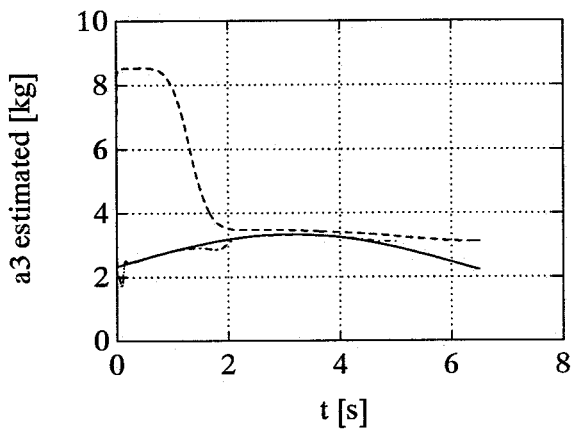

Figure C.88: estimated parameter a_3
—— :real, ----:dir., -·-·:ind. and comp.

Appendix D: Controller design for the XY-table

Control law

All three controllers: $\tau = Y(q,\dot{q},\dot{q}_r,\ddot{q}_r)\hat{a} - K_D s$

Adaptation law

Direct controller: $\dot{\hat{a}} = -\Gamma Y^T(q,\dot{q},\dot{q}_r,\ddot{q}_r)s$

Indirect controller: $\dot{\hat{a}} = -PW^T(q,\dot{q})e$

Composite controller: $\dot{\hat{a}} = -P[Y^T s + W^T R(t)e]$

BGF estimator:

$$\dot{P} = \lambda(t)P - PW^T WP$$
$$\lambda(t) = \lambda_0(1 - \frac{\|P\|}{k_0})$$

This yields for the XY-table:

$$\tau = \begin{bmatrix} T_1 \\ T_3 \end{bmatrix}, \quad q = \begin{bmatrix} \varphi_1 \\ \varphi_3 \end{bmatrix}, \quad a = \begin{bmatrix} J_1 + (m_1 + m_2 + m_e + m_y)r_x^2 \\ J_3 + m_e r_y^2 \\ W_1 + W_2 \\ W_3 \end{bmatrix}, \quad s = \begin{bmatrix} \dot{\varphi}_1 - \dot{\varphi}_{1r} \\ \dot{\varphi}_3 - \dot{\varphi}_{3r} \end{bmatrix}, \quad e = W(\hat{a} - a)$$

$$Y(q_r,\dot{q}_r,\ddot{q}_r) = \begin{bmatrix} \ddot{\varphi}_{1r} & 0 & \text{sign}(\dot{\varphi}_1) & 0 \\ 0 & \ddot{\varphi}_{3r} & 0 & \text{sign}(\dot{\varphi}_3) \end{bmatrix} \tag{D.1}$$

with

$$\dot{\varphi}_{1r} = \dot{\varphi}_{1d} - \Lambda_{11}(\varphi_1 - \varphi_{1d})$$

$$\dot{\varphi}_{3r} = \dot{\varphi}_{3d} - \Lambda_{22}(\varphi_3 - \varphi_{3d})$$

$$\ddot{\varphi}_{1r} = \ddot{\varphi}_{1d} - \Lambda_{11}(\dot{\varphi}_1 - \dot{\varphi}_{1d})$$

$$\ddot{\varphi}_{3r} = \ddot{\varphi}_{3d} - \Lambda_{22}(\dot{\varphi}_3 - \dot{\varphi}_{3d})$$

The matrix $W(q,\dot{q})$ is generated by filtering the matrix $Y_1(q,\dot{q},\ddot{q})$ through a first-order filter:

$$W(q,\dot{q}) = \begin{bmatrix} \lambda_f\dot{\varphi}_1 - \lambda_f^2\dfrac{\dot{\varphi}_1}{p+\lambda_f} & 0 & \text{sign}(\dot{\varphi}_1) & 0 \\ 0 & \lambda_f\dot{\varphi}_3 - \lambda_f^2\dfrac{\dot{\varphi}_3}{p+\lambda_f} & 0 & \text{sign}(\dot{\varphi}_3) \end{bmatrix} \qquad \text{(D.2)}$$

Appendix E: Results of simulations with the XY-table

E.1 Data

The simulations are executed with the following data:

XY-table parameters:

b=1 [m]	m_1=2.3 [kg]	J_1=2.2e-3 [kgm^2]
l=1.25 [m]	m_2=2.3 [kg]	J_3=1.58e-4 [kgm^2]
r_x=0.01 [m]	m_e=2.3 [kg]	W_1=0.447 [Nm]
r_y=0.01 [m]	m_y=8.5 [kg]	W_3=0.154 [Nm]

Trajectory parameters:

r=0.25 [m]
$\omega=2\pi$ [rad/s]

Manipulator state variables:

φ_1	angular displacement of belt wheel 1
φ_3	angular displacement of belt wheel 3
$\dot{\varphi}_1$	angular velocity of belt wheel 1
$\dot{\varphi}_3$	angular velocity of belt wheel 3

The initial system state conditions:

	$\varphi_1(t_0)$ [rad]	$\varphi_3(t_0)$ [rad]	$\dot{\varphi}_1(t_0)$ [rad/s]	$\dot{\varphi}_3(t_0)$ [rad/s]
ideal initial state variables	25	50	0	50π

The initial mass parameters:

$a_1(t_0)=0$ [kgm^2] $a_2(t_0)=0$ [kgm^2] $a_3(t_0)=0$ [Nm] $a_4(t_0)=0$ [Nm]

The real mass parameters are:

a_1=3.7e-3 [kgm^2] a_2=3.88e-4 [kgm^2] a_3=0.447 [Nm] a_4=0.154 [Nm]

E.2 Results of situation 1

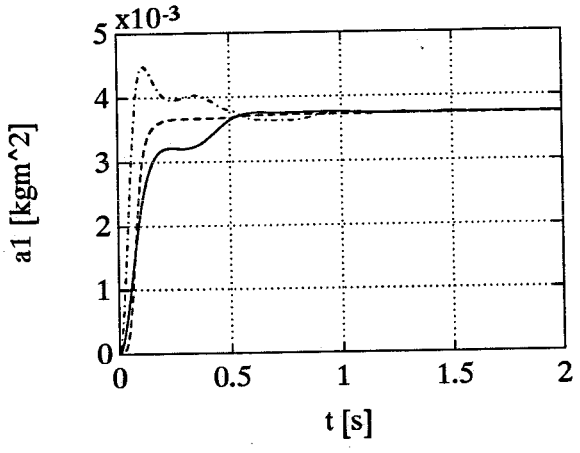

Figure E.1: estimated parameter a_1
—— :direct, ----:indirect, -·-·:composite

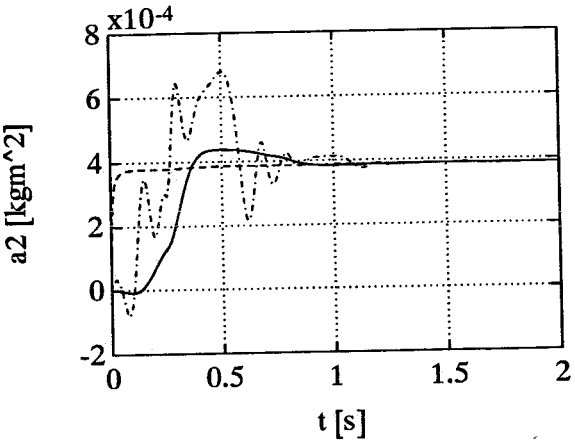

Figure E.2: estimated parameter a_2
—— :direct, ----:indirect, -·-·:composite

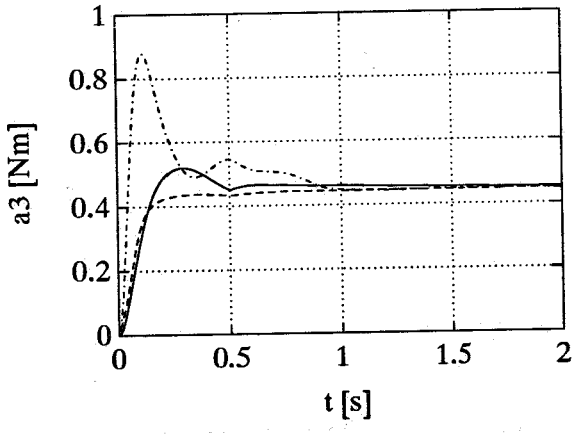

Figure E.3: estimated parameter a_3
—— :direct, ----:indirect, -·-·:composite

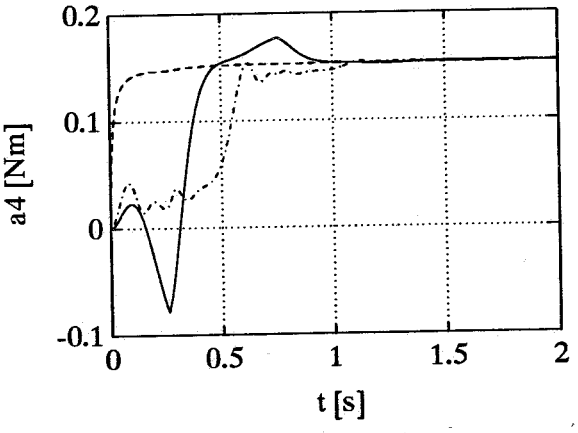

Figure E.4: estimated parameter a_4
—— :direct, ----:indirect, -·-·:composite

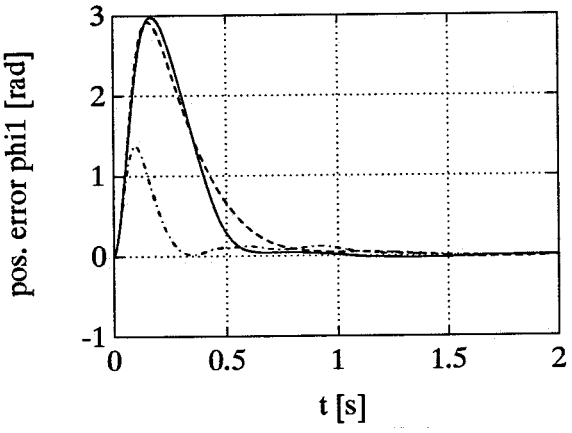

Figure E.5: Pos. tr. error x-direction
—— :direct, ----:indirect, -·-·:composite

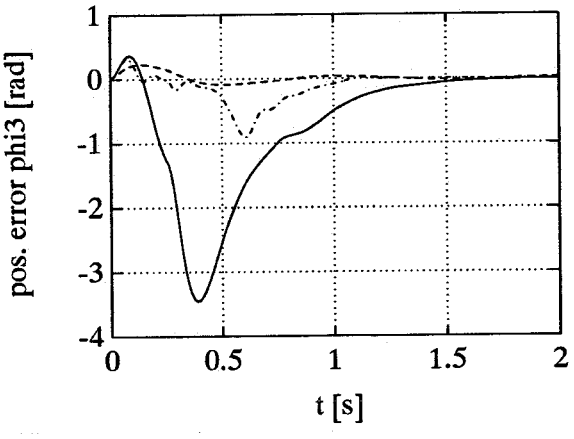

Figure E.6: Pos. tr. error y-direction
—— :direct, ----:indirect, -·-·:composite

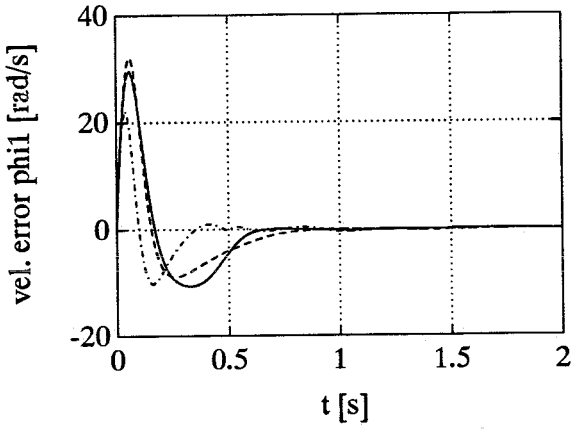

Figure E.7: Vel. tr. error x-direction
—— :direct, ----:indirect, -·-·:composite

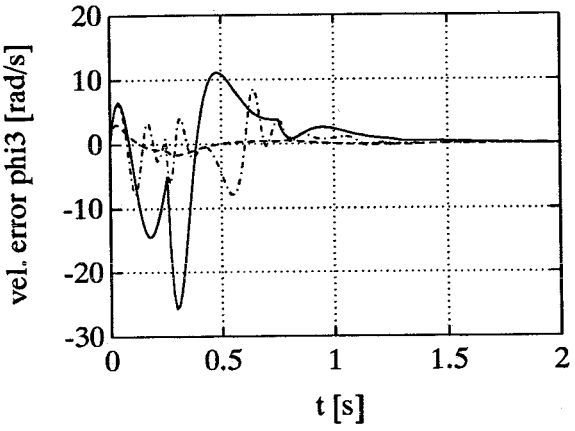

Figure E.8: Vel. tr. error y-direction
—— :direct, ----:indirect, -·-·:composite

E.3 Results of situation 2

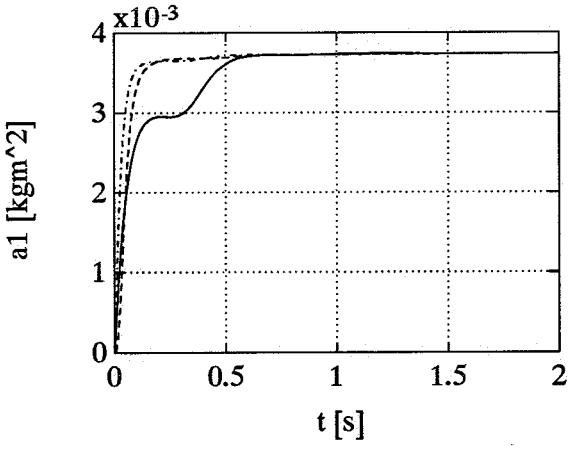

Figure E.9: estimated parameter a_1
—— :direct, ----:indirect, -·-·:composite

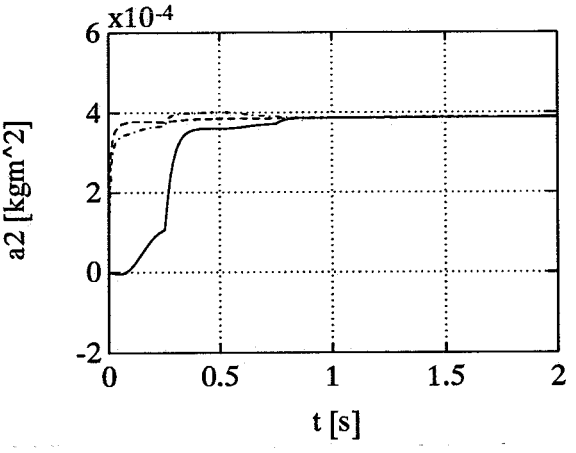

Figure E.10: estimated parameter a_2
—— :direct, ----:indirect, -·-·:composite

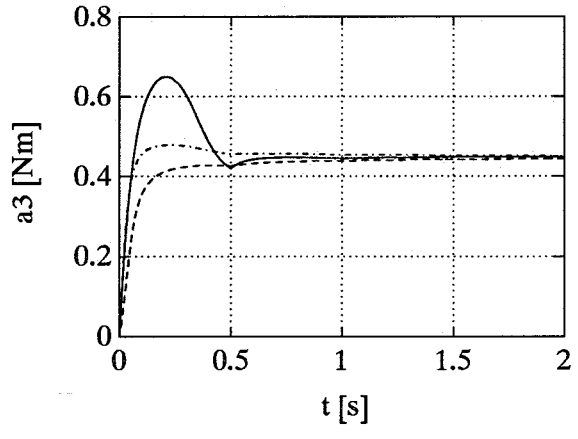

Figure E.11: estimated parameter a_3
—— :direct, ----:indirect, -·-·:composite

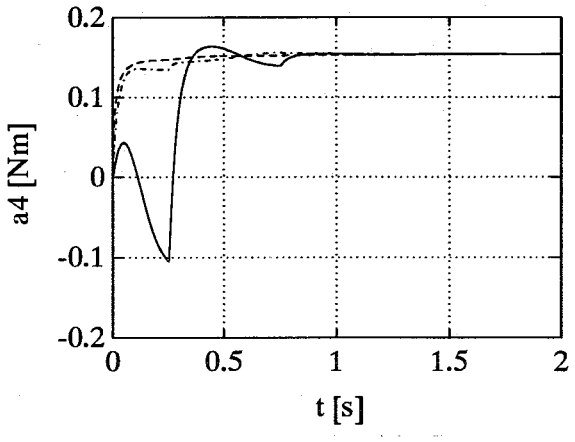

Figure E.12: estimated parameter a_4
—— :direct, ----:indirect, -·-·:composite

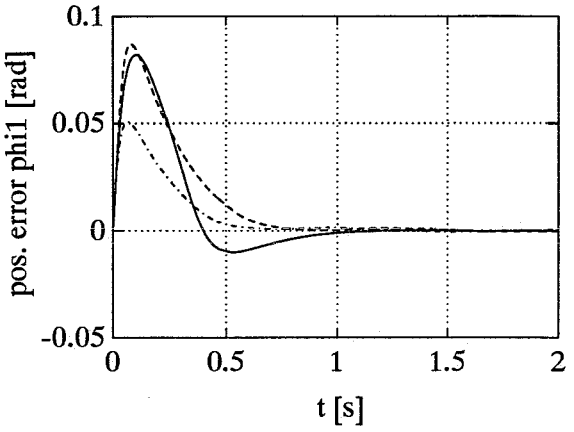

Figure E.13: Pos. tr. error x-direction
—— :direct, ----:indirect, -·-·:composite

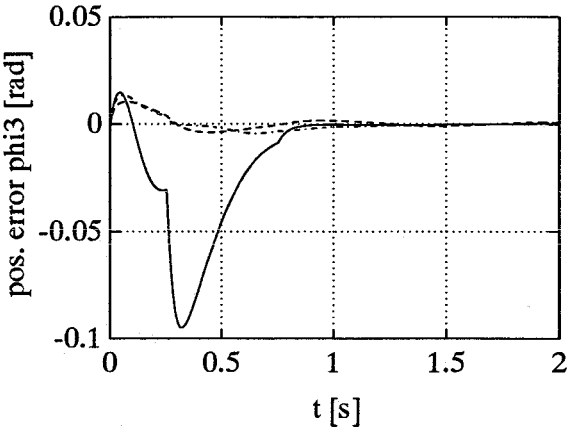

Figure E.14: Pos. tr. error y-direction
—— :direct, ----:indirect, -·-·:composite

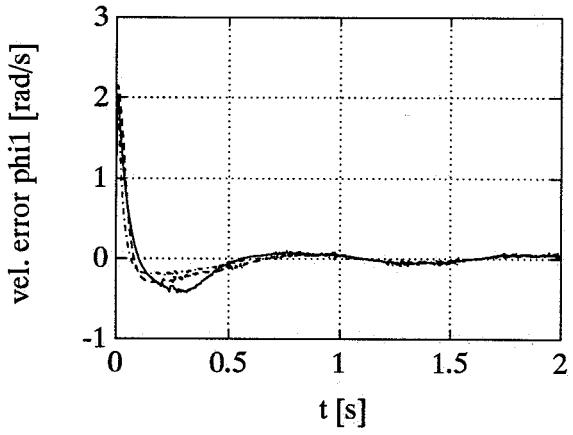

Figure E.15: Vel. tr. error x-direction
—— :direct, ----:indirect, -·-·:composite

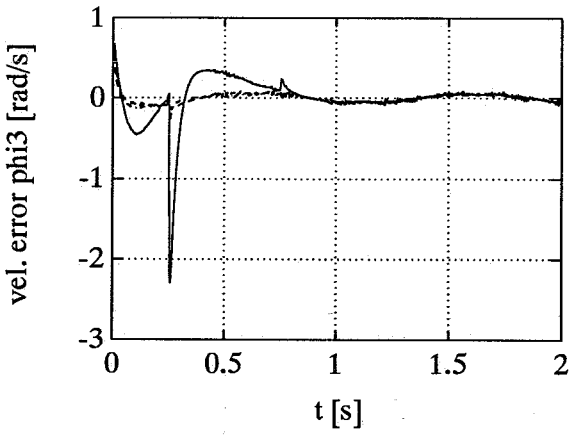

Figure E.16: Vel. tr. error y-direction
—— :direct, ----:indirect, -·-·:composite

Appendix F: The observer

The simplified model of the XY-table is used to design the observer:

$$\frac{a_1}{k_1}\ddot{x} = u_1 - \frac{a_3}{k_1}\text{sign}(\dot{x}) \tag{F.1}$$

$$\frac{a_2}{k_2}\ddot{y} = u_2 - \frac{a_4}{k_2}\text{sign}(\dot{y}) \tag{F.2}$$

The state vector, the control inputs and the outputs are defined as follows:

$$x(t) = \begin{bmatrix} x(t) \\ y(t) \\ \dot{x}(t) \\ \dot{y}(t) \end{bmatrix}, \qquad u(t) = \begin{bmatrix} u_1 - \frac{a_3}{k_1}\text{sign}(\dot{x}) \\ u_2 - \frac{a_4}{k_2}\text{sign}(\dot{y}) \end{bmatrix}, \qquad y(t) = \begin{bmatrix} x(t) \\ y(t) \end{bmatrix}$$

With the process noise $w(t)$, that is modelled as noise on the input $u(t)$ and with measurement noise $v(t)$ the model can be written as:

$$\dot{x} = Ax + Bu + Ew \tag{F.3}$$

$$y = Cx + v \tag{F.4}$$

with:

$$A = \begin{bmatrix} 0 & 0 & 1 & 0 \\ 0 & 0 & 0 & 1 \\ 0 & 0 & 0 & 0 \\ 0 & 0 & 0 & 0 \end{bmatrix}, \qquad B = E = \begin{bmatrix} 0 & 0 \\ 0 & 0 \\ k_1/a_1 & 0 \\ 0 & k_2/a_2 \end{bmatrix}, \qquad C = \begin{bmatrix} 1 & 0 & 0 & 0 \\ 0 & 1 & 0 & 0 \end{bmatrix}$$

According te equation (5.37) of Kok [4] the following estimate can be made:

$$\dot{\hat{x}} = A\hat{x} + Bu + K(y - C\hat{x}) \tag{F.5}$$

with the optimum gain matrix K^0 according to

$$K^0 = \tilde{Q}(t)C^T(t)V_v^{-1}(t) \tag{F.6}$$

This optimal gain matrix K^0 is calculated with the function lqe of the software package MATLAB:

$$K^0 = \text{lqe}(A,E,C,Q,R)$$

with

$$Q = \text{covariance}(w)$$
$$R = \text{covariance}(v)$$

To calculate K^0 the covariances Q and R have to be known. From L.J.W. van Gerwen [3], the covariance of the measurement v is known:

$$R_x = 3.5*10^{-12} \quad [m^2]$$
$$R_y = 8.4*10^{-11} \quad [m^2]$$

However, the covariance Q of the process noise is not known. The solution to this problem is found by looking at the filterpoles. Two filterpoles are determined by the covariance R and two filterpoles are determined by the covariance Q. The two filterpoles determined by R are:

$$-37.27 \pm 37.27i$$

Now we demand that the two filterpoles determined by Q must exactly be the same. This leads to a gain matrix K:

$$K = 1*10^3 \begin{bmatrix} 0.0745 & 0 \\ 0 & 0.0745 \\ 2.7775 & 0 \\ 0 & 2.7775 \end{bmatrix}$$

Furthermore, we can use in the matrix B of equation (F.5) the constant parameters a_1 and a_2 with respectivily the values 40 and 4 or the estimated parameters of the adaptation mechanism. A disadvantage of the adaptive version of the observer is that if the initial parameter values are very small the matrix B is very large. A large matrix B leads to a fluctuating estimation of the state vector $x(t)$ and as a result of that to larger tracking errors. If the initial parameter values are large there is no problem with the adaptive version of the observer. To avoid any problem I have chosen the observer with a constant matrix B.

Appendix G: The control parameters K_D and Λ

To determine the control matrices the simplified model of the XY-table without friction will be used:

$$\ddot{x} = \frac{k_1}{a_1} u_1 \tag{G.1}$$

$$\ddot{y} = \frac{k_2}{a_2} u_2 \tag{G.2}$$

The input can be written as a PD-feedback:

$$u_1 = -K_{D1}(\dot{x} - \dot{x}_d) - K_{P1}(x - x_d) \tag{G.3}$$

$$u_2 = -K_{D3}(\dot{y} - \dot{y}_d) - K_{P3}(y - y_d) \tag{G.4}$$

Substitution of (G.3) in (G.1) and (G.4) in (G.2) leads to the following equations:

$$\ddot{x} + K_{D1}\frac{k_1}{a_1}\dot{x} + K_{P1}\frac{k_1}{a_1}x = K_{D1}\frac{k_1}{a_1}\dot{x}_d + K_{P1}\frac{k_1}{a_1}x_d \tag{G.5}$$

$$\ddot{y} + K_{D3}\frac{k_2}{a_2}\dot{y} + K_{P3}\frac{k_2}{a_2}y = K_{D3}\frac{k_2}{a_2}\dot{y}_d + K_{P3}\frac{k_2}{a_2}y_d \tag{G.6}$$

This can be written as:

$$\ddot{x} + 2\beta_x\omega_{0x}\dot{x} + \omega_{0x}^2 x = 2\beta_x\omega_{0x}\dot{x}_d + \omega_{0x}^2 x_d \tag{G.7}$$

$$\ddot{y} + 2\beta_y\omega_{0y}\dot{y} + \omega_{0y}^2 y = 2\beta_y\omega_{0y}\dot{y}_d + \omega_{0y}^2 y_d \tag{G.8}$$

This yields:

$$K_P = \begin{bmatrix} \omega_{0x}^2 a_1/k_1 & 0 \\ 0 & \omega_{0y}^2 a_2/k_2 \end{bmatrix}, \qquad K_D = \begin{bmatrix} 2\beta_x\omega_{0x} a_1/k_1 & 0 \\ 0 & 2\beta_y\omega_{0y} a_2/k_2 \end{bmatrix}$$

In L.J.W. van Gerwen [3] is found that the largest possible eigenfrequency and damping, without causing undesirable chattering, is:

$$\omega_{0x} = \omega_{0y} = 4*2\pi \quad [\text{rad/s}]$$
$$\beta_x = \beta_y = 0.7 \quad [-]$$

These values are valid for the XY-table with the rigid bar. For these values the control matrices are:

$$K_D = \begin{bmatrix} 11700 & 0 \\ 0 & 7000 \end{bmatrix}, \qquad \Lambda = \begin{bmatrix} 18 & 0 \\ 0 & 18 \end{bmatrix}$$

The control poles can be determined as follows:

- the input in x-direction is:

$$u_i = \frac{a_1}{k_1}\ddot{x}_r - K_{D1}s_i \tag{G.9}$$

with

$$\ddot{x}_r = \ddot{x}_d - \Lambda_{11}\dot{e}_x$$

$$s_1 = \dot{e}_x + \Lambda_{11}e_x$$

$$e_x = x - x_d$$

Substitution of (G.9) in (G.1) leads to:

$$\ddot{x} = \ddot{x}_r - \frac{k_1}{a_1}K_{D1}(\dot{e}_x + \Lambda_{11}e_x)$$

$$\ddot{x} = \ddot{x}_d - \Lambda_{11}\dot{e}_x - \frac{k_1}{a_1}K_{D1}(\dot{e}_x + \Lambda_{11}e_x)$$

$$\ddot{e}_x + \Lambda_{11}\dot{e}_x + \frac{k_1}{a_1}K_{D1}(\dot{e}_x + \Lambda_{11}e_x) = 0$$

$$\ddot{e}_x + (\Lambda_{11} + \frac{k_1}{a_1} K_{D1})\dot{e}_x + \Lambda_{11}\frac{k_1}{a_1} K_{D1} e_x = 0$$

$$s^2 e_x + (\Lambda_{11} + \frac{k_1}{a_1} K_{D1}) s e_x + \Lambda_{11}\frac{k_1}{a_1} K_{D1} e_x = 0$$

$$(s + \Lambda_{11})\ (s + \frac{k_1}{a_1} K_{D1}) e_x = 0$$

The control poles are in x-direction:

$$s_1 = -\Lambda_{11}\ , \qquad s_2 = -\frac{k_1}{a_1} K_{D1} \tag{G.10}$$

The control poles in y-direction are:

$$s_3 = -\Lambda_{22}\ , \qquad s_4 = -\frac{k_2}{a_2} K_{D3} \tag{G.11}$$

With the above values of K_D and Λ the control poles are:

$$s_1 = s_3 = -18$$
$$s_2 = s_4 = -35$$

However, for these values of K_D and Λ there occurs a saturation of the inputs. If we demand that all the control poles are -18, then from (G.10) and (G.11) we get the following control matrices:

$$K_D = \begin{bmatrix} 6000 & 0 \\ 0 & 3600 \end{bmatrix}, \qquad \Lambda = \begin{bmatrix} 18 & 0 \\ 0 & 18 \end{bmatrix}$$

For these control matrices there is less saturation of the inputs. In the experiments these control matrices are used.

Appendix H. Results of the expriments

The results of the experiments discussed in this appendix are executed for the following situations:

situation 1: $\omega=0.5\pi$ [rad/s]

$$\hat{a}(t_0) = [40/0.12 \quad 4/0.02 \quad 50/0.12 \quad 15/0.02]^T$$

situation 2: $\omega=0.5\pi$ [rad/s]

$$\hat{a}(t_0) = \frac{1}{2}[40/0.12 \quad 4/0.02 \quad 50/0.12 \quad 15/0.02]^T$$

situation 3: $\omega=\pi$ [rad/s]

$$\hat{a}(t_0) = [40/0.12 \quad 4/0.02 \quad 50/0.12 \quad 15/0.02]^T$$

H.1 Results of the rigid XY-table

First, the desired and real trajectory of the three controllers are given for <u>situation 1</u>:

- direct adaptive controller

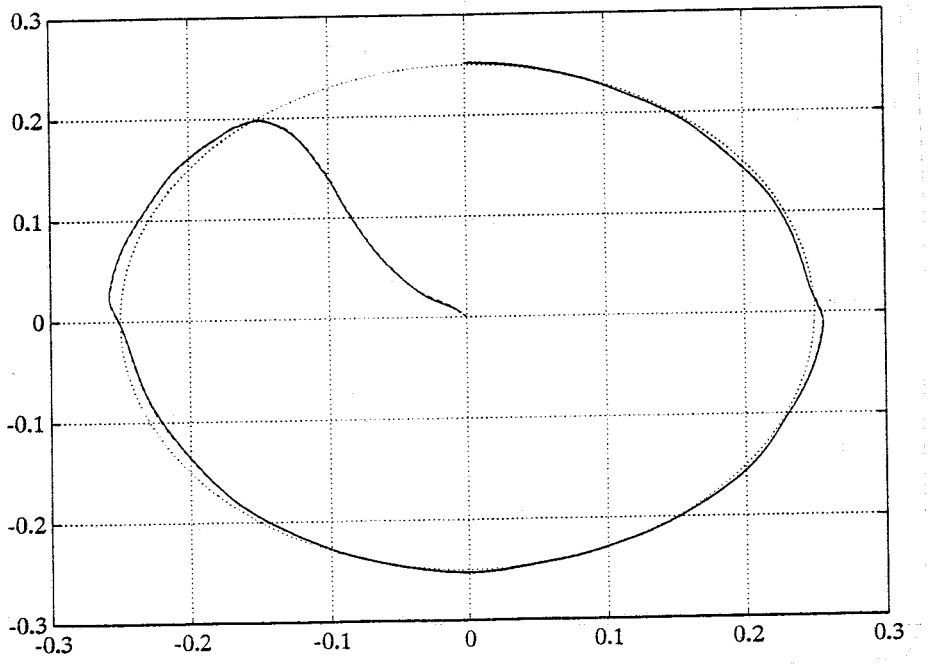

Figure H.1: desired and real trajectory
—— :real, ----:desired

- indirect adaptive controller

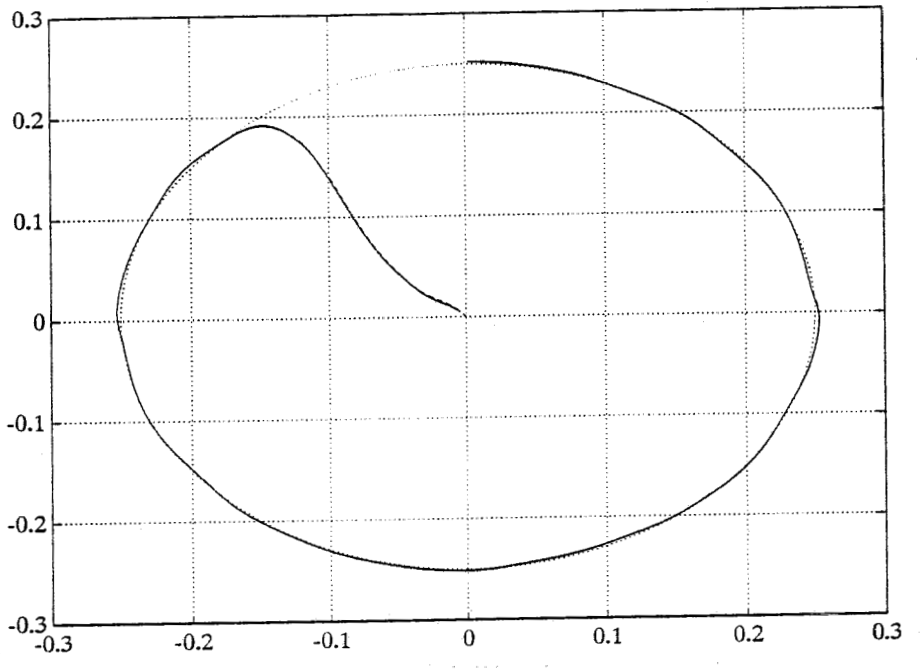

Figure H.2: desired and real trajectory
—— :real, ----:desired

- composite adaptive controller

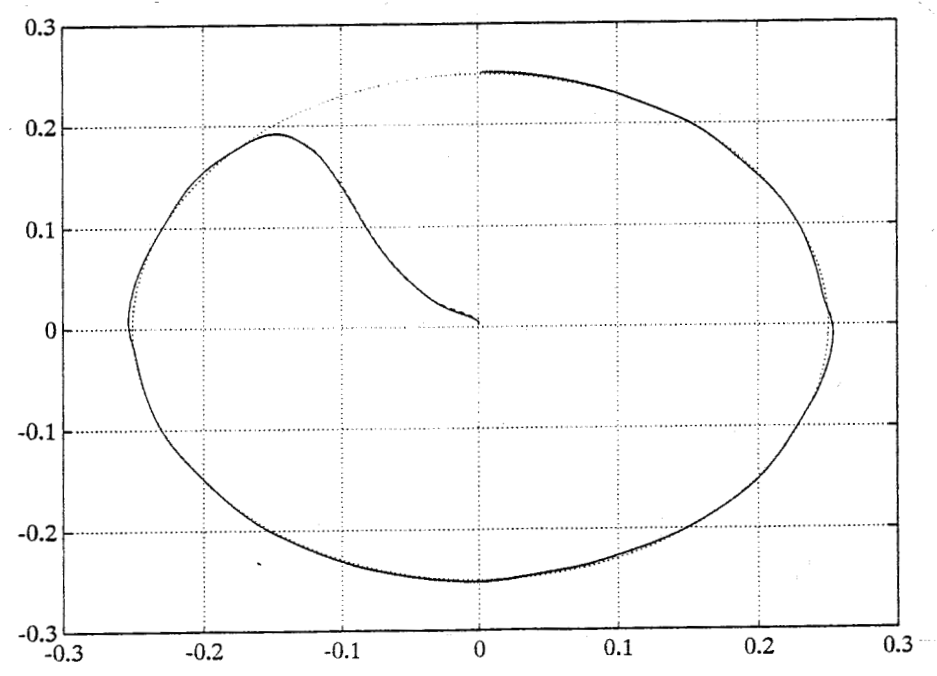

Figure H.3: desired and real trajectory
—— :real, ----:desired

From these figures we see that the transient response of the direct controller lasts longer than the transient response of the indirect and composite controller. The indirect and composite controller go from the starting point of the experiment (centre of the desired circle) quicker to the desired trajectory than the direct controller.

Furthermore, we see that at the point where the motion in y-direction changes from sign the direct controller has the largest tracking error. This is caused by the worse parameter estimates in the direct controller. The direct controller estimates the friction in y-direction too large. So, the controller calculates a too large input for the y-axis servomotor. As a result of this the real trajectory has an overshoot with regard to the desired trajectory. If the motion in y-direction changes from sign, also the friction term changes from sign and the controller calculates a too large input, but now in the opposite direction as before. This explains the oscillation in the real trajectory of the direct controller at the point where the motion in the y-direction changes from sign.

In the following figures the calculated and the real inputs to the servomotors of the direct adaptive controller are shown (the inputs of the indirect and composite adaptive controller are almost the same):

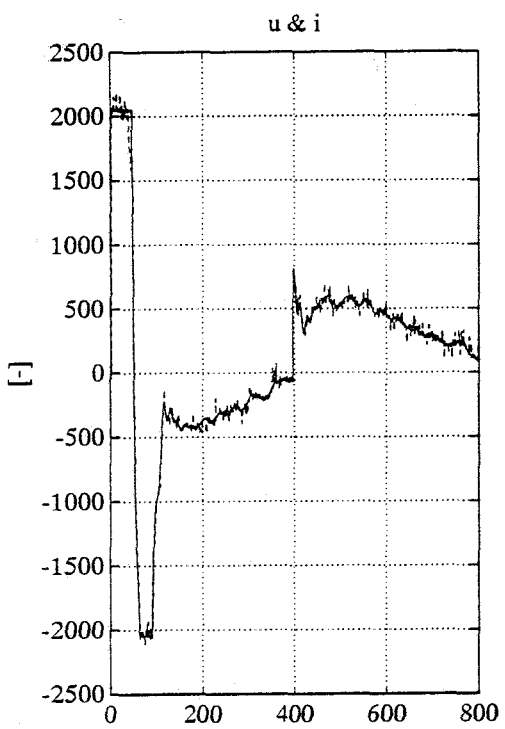

Figure H.4: Input to x-axis motor
—— :calculated, ----:real

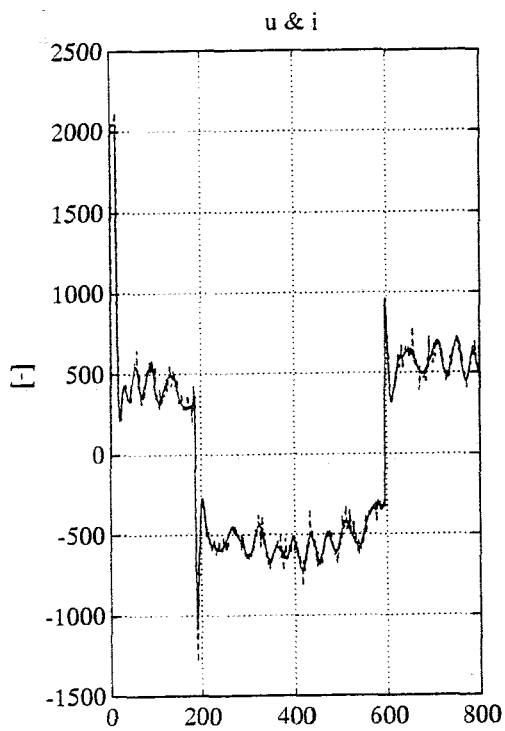

Figure H.5: Input to y-axis motor
—— :calculated, ----:real

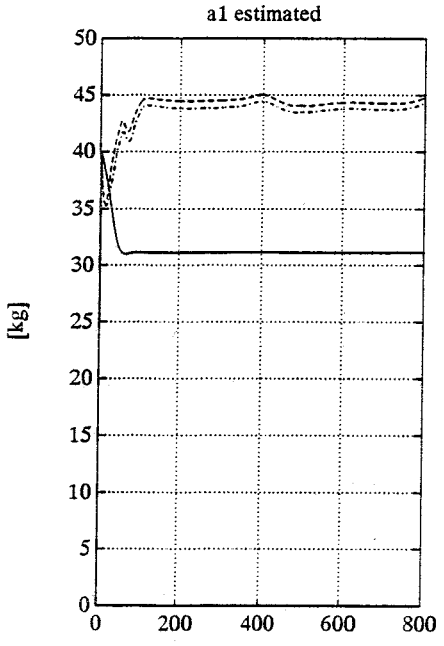

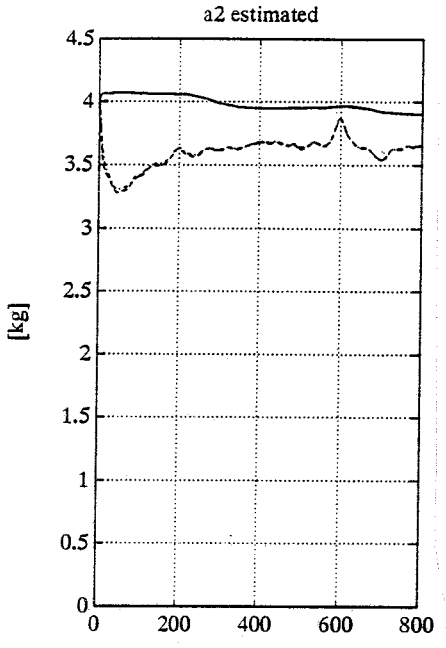

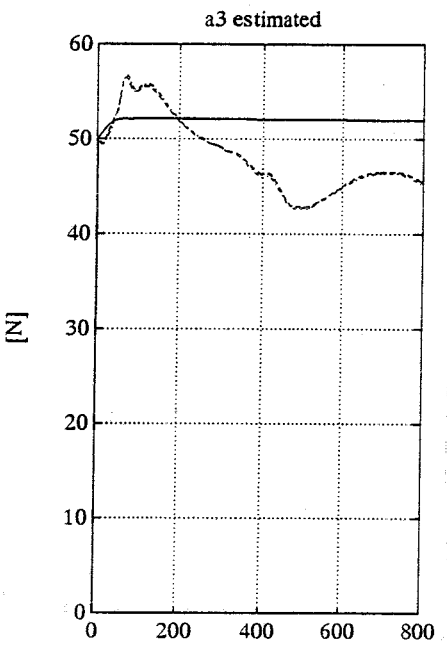

Figure H.6: estimated a_1 Figure H.7: estimated a_2 Figure H.8: estimated a_3
—— :direct, ----:indirect, -·-·:composite

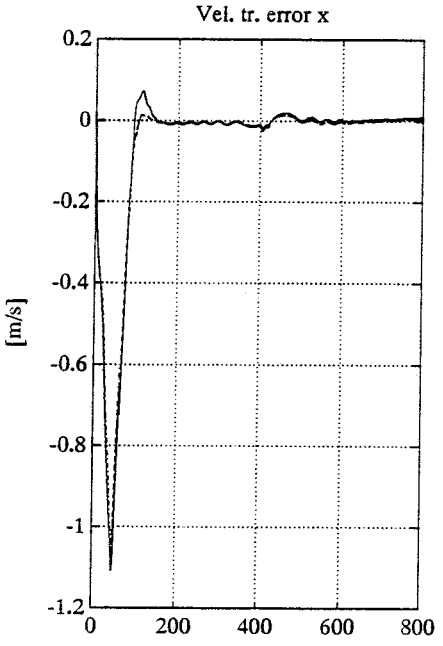

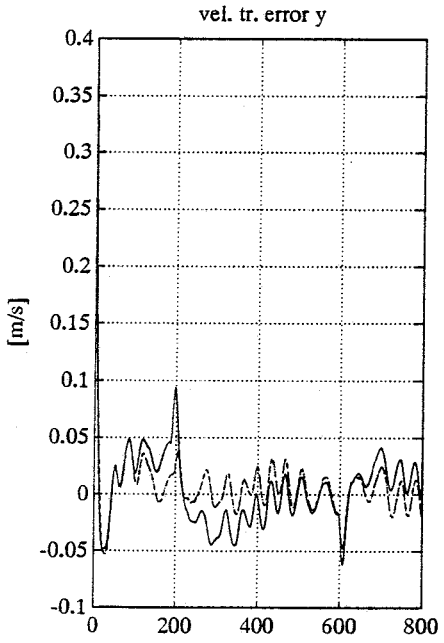

Figure H.9: Vel. error x Figure H.10: Vel. error y
—— :direct, ----:indirect, -·-·:composite

Situation 2:

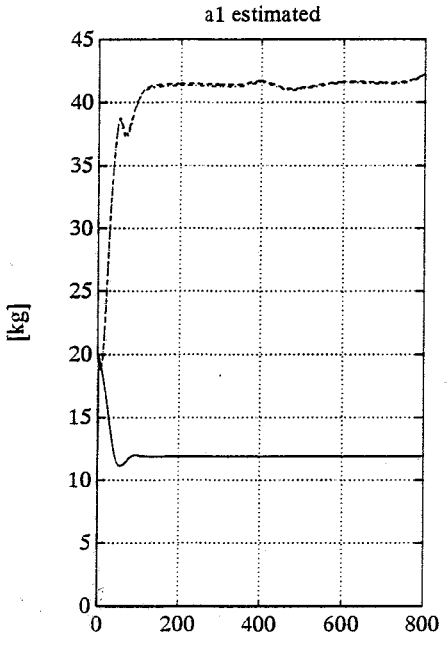

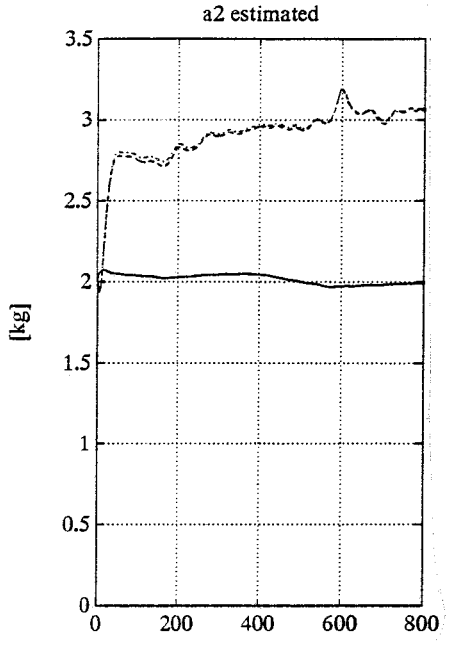

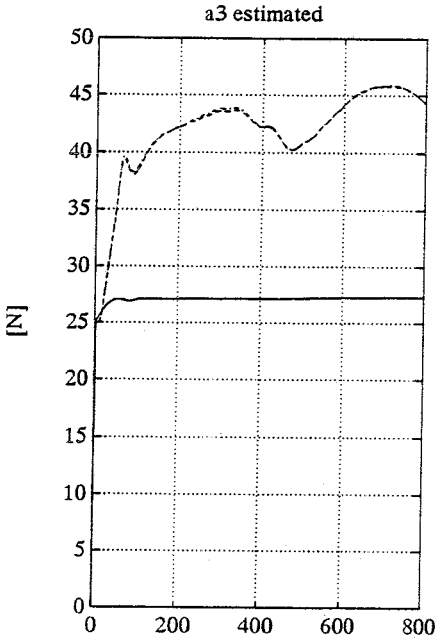

Figure H.11: estimated a_1 Figure H.12: estimated a_2 Figure H.13: estimated a_3
—— :direct, ----:indirect, -·-·:composite

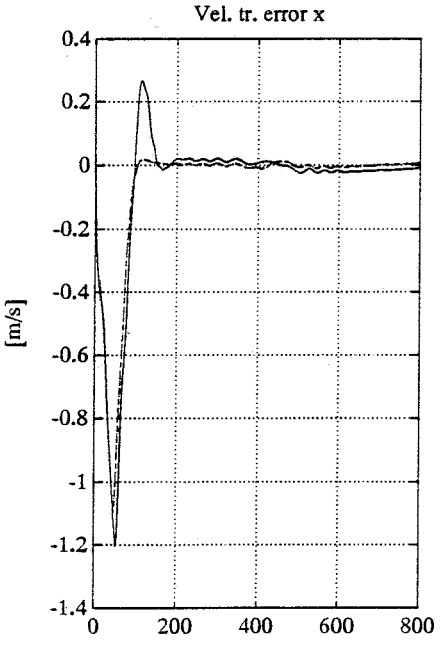

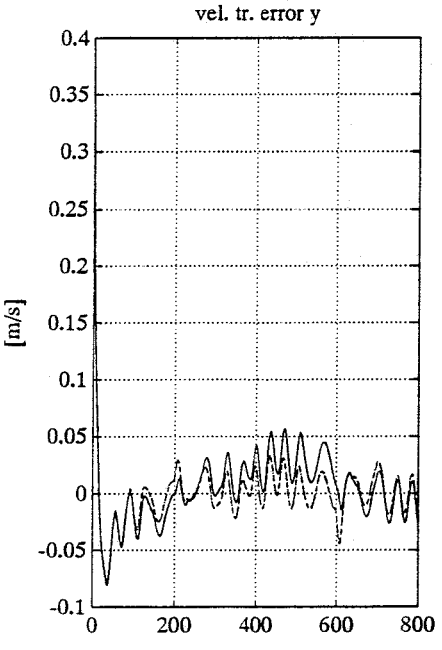

Figure H.14: Vel. error x Figure H.15: Vel. error y
—— :direct, ----:indirect, -·-·:composite

Situation 3:

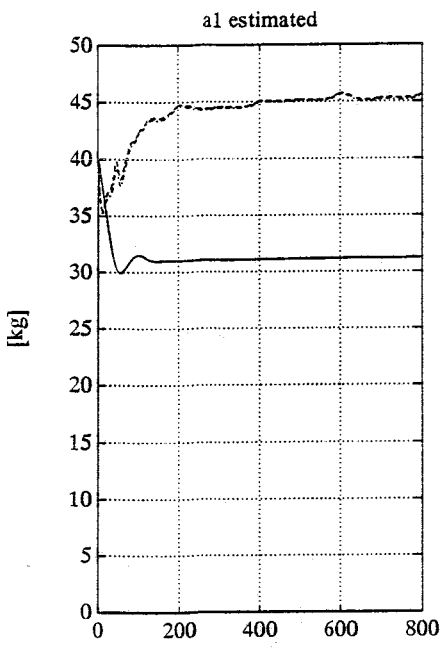

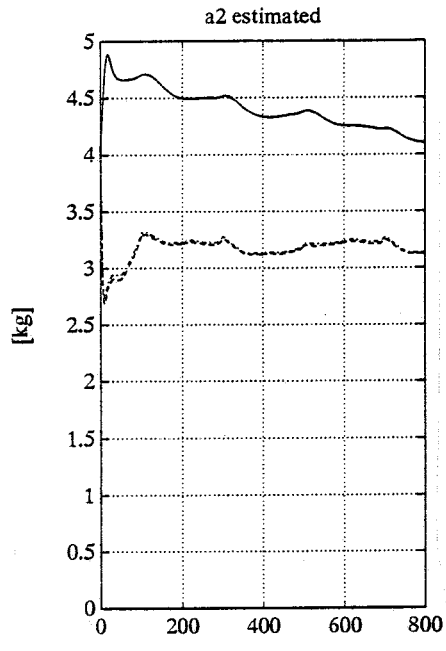

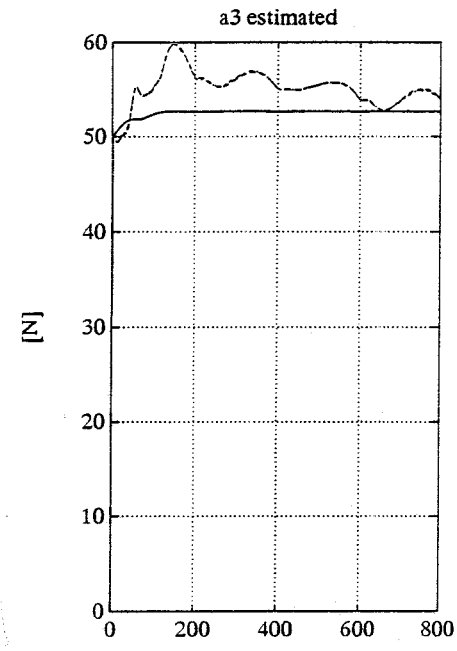

Figure H.16: estimated a_1 Figure H.17: estimated a_2 Figure H.18: estimated a_3
—— :direct, ----:indirect, -·-·:composite

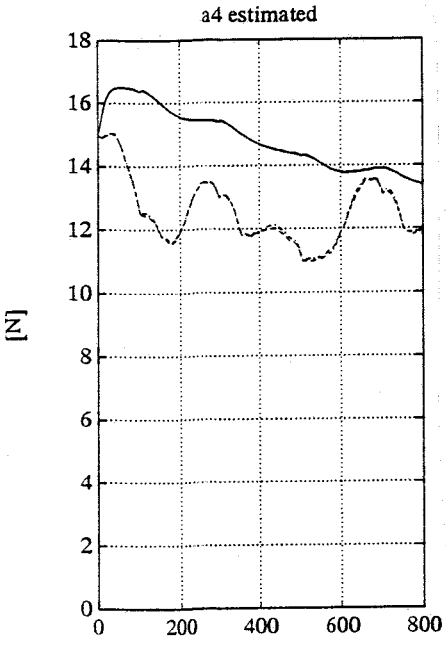

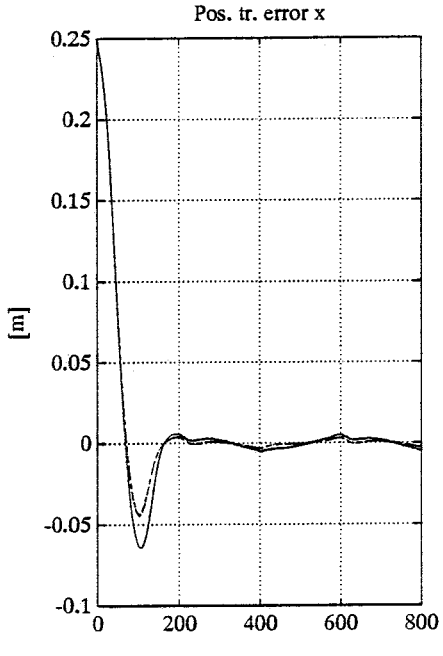

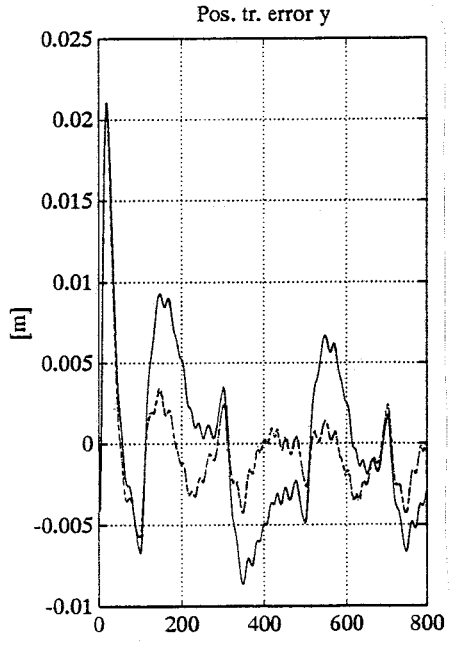

Figure H.19: estimated a_4 Figure H.20: Pos. error x Figure H.21: Pos. error y
—— :direct, ----:indirect, -·-·:composite

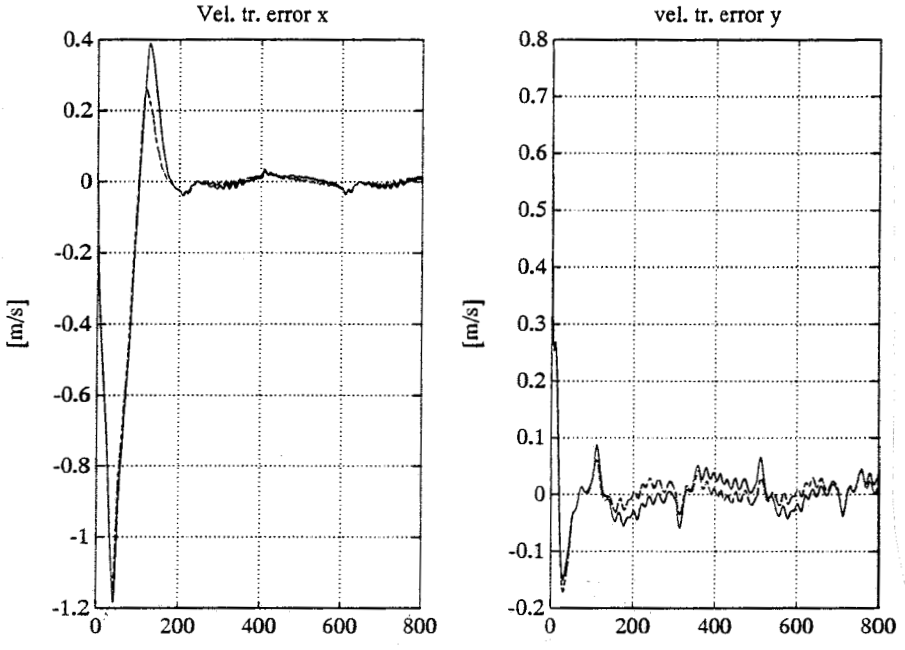

Figure H.22: Vel. error x Figure H.23: Vel. error y
—— :direct, ----:indirect, -·-·:composite

H.2 Results of the flexible XY-table

Situation 1:

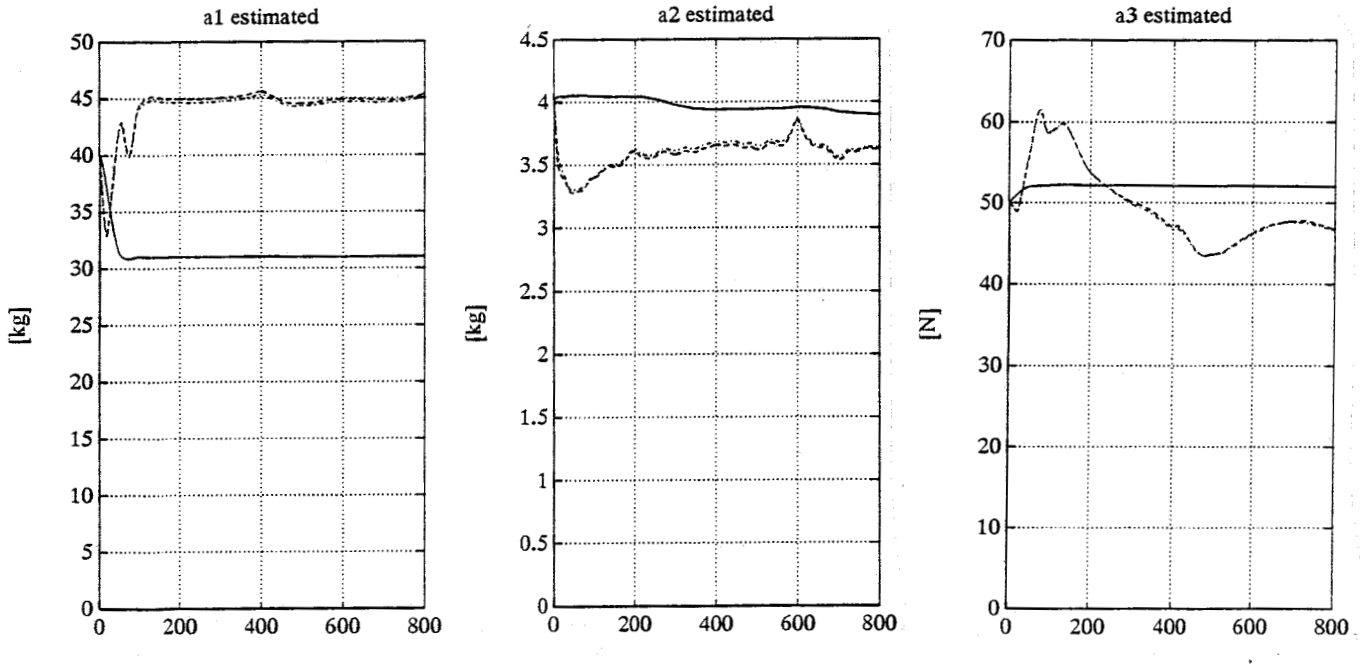

Figure H.24: estimated a_1 Figure H.25: estimated a_2 Figure H.26: estimated a_3
—— :direct, ----:indirect, -·-·:composite

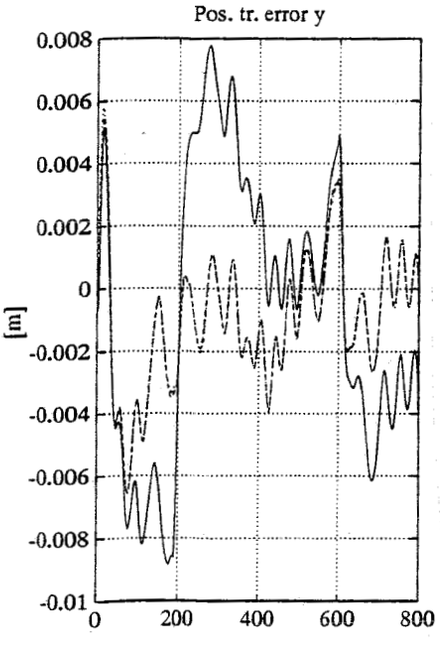

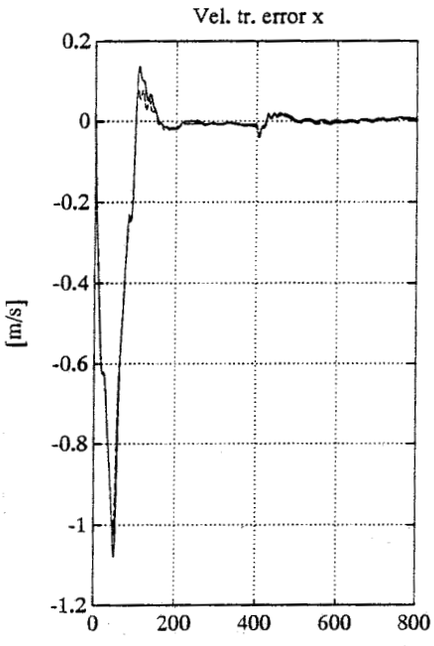

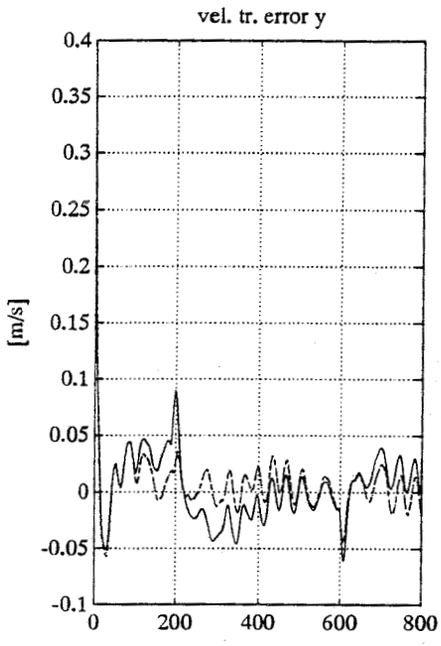

Figure H.27: Pos. error y Figure H.28: Vel. error x Figure H.29: Vel. error y
—— :direct, ----:indirect, -·-·:composite

H.3 Results of a non-adaptive controller

The non-adaptive controller has the following control law:

$$\tau = Y(q,\dot{q},\dot{q}_r,\ddot{q}_r)a - K_D s$$

The results of the non-adaptive controller is much dependent on the choice of the parameters a. If we choose the parameters reasonably well, the results of the non-adaptive controller are almost as good as the results of the direct adaptive controller.

Now, the results are shown for the situation with a=[40/0.12 4/0.02 50/0.12 15/0.02]^T. The control parameters K_D and Λ are chosen the same as in case of the direct adaptive controller.

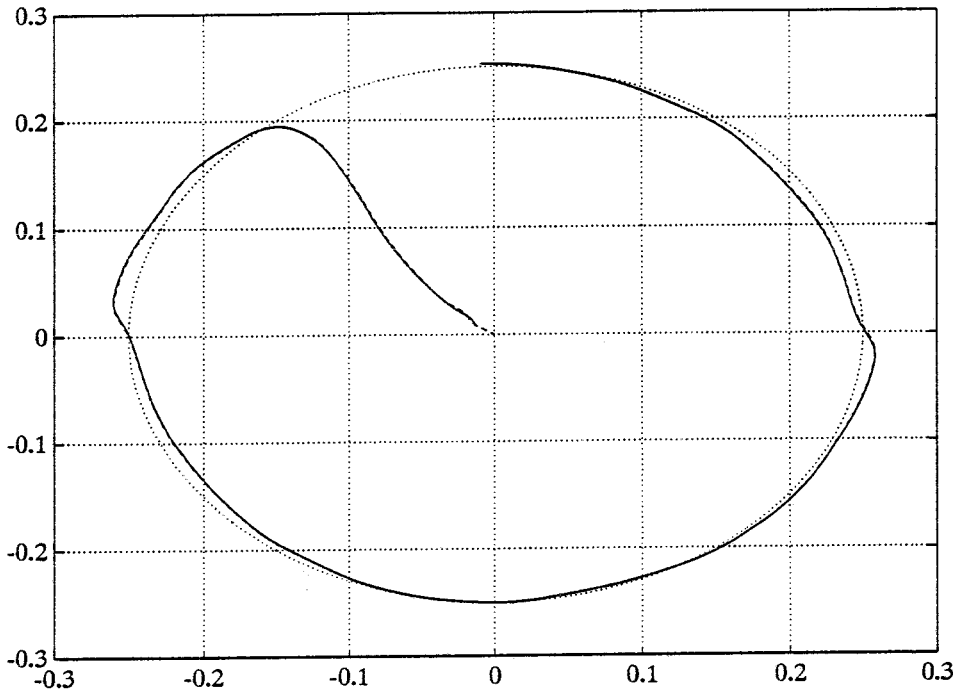

Figure H.30: desired and real trajectory
—— :real, ----:desired

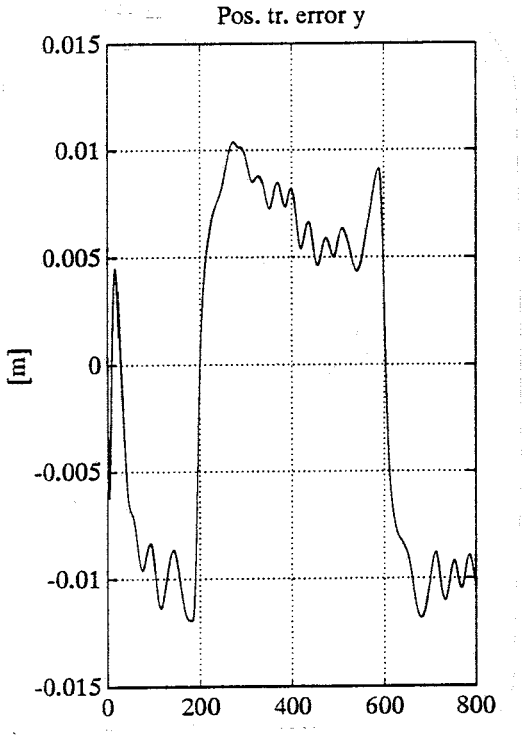

Figure H.31: Pos. error y

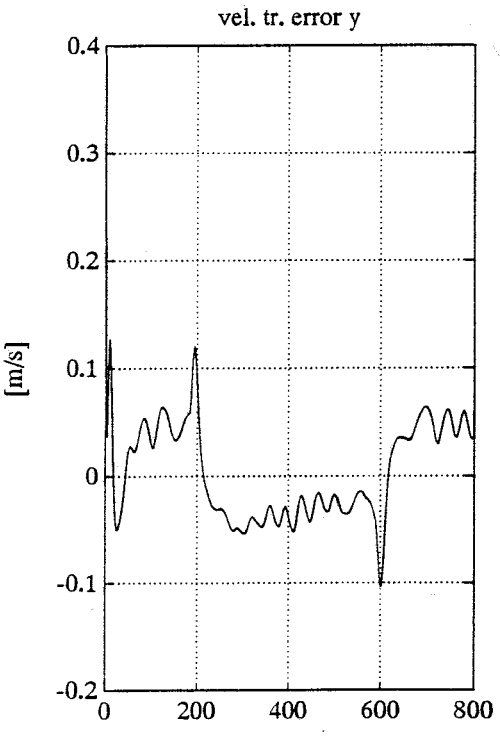

Figure H.32: Vel. error y

If we choose a=1/2*[40/0.12 4/0.02 50/0.12 15/0.02]^T, the results of the non-adaptive controller become better. In this case, the results are the same as for the direct adaptive controller in situation 1. But if we choose a=2*[40/0.12 4/0.02 50/0.12 15/0.02]^T, the results of the non-adaptive controller become unstable:

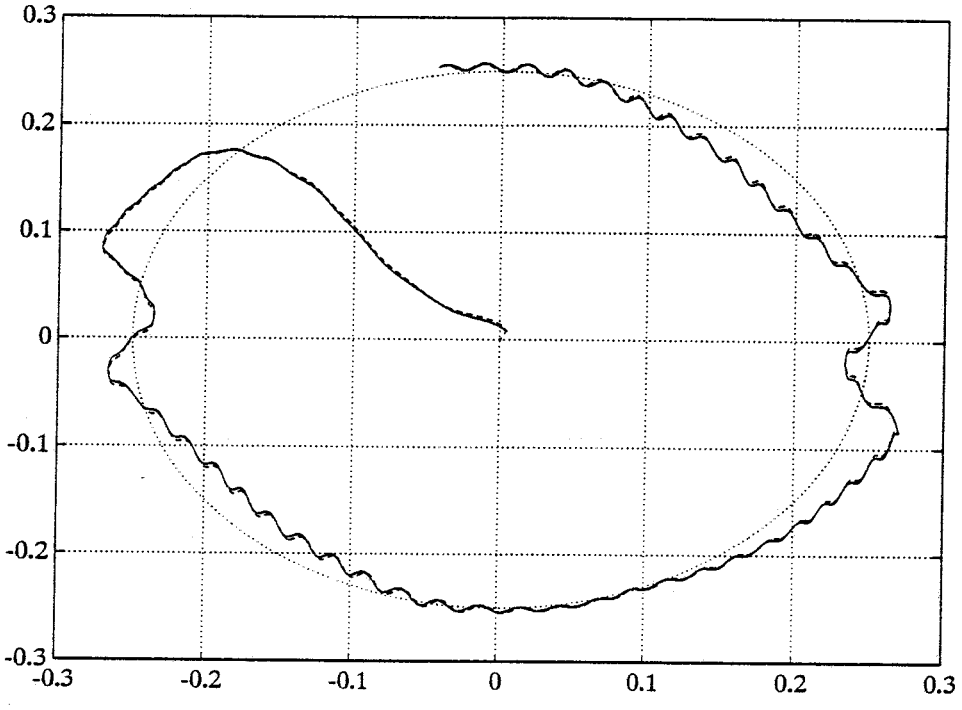

Figure H.33: desired and real trajectory
—— :real, ----:desired